## AN ABSTRACT OF THE THESIS OF

Kenneth Stefan Werner for the degree of Master of Science in Geosciences presented on October 11, 1990

Title: I. Direction of Maximum Horizontal Compression in Western Oregon Determined by Borehole Breakouts. II. Structure and Tectonics of the Northern Willamette Valley, Oregon

Redacted for privacy

Abstract approved: _____
Robert Yeats

Elliptical borehole enlargements or "breakouts" caused by systematic spalling of a borehole wall due to regional maximum horizontal stresses were identified in 18 wells drilled in the Coast Range and Willamette Valley of western Oregon. The breakouts generally indicate a NNW to NNE orientation of maximum horizontal compression ($\sigma H_{max}$) that agrees with the predominant direction of $\sigma H_{max}$ determined from earthquake focal mechanisms, from post-middle Miocene structural features, and from alignments of Holocene volcanic centers in the Pacific Northwest. However, this orientation is inconsistent with the N50°E convergence between the Juan de Fuca and North American plates determined by Riddihough [1984] from Juan de Fuca plate magnetic lineations as young as 730 ka (the Brunhes-Matuyama boundary). The predominant NNW to NNE orientation of $\sigma H_{max}$ may be due to the complex interaction of a northwestward-moving Pacific plate driving into the Gorda and Juan de Fuca plates and indirectly transmitting N-S compression across the strongly coupled Cascadia subduction zone into the overriding North American plate [Spence, 1989]. Alternatively, the predominant NNW to NNE

orientation of $\sigma H_{max}$ may be due to a landward counterclockwise rotation of the direction of $\sigma H_{max}$ from N50°E compression offshore to N-S compression in the Coast Range.

The northern Willamette Valley lies on the eastern flank of the broad north-northeast-trending Oregon Coast Range structural arch. Eocene to Oligocene marine sedimentary rocks crop out along the western side of the northern Willamette Valley and form a gently eastward dipping homocline. However, beneath the center of the Willamette Valley, Eocene to Oligocene strata are structurally warped up.

During the Eocene several major volcanic centers subdivided the Coast Range forearc region into shallow to deep marine basins. Several such volcanic centers occur adjacent to the northern Willamette Valley and are associated with residual gravity anomaly highs and lineations.

The top of basalt in the northern Willamette Valley (middle Miocene Columbia River basalt except near the valley margins) is contoured based on petroleum exploration wells, water wells, and seismic-reflection data. It is structurally downwarped to an altitude of less than -500 m just north of Woodburn. The downwarp is bounded to the south by the NE-trending Waldo Hills range-front fault and in part to the north by the NE-trending Yamhill River-Sherwood fault zone.

The NW-trending Mt. Angel fault extends across the northern Willamette Valley between Mt. Angel and Woodburn and deforms middle Miocene Columbia River basalt and overlying Pliocene and Miocene fluvial and lacustrine deposits. The top of Columbia River basalt is vertically separated, NE side up, roughly 100 m based on seismic-reflection data near Woodburn, and 250+ m based on water-well data near Mt. Angel. The Mt. Angel fault is part of a NW-trending structural zone that includes the Gales Creek fault west of the Tualatin basin; however, a connection between the Gales Creek and Mt. Angel faults does not occur through Willamette River alluvial deposits.

A series of small earthquakes (6 events with $m_C$ = 2.0, 2.5, 2.4, 2.2, 2.4, 1.4) occurred on August 14, 22, and 23, 1990 with epicenters near the northwest end of the Mt.

Angel fault. Routine locations indicate a depth of about 30 km. The preferred composite focal mechanism is a right-lateral strike-slip fault with a small normal component on a plane striking north and dipping steeply to the west.

Both recent mapping of the Mt. Angel fault and the recent seismicity suggest that the Gales Creek-Mt. Angel lineament is similar to the Portland Hills-Clackamas River lineament found to the north. Together, these two lineaments may take up right-lateral strike-slip motions imposed on the upper plate by oblique subduction.

Boring Lava appears to occur extensively in the subsurface of the northeastern portion of the northern Willamette Valley based on seismic data. Many of the faults in the area are interpreted to be largely caused by doming from influx of Boring magma or subsidence associated with evacuation of Boring magma. Such faults occur at Petes Mountain, at Parrett Mountain, along the Molalla River, and possibly near Curtis. The fault along the Molalla River appears to offset the Pleistocene (?) Rowland Formation 1 m (Glenn, 1965).

# I. Direction of Maximum Horizontal Compression in Western Oregon Determined by Borehole Breakouts
# II. Structure and Tectonics of the Northern Willamette Valley, Oregon

by

Kenneth Stefan Werner

A THESIS

submitted to

Oregon State University

in partial fulfillment of
the requirements for the
degree of

Master of Science

Completed October 11, 1990

Commencement June, 1991

APPROVED:

Redacted for privacy

Professor of Geosciences in charge of major

Redacted for privacy

Chairman of department of Geosciences

Redacted for privacy

Dean of Graduate School

Date thesis is presented October 11, 1990

Typed by Kenneth S. Werner

## ACKNOWLEDGEMENTS

Support was provided by U.S. Geological Survey National Earthquake Hazard Reduction Program Grant no. 14-08-0001-G1522 awarded to R. S. Yeats. Additional funding was provided by ARCO Oil and Gas Company and the Peter P. Johnsen scholarship committee.

Many people and companies were helpful in supplying data and facilities. Gravity data were supplied by Northwest Geophysical Associates, A. Johnsen, and C. Goldfinger. All reduction of gravity data was completed at CONMAR, College of Oceanography, Oregon State University, with much help from B. O'Malley. J. Shay donated a great deal of time to writing the synthetic seismogram program. Air photos (taken in 1980) were supplied by the Environmental Remote Sensing Applications Laboratory (ERSAL) at the College of Forestry. Thank you Paula Pitts, Linda Haygarth, and Camela Carstarphen for doing a great job of drafting the plates and many of the figures, an arduous task.

I would like to thank Dr. R. Yeats for his guidance and insightful discussions on Willamette Valley geology. I also greatly benefitted from discussions with Dr. R. Couch, Dr. M. Beeson, Dr. A. R. Niem, W. Niem, J. Meyer, and D. Sherrod. Thanks very much to the many graduate students who helped along the way including E. Graven, G. Huftile, T. Popowski, C. Goldfinger, T. Berkman, M. Parker, and C. Carstarphen. I would especially like to thank my family for encouragement, support, and financial assistance.

## TABLE OF CONTENTS

## LIST OF FIGURES

## LIST OF TABLES

## LIST OF PLATES

# PREFACE

The thesis has been divided into two sections: I. Direction of Maximum Horizontal Compression in Western Oregon Determined by Borehole Breakouts, and II. Structure and Tectonics of the Northern Willamette Valley, Oregon. The first section corresponds to a publication coauthored with E. P. Graven, T. A. Berkman, and M. P. Parker. The publication is currently in press in Tectonics. The coauthors contributed to the paper by examining dip-meter logs to pick borehole breakouts and reviewing drafts of the paper. In addition, E. P. Graven and the author constructed rose diagrams for each well showing the direction of maximum horizontal compression (Table 2).

The second section was completed independently. Portions of the second section will be included in a publication by R. Yeats, E. P. Graven, K. S. Werner, C. Goldfinger, and T. Popowski, which will be part of a Professional Paper by the U.S. Geological Survey. In addition, portions of the thesis on the Gales Creek-Mt. Angel structural zone will be submitted by K. Werner, J. Nábelek, and R. Yeats to Oregon Geology for publication.

# I. DIRECTION OF MAXIMUM HORIZONTAL COMPRESSION IN WESTERN OREGON DETERMINED BY BOREHOLE BREAKOUTS

# II. STRUCTURE AND TECTONICS OF THE NORTHERN WILLAMETTE VALLEY, OREGON

## INTRODUCTION

### GEOLOGIC SETTING

This thesis consists of two parts: a regional study of the direction of maximum horizontal compression in western Oregon, and a study of the structure and tectonics of the northern Willamette Valley. The two parts are closely related in that the direction of compression from plate interactions near western Oregon is important in understanding the structural geology and possible seismic hazards of western Oregon, including the northern Willamette Valley.

The northern Willamette Valley, the focus of the second part of the study, is located between the Oregon Coast Range and Cascade mountains. It is part of a linear depression, the Willamette-Puget lowland, which extends from Georgia Strait, Washington to Eugene, Oregon (Figure 6). During the early Eocene, the subduction zone between the Farallon and North American plates occupied a position east of the Willamette-Puget lowland [Snavely et al., 1968; Niem and Niem, 1984]. The subduction zone shifted to its present position as oceanic basalt of the Oregon Coast Range block accreted to the North American plate margin. Currently, the Juan de Fuca plate is obliquely subducting beneath North America along the Cascadia subduction zone (Figure 6).

## OBJECTIVES

The purpose of the thesis is to:

(1.) Determine the present direction of maximum horizontal compression ($\sigma H_{max}$) in western Oregon based on the analysis of borehole breakouts from petroleum exploration wells.

(2.) Identify structures which may be potential seismic hazards. This thesis represents part of the effort by the Oregon Department of Geology and Mineral Industries (DOGAMI) and the United States Geological Survey (USGS) to evaluate the seismic risk from subduction-zone and intraplate earthquakes in the more populated part of Oregon. Several metropolitan centers including the state capital (Salem) lie within the study area.

(3.) Determine the general structure of the northern Willamette Valley by integrating surface and subsurface data, collected largely during oil and gas exploration in the 1970's and 1980's. The distribution of older structures and strata is important in controlling recent deformation.

(4.) Establish a geologic framework for analyzing ground shaking potential from either subduction zone earthquakes or intraplate earthquakes. The shaking potential should depend in part on the thickness of unconsolidated sediments overlying Columbia River basalt because the sediment/basalt contact corresponds to a large acoustic impedance contrast.

# I. DIRECTION OF MAXIMUM HORIZONTAL COMPRESSION IN WESTERN OREGON DETERMINED BY BOREHOLE BREAKOUTS

## ABSTRACT

Elliptical borehole enlargements or "breakouts" caused by systematic spalling of a borehole wall due to regional maximum horizontal stresses were identified in 18 wells drilled in the Coast Range and Willamette Valley of western Oregon. The breakouts generally indicate a NNW to NNE orientation of maximum horizontal compression ($\sigma H_{max}$) that agrees with the predominant direction of $\sigma H_{max}$ determined from earthquake focal mechanisms, from post-middle Miocene structural features, and from alignments of Holocene volcanic centers in the Pacific Northwest. However, this orientation is inconsistent with the N50°E convergence between the Juan de Fuca and North American plates determined by Riddihough [1984] from Juan de Fuca plate magnetic lineations as young as 730 ka (the Brunhes-Matuyama boundary). The predominant NNW to NNE orientation of $\sigma H_{max}$ may be due to the complex interaction of a northwestward-moving Pacific plate driving into the Gorda and Juan de Fuca plates and indirectly transmitting N-S compression across the strongly coupled Cascadia subduction zone into the overriding North American plate [Spence, 1989]. Alternatively, the predominant NNW to NNE orientation of $\sigma H_{max}$ may be due to a landward counterclockwise rotation of the direction of $\sigma H_{max}$ from N50°E compression offshore to N-S compression in the Coast Range.

# INTRODUCTION

Western Oregon lies in an area of complex and dynamic plate motions (Figure 1). The direction of compression from plate interactions near western Oregon is important in understanding the tectonic development as well as possible seismic hazards of the area. The Pacific Northwest region, which includes western British Columbia, Washington, northeastern Idaho, Oregon, and northern California, is the dominant stress province surrounding western Oregon [Zoback and Zoback, 1989]. This province is characterized by NNW to NNE maximum horizontal compression ($\sigma H_{max}$) based on earthquake focal mechanism solutions, fault surfaces, volcanic alignments, and hydraulic fracturing tests (in southeastern Washington) [Crosson, 1972; Smith, 1977; Sbar, 1982; Zoback and Zoback, 1980, 1989; Paillet and Kim, 1987]. However, a second stress province, the Cascade convergence zone, has recently been proposed by Zoback and Zoback [1989] and is characterized by NE compression based largely on earthquake focal mechanism solutions around Mt. St. Helens and Mt. Hood. The stress orientation has been difficult to determine in western Oregon due to relatively few earthquakes and limited data on volcanism and faulting. The purpose of this study was to determine the present direction of $\sigma H_{max}$ in western Oregon using the analysis of borehole breakouts from petroleum exploratory wells.

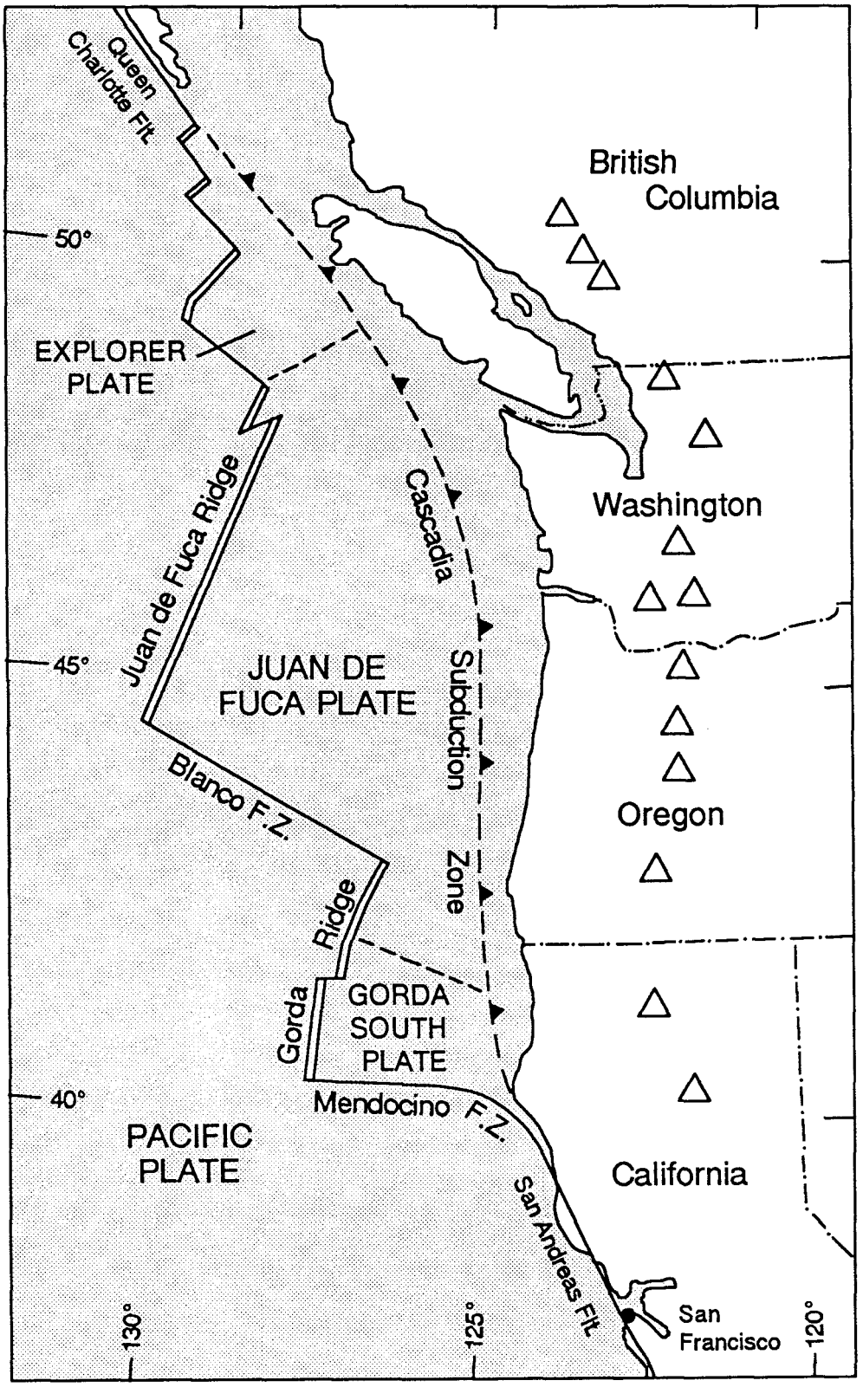


Figure 1: Tectonic map of the Pacific Northwest. Major stratovolcanoes are shown as open triangles [after Riddihough, 1984].

## FORMATION OF BOREHOLE BREAKOUTS

A borehole breakout is the elongation of a once-circular borehole due to stress concentration around the borehole arising from differential horizontal stress [Bell and Gough, 1979; Zoback et al., 1985; Springer, 1987]. In a matter of hours after drilling [Gough and Bell, 1982], tangential stress is concentrated in the direction of minimum horizontal compression resulting in spalling and subsequent borehole elongation (along the dashed line in Figure 2). The direction of $\sigma H_{max}$ is thus perpendicular to the direction of elongation. Borehole breakouts have been shown to be independent of both lithology [Bell and Gough, 1979] and bedding dip [Babcock, 1978; Bell and Gough, 1979; Plumb and Hickman, 1985].

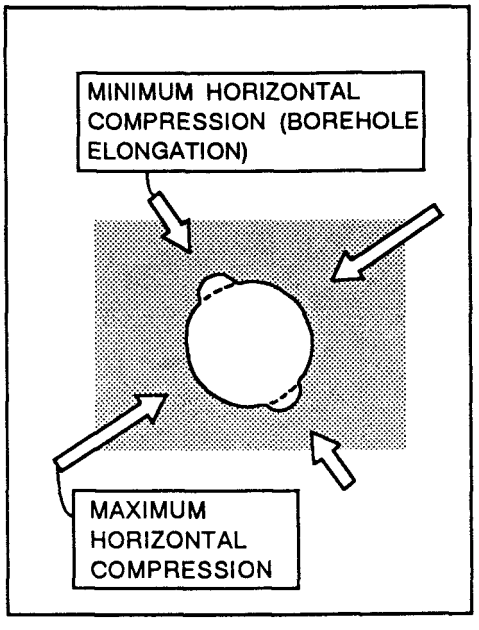


Figure 2. A horizontal cross section through a borehole showing a breakout [after Plumb and Cox, 1987].

Borehole breakouts in this study were picked using unprocessed, four-arm dual-caliper dipmeter logs. The dipmeter tool has four orthogonal arms that are forced against the borehole wall. Pads on these arms measure microconductivity, while the arms

themselves act as two independent sets of calipers measuring the diameter of the hole. Torque on the logging cable generally causes the tool to rotate as it is pulled upward except where the hole is elongated and two opposing pads of the tool become temporarily locked within the elongated interval.

Enlargement of the borehole may occur from mechanisms other than spalling due to differential horizontal stress. These include (1) washout of poorly consolidated material by drilling fluid, (2) drilling-induced hydraulic fractures [Zoback et al., 1986], (3) intersection with one or more pre-existing fractures [Babcock, 1978; Hickman et al., 1985], or (4) drill pipe wear as the hole deviates from vertical [Plumb and Hickman, 1985]. In addition, "caking" of drilling-mud on the wall of the hole [Babcock, 1978; Plumb and Hickman, 1985; Springer, 1987] or hole closure from elastic or plastic deformation [Plumb and Hickman, 1985; Zoback et al., 1986; Plumb and Cox, 1987] can make identification of borehole breakouts difficult. We used several criteria modified from Plumb and Hickman [1985], Springer [1987], and Fuchs and Clauß [1988] to exclude intervals of the borehole affected by the mechanisms listed above. The criteria are as follows:

1. The tool must stop rotating, because the stress responsible for the elongation should have a relatively consistent orientation
2. The resistivity curves for all four pads must be consistent. Natural fractures intersecting the hole are commonly associated with resistivity anomalies due to fluids or a drilling-mud precipitate. Drilling-induced hydraulic fractures may also cause a resistivity anomaly due to infiltrating drilling fluid. In addition, resistivity anomalies may occur when the logging tool is not centered.
3. The larger caliper curve must be larger than hole gauge, and the smaller caliper curve must not be significantly less than hole gauge. Mudcaking

often results in a diameter less than hole gauge as does plastic deformation of the borehole (in contrast to brittle failure).

4. The two caliper curves cannot mimic each other, as this is a common characteristic of washouts.
5. The well cannot deviate more than 7°, because drill-pipe wear against the borehole wall often elongates the hole in the direction of hole deviation. If the deviation is greater than 1°, the direction of elongation must not be within 10° of the azimuth of hole deviation.
6. The minimum caliper (or diameter) difference allowed was 0.25 in or 6 mm.

# MAXIMUM HORIZONTAL COMPRESSION IN WESTERN OREGON

## BOREHOLE BREAKOUTS

In western Oregon, from Coos Bay northward to the Columbia River, we found borehole breakouts in 18 of 23 wells examined (all wells were deviated < 7°). The 5 wells without breakouts all had elongated intervals; however, the intervals failed to meet the criteria previously listed. The location and direction of $\sigma H_{max}$ for each well with breakouts is shown in Figure 3. The convergent arrows show the mean azimuth-cumulative length weighted direction of $\sigma H_{max}$ (weighting methods are discussed below). The length of each pair of arrows indicates the reliability of the breakouts found in a well, using the tectonic stress quality ranking scheme of Zoback and Zoback [1989] shown in Table 1. An 'A' ranking indicates the most reliable direction and a 'D' ranking indicates the least reliable direction. The ranking scheme is a function of both the number of breakouts and the standard deviation of the breakout directions for a given well.

Table 1. Criteria for ranking the quality of breakout data as a stress indicator [from Zoback and Zoback, 1989]. S.D. = standard deviation.

| Rank | Criteria |
|---|---|
| A | Ten or more distinct breakout zones in a single well with S.D.≤12° and/or combined length >300 m. Alternatively, average of breakouts in two or more wells in close geographic proximity with combined length >300 m and S.D.≤12°. |
| B | At least six distinct breakout zones in a single well with S.D.≤20° and/or combined length >100 m. |
| C | At least four distinct breakouts with S.D.<25° and/or combined length >30 m. |
| D | Less than four consistently oriented breakouts or <30 m combined length in a single well. Alternatively, breakouts in a single well with S.D.≥25°. |

Figure 3: Orientation of $\sigma H_{max}$ as determined by borehole breakouts from 18 wells in western Oregon. The wells are located where the arrows meet and the numbers refer to Table 2. Wells 5 and 14 have bimodel directions of $\sigma H_{max}$ shown by two sets of convergent arrows. Offshore faults and folds deform Pleistocene-late Miocene strata and are from Peterson et al. [1986].

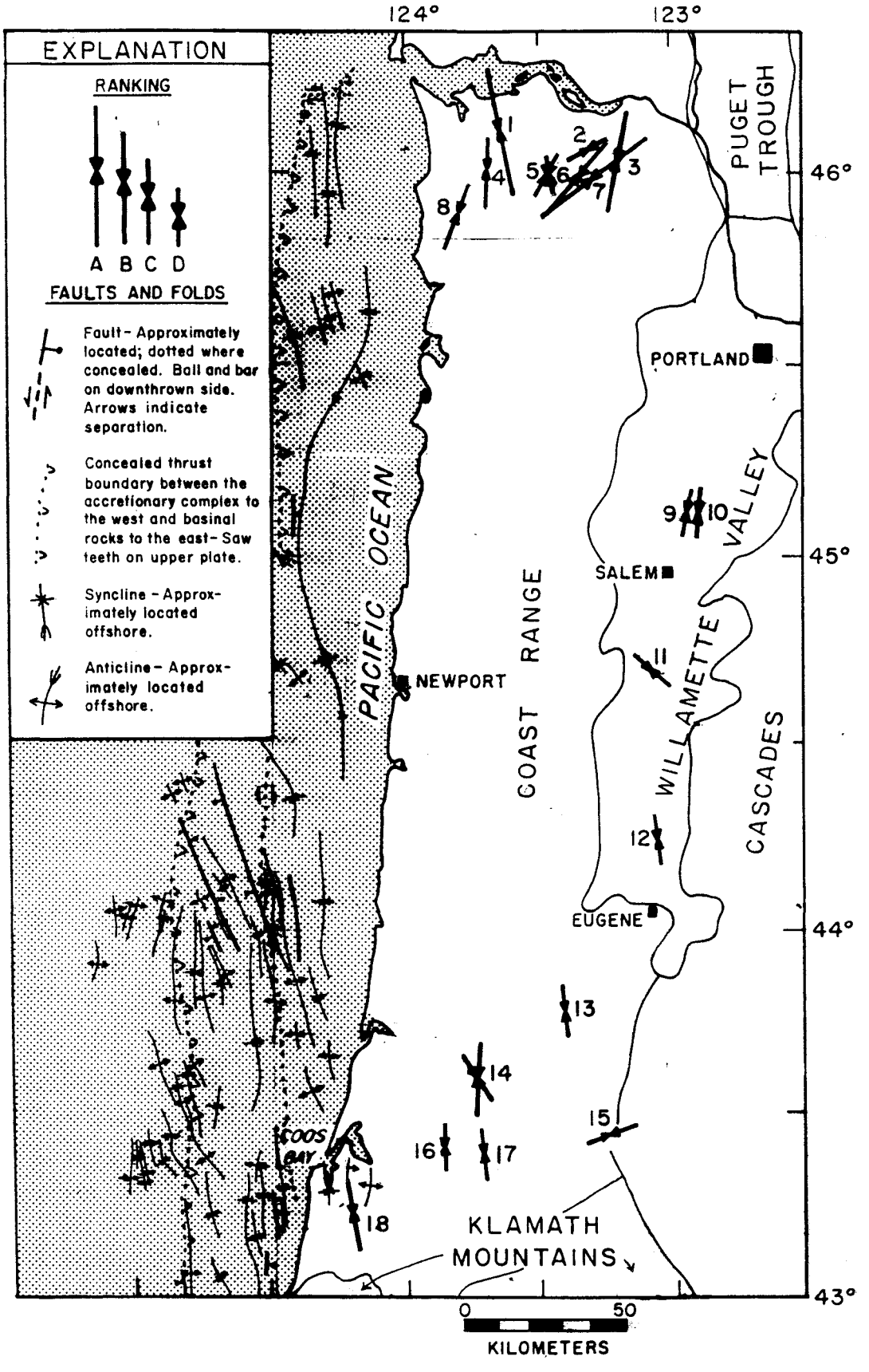
124°
123°
EXPLANATION
RANKING
A B C D
FAULTS AND FOLDS
Fault - Approximately located; dotted where concealed. Ball and bar on downthrown side. Arrows indicate separation.
Concealed thrust boundary between the accretionary complex to the west and basinal rocks to the east - Saw teeth on upper plate.
Syncline - Approximately located offshore.
Anticline - Approximately located offshore.
PUGET TROUGH
46°
PORTLAND
PACIFIC OCEAN
COAST RANGE
WILLAMETTE VALLEY
CASCADES
SALEM
NEWPORT
45°
EUGENE
44°
COOS BAY
KLAMATH MOUNTAINS
43°
1
2
3
4
5
6
7
8
9
10
11
12
13
14
15
16
17
18
0
50
KILOMETERS

The number of borehole breakouts per well ranges up to 13, with two-thirds of the borehole breakouts occurring in the northern 8 wells (Table 2). The direction of $\sigma H_{max}$ for each well is represented in Table 2 by an azimuth-frequency rose diagram and by an azimuth-cumulative-length rose diagram [terminology from Plumb and Hickman, 1985]. Azimuth-frequency rose diagrams weight the direction of $\sigma H_{max}$ from each breakout equally regardless of its length (e.g., one 50 meter breakout would be weighted the same as one 5 meter breakout). Azimuth-cumulative-length rose diagrams weight the direction of $\sigma H_{max}$ based on the downhole length of a breakout with a given direction regardless of the number of breakouts (e.g., one 50 meter breakout would be weighted the same as ten 5 meter breakouts).

The mean direction, standard deviation, and 95% confidence interval of $\sigma H_{max}$ was calculated for all breakouts using both weighting methods. The statistics are based on the methods of Mardia [1972] for nonpolar directional data. Assuming the distribution of all breakouts is unimodal and symmetric, which is not strictly the case, the mean frequency weighting method results in a mean azimuth of N9.7°E, a standard deviation of 32.8°, and a 95% confidence interval of 13.9°. The azimuth-cumulative-length weighting results in a mean azimuth of N13.0°E, a standard deviation of 27.8°, and a 95% confidence interval of 12.0°.

Table 2 shows the mean direction and standard deviation of $\sigma H_{max}$ for individual wells based on both frequency and cumulative-length weighting. The mean directions for each well determined using either weighting method agree to within 5° (except for well 8), which indicates the mean directions are relatively reliable [M. L. Zoback, personal communication, 1989]. Some scatter in the direction of $\sigma H_{max}$ is evident on the rose diagrams (e.g. wells 5 and 14). This scatter is probably the result of inclusion of a few wellbore elongations which may not be borehole breakouts. Similarly, the direction of $\sigma H_{max}$ in well 15 is based on only one elongation at roughly right angles to the directions of $\sigma H_{max}$

Table 2: Statistical data on borehole breakouts in western Oregon. The wells are listed from north to south, and the numbers refer to the locations in Figure 3. The shallowest breakout depth corresponds to the top of the shallowest breakout, and the deepest breakout depth to the base of the deepest breakout (measured from the kelly bushing). S.D. = standard deviation. The rose diagrams show the direction of $\sigma H_{max}$ (the tick marks indicate west, north, and east) and have a class width of 20°, positioned to best center the directions in all sectors. The area of each sector is proportional to the class frequency. Thus, each additional breakout to fall within a sector adds an equal amount to the area, but progressively less to the radius of that sector. This avoids slightly larger class frequencies appearing out of proportion to their significance [Cheeney, 1983].

TABLE 2.

| | | | | | | | | FREQUENCY WEIGHTED DATA | | | | LENGTH WEIGHTED DATA | | | |
|---|---|---|---|---|---|---|---|---|---|---|---|---|---|---|---|
| WELL # | WELL NAME | LAT. | LONG. | # of B.O. | TOTAL LENGTH (FT) | SHALLOWEST B.O. (FT) | DEEPEST B.O. (FT) | MEAN AZIMUTH MAX. HORIZ. COMPRESSION | S.D. | RANK | ROSE DIAGRAM | MEAN AZIMUTH MAX. HORIZ. COMPRESSION | S.D. | RANK | ROSE DIAGRAM |
| 1 | Patton 32-9 | 46.106 | -123.677 | 13 | 798 | 5722 | 9728 | 167.7 | 10.8 | A | | 167.9 | 10.1 | A | |
| 2 | Adams 32-34 | 46.050 | -123.300 | 3 | 137 | 1989 | 2230 | 56.7 | 6.3 | D | | 59.1 | 5.5 | D | |
| 3 | Wilna et al. 5-23 | 46.032 | -123.208 | 8 | 306 | 1006 | 4286 | 12.3 | 20.0 | B | | 12.4 | 15.9 | B | |
| 4 | Crown Zellerbach 31-17 | 46.007 | -123.698 | 5 | 452 | 2033 | 5016 | 13.3 | 28.7 | C | | 7.7 | 14.7 | C | |
| 5 | Watzek 22-19 | 45.993 | -123.472 | 4 | 660 | 1676 | 3898 | 27.5, 164.0 | 23.9 | C | | 27.9, 169.7 | 20.1 | C | |
| 6 | Columbia County 44-21 | 45.984 | -123.299 | 7 | 966 | 1138 | 3840 | 40.7 | 16.1 | B | | 39.4 | 15.0 | B | |
| 7 | Columbia County 33-8 | 45.967 | -123.306 | 10 | 503 | 950 | 3303 | 52.0 | 6.8 | A | | 51.6 | 7.4 | A | |
| 8 | Crown Zellerbach 11-28 | 45.893 | -123.809 | 4 | 1826 | 1014 | 4010 | 26.8 | 14.2 | C | | 19.3 | 10.8 | C | |
| 9 | Werner 14-21 | 45.117 | -122.945 | 2 | 58 | 2090 | 2212 | 1.0 | 4.0 | D | | 3.4 | 3.2 | D | |
| 10 | Werner 34-21 | 45.116 | -122.934 | 1 | 54 | 1672 | 1726 | 10.0 | N/A | D | | 10.0 | N/A | D | |
| 11 | Henschell 17-34 | 44.696 | -123.076 | 2 | 163 | 2180 | 2355 | 132.5 | 12.7 | D | | 129.2 | 12.3 | D | |
| 12 | Ira Baker no. 1 | 44.240 | -123.055 | 2 | 124 | 2130 | 3160 | 172.5 | 2.5 | D | | 172.0 | 2.5 | D | |
| 13 | Harris 1-4 | 43.780 | -123.409 | 1 | 60 | 5610 | 5670 | 174.0 | N/A | D | | 174.0 | N/A | D | |
| 14 | Sawyer Rapids no. 1 | 43.603 | -123.747 | 7 | 878 | 924 | 3816 | 150.0, 3.0 | 15.7 | B | | 148.4, 2.6 | 17.9 | B | |
| 15 | Sutherlin Unit no. 1 | 43.446 | -123.238 | 1 | 62 | 8816 | 8878 | 69.0 | N/A | D | | 69.0 | N/A | D | |
| 16 | Amoco-Weyerhauser F-1 | 43.413 | -123.864 | 3 | 297 | 1444 | 1960 | 177.7 | 13.3 | D | | 178.8 | 13.3 | D | |
| 17 | Amoco-Weyerhauser B-1 | 43.390 | -123.715 | 1 | 110 | 1450 | 1560 | 174.0 | N/A | D | | 174.0 | N/A | D | |
| 18 | Coos County no. 1 | 43.229 | -124.212 | 4 | 388 | 2910 | 6428 | 169.7 | 7.0 | C | | 170.3 | 7.1 | C | |

in adjacent wells (Figure 3). This elongation may be caused by a drilling-induced hydraulic fracture or a pre-existing fracture rather than a borehole breakout.

In situ stress is the resultant of one or more components of contemporary tectonic stress, local stress, or residual stress [Engelder and Sbar, 1984]. Several studies [Plumb and Cox, 1987; Zoback et al., 1986; and others] have shown that borehole breakouts generally measure contemporary regional tectonic stresses. Local stresses typically occur at shallow depth and may be caused by topography, nearby geologic structures, or periodic heating and cooling of near-surface rocks [Engelder and Sbar, 1984]. In order to filter out local stresses, Zoback et al. [1987] included only in situ stress measurements (such as hydraulic fracturing) in California from depths greater than 330 ft (100 m). Breakouts that did not extend below 1000 ft (305 m) were excluded from this data set. In spite of this added constraint, the northern eight wells (1-8) still have a high variance in their direction of $\sigma H_{max}$ (Figure 3). These wells occur in an area that is characterized by complex structure, consisting of many steeply-dipping NW- and NE-trending oblique slip faults, and the borehole breakouts there may be recording a complex local stress field related to local structure.

The effect of residual stress on borehole breakouts appears minimal. The direction of $\sigma H_{max}$ as recently as 4 Ma was NW based on dike and vein orientations in the western part of the Cascades province [Sherrod and Pickthorn, 1989]. Well 11 is the only well that is consistent with this direction and may be recording a residual stress orientation.

## RECENT DEFORMATION IN COOS BAY AREA AND NORTHERN OREGON COAST RANGE

Coos Bay and the northern Oregon Coast Range are two areas which provide information regarding the age and direction of the most recent period of principal shortening in western Oregon. The Coos Bay area has experienced shortening on numerous N- to NNW-trending fold axes that comprise the Coos Bay synclinorium.

Progressive warping of the synclinorium has continued through late Quaternary time based on tilted and faulted wave-cut platforms [Adams, 1984; McInelly and Kelsey, in press]. Furthermore, late Holocene subsidence has been inferred by Peterson and Darienzo [1989] along one of the N-trending synclinal axes based on Holocene salt-marsh stratigraphy. McInelly and Kelsey [in press] estimate that the direction of maximum horizontal shortening just south in the Cape Arago area is N60°E based on the down-to-the-east tilt direction of one wave-cut platform. The Coos Bay synclinorium continues northward onto the Oregon continental shelf and slope (Figure 3), where deformation consists of several N- to NNW-trending low-angle imbricate thrust faults and folds in unconsolidated Plio-Pleistocene sediments [Kulm and Fowler, 1974; Peterson et al., 1986]. Assuming the deformation both on- and offshore is compressional, the orientation of the fold axes and faults suggests an E to ENE direction of principal horizontal shortening. This direction of maximum horizontal shortening is roughly orthogonal to the direction of $\sigma H_{max}$ determined for well 18 (Figure 3). The direction of $\sigma H_{max}$ for well 18 is NNW based on borehole breakouts at a depth of 2910-6428 ft (887-1960 m).

The direction $\sigma H_{max}$ (which does not necessarily correspond to the direction of maximum horizontal shortening) may rotate between the shallower deformation in Coos Bay and the deeper breakout data. Alternatively, the discrepancy between the direction of principal shortening determined from structural geology and the direction of $\sigma H_{max}$ determined from borehole breakouts may indicate the direction of $\sigma H_{max}$ has recently rotated counterclockwise as suggested by McInelly and Kelsey [in press]. They show an apparent recent decrease in the amount of shortening of structures with N-S trending fold-axes. In addition, Kelsey [1990] found an E-W trending anticline near Cape Blanco based on altitudinal surveys of terraces combined with numerical and correlation age determinations (Figure 4). The latest movement on the anticline occurred 3000 years ago, but it also deforms strata as old as middle Miocene [Kelsey, 1990]. The anticline is consistent with the N-S direction of $\sigma H_{max}$ determined for well 18.

In the northern Coast Range west of the north-trending part of the Columbia River (Figure 3), Olbinski [1983], Peterson [1983], Nelson [1985], and Niem and Niem [1985] have mapped oblique slip conjugate right-lateral NW-trending and left-lateral NE-trending high-angle faults with abundant subhorizontal slickenside lineations. Both the fault orientations and sense of motion are consistent with N-S principal horizontal shortening in a wrench tectonic setting. The faults offset middle Miocene dikes of the Grande Ronde and Wanapum Basalts of the Columbia River Basalt Group, and seem to represent the most recent period of structural deformation. In addition, Nelson [1985], Olbinski [1983] and Parker [1990] have mapped E-striking thrust faults of the same age. The direction of maximum horizontal shortening determined from faulting in this region may be complicated by rotational tectonics. The Grande Ronde and Wanapum Basalts along coastal sites in Oregon have rotated clockwise an average of 22° since their extrusion during the middle Miocene based on paleomagnetism [Wells and Heller, 1988]; therefore, the direction of maximum horizontal shortening at the time of faulting could have been between N22°W and north. This direction is roughly consistent with borehole breakouts from nearby wells.

Figure 4: Stress-orientation indicators for the Pacific Northwest. The symbols denote the type of indicator: earthquake focal mechanism, borehole, or geologic (all Quaternary). The latitude and longitude of each indicator are listed in Table 3. The date, depth, and magnitude for all earthquakes are listed in the comments column of Table 3. The Mt. St. Helens Seismic Zone is outlined by a hachured line that encircles the epicenters of earthquakes used to calculate the direction of $\sigma H_{max}$. The location of the triple junction is from B. C. McPherson [written comm., 1988]. The area shown in Figure 3 is outlined.

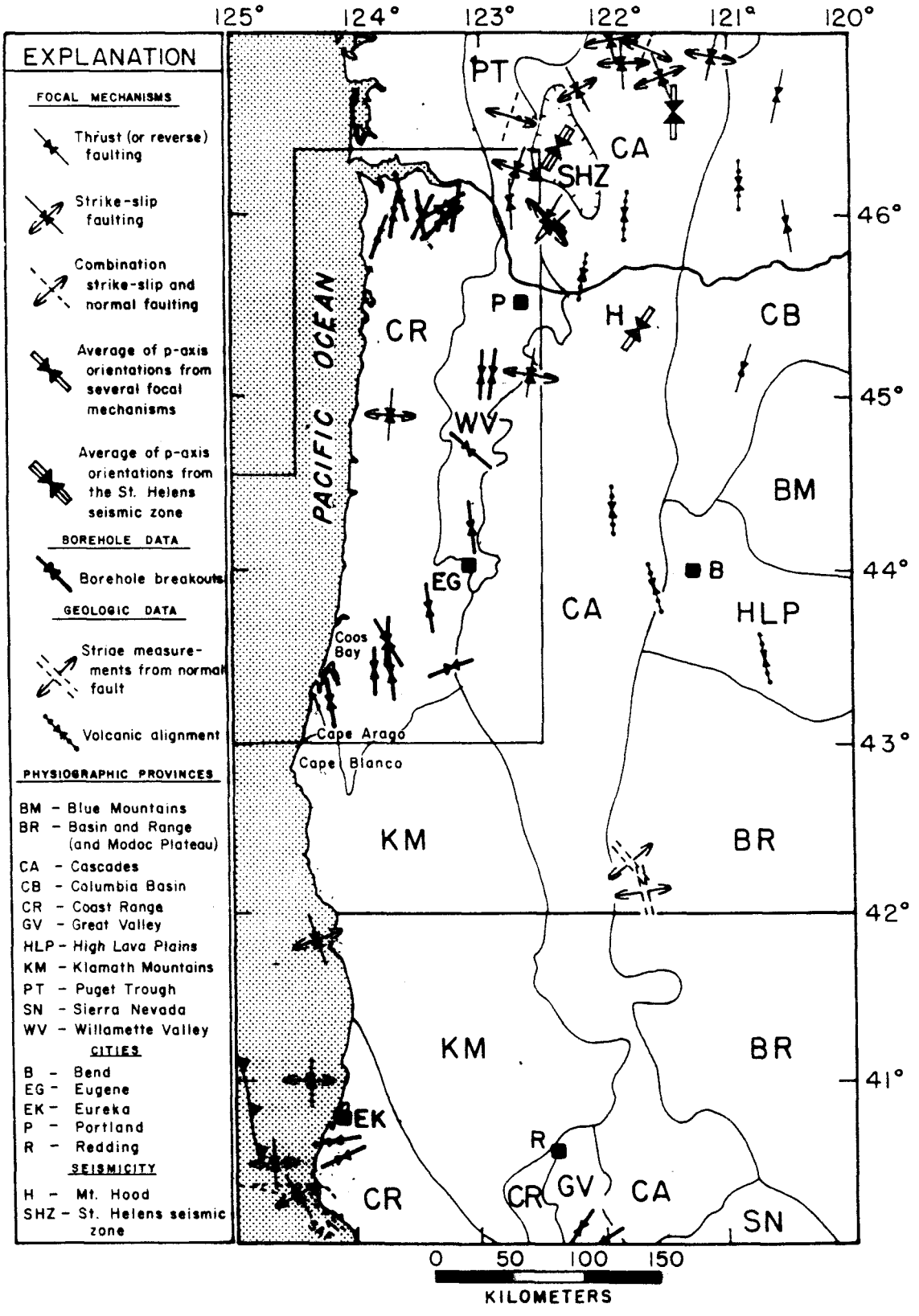
125°
124°
123°
122°
121°
120°
46°
45°
44°
43°
42°
41°
EXPLANATION
FOCAL MECHANISMS
Thrust (or reverse) faulting
Strike-slip faulting
Combination strike-slip and normal faulting
Average of p-axis orientations from several focal mechanisms
Average of p-axis orientations from the St. Helens seismic zone
BOREHOLE DATA
Borehole breakouts
GEOLOGIC DATA
Striae measurements from normal fault
Volcanic alignment
PHYSIOGRAPHIC PROVINCES
BM - Blue Mountains
BR - Basin and Range (and Modoc Plateau)
CA - Cascades
CB - Columbia Basin
CR - Coast Range
GV - Great Valley
HLP - High Lava Plains
KM - Klamath Mountains
PT - Puget Trough
SN - Sierra Nevada
WV - Willamette Valley
CITIES
B - Bend
EG - Eugene
EK - Eureka
P - Portland
R - Redding
SEISMICITY
H - Mt. Hood
SHZ - St. Helens seismic zone
PACIFIC OCEAN
PT
CA
SHZ
CR
P
H
CB
WV
BM
EG
B
CA
HLP
Coos Bay
Cape Arago
Cape Blanco
KM
BR
KM
BR
EK
R
CR
CR
GV
CA
SN
0
50
100
150
KILOMETERS

# MAXIMUM HORIZONTAL STRESS IN THE REGION SURROUNDING WESTERN OREGON

Most of the Pacific Northwest, including western Oregon, is an area of compressional tectonics characterized by crustal earthquakes with strike-slip or thrust focal mechanisms [Zoback and Zoback, 1980; Sbar, 1982]. The direction of maximum horizontal compression determined from focal-mechanism solutions corresponds to the maximum principal stress ($\sigma H_{max}=\sigma_1$). However, much of the southern and central Oregon Cascade mountains are undergoing extensional tectonics based on N-S trending normal faults [Weaver et al., 1981; Macleod and Sherrod, 1988]. The presence of these faults is consistent with the direction of maximum horizontal compression corresponding to the intermediate principal stress ($\sigma H_{max}=\sigma_2$ and $\sigma_1$ is vertical).

Figure 4 shows stress-orientation indicators for northern California, Oregon, and southern Washington. These indicators include the borehole breakout data, earthquake focal mechanisms, volcanic alignments, and slickenside lineations on fault surfaces. The predominant direction of $\sigma H_{max}$ from all indicators is NNW to NNE. Zoback and Zoback [1989] note a slight rotation from a N-S direction of $\sigma H_{max}$ in central Oregon to a NNE direction in southern Washington, based on earthquake focal mechanisms and volcanic alignments. Both the NNW to NNE predominant orientation of $\sigma H_{max}$ and the slight clockwise rotation of $\sigma H_{max}$ toward the north are corroborated by borehole breakouts from this study.

## FOCAL MECHANISMS

Very few earthquake focal-mechanism solutions are available for Oregon due to the paucity of instrumental seismicity, but numerous well-constrained focal mechanisms define the direction of $\sigma H_{max}$ in southwestern Washington (Figure 4). The direction of $\sigma H_{max}$ in Figure 4 determined from earthquake focal-mechanism solutions corresponds to the P axis

(compression axis), which is plotted at 45° from either nodal plane. Error in the direction of $\sigma H_{max}$ as determined by focal mechanisms can be substantial for two main reasons: (1) rock fails at approximately 30° from the greatest principal stress direction in rheological experiments rather than 45°; (2) the rock could fail along a pre-existing fracture not parallel to a plane of maximum shearing stress [Raleigh et al., 1972; Zoback and Zoback, 1980]. The error in directions of $\sigma H_{max}$ for focal mechanisms due to these two factors is no more than 35°-40° [Raleigh et al., 1972]. However, despite this large margin of error for individual indicators and their location in several physiographic provinces, the direction of $\sigma H_{max}$ from earthquake focal mechanisms is fairly consistent (Figure 4).

In western Oregon, a N to NNE orientation of $\sigma H_{max}$ from two strike-slip earthquake focal mechanisms [Bolt et al., 1968; S. D. Malone, unpub. data] agrees with the direction of $\sigma H_{max}$ determined from borehole breakout data, despite the fact that the earthquake foci are >20 km deep and the borehole breakouts are shallower than 3 km (Table 3). Several strike-slip events in the Portland area were not included in Figure 4, because they are poorly constrained. However, the focal-plane solutions for these events are consistent with approximate north-south compression [Dehlinger et al. 1963; Heinrichs and Pietrafesa, 1968; Couch et al., 1968; Yelin and Patton, 1989].

Based on average P-axis orientations, both the Mt. St. Helens seismic zone (SHZ) and Mt. Hood region have anomalous directions of $\sigma H_{max}$. The SHZ is a north-northwest striking linear zone of seismicity in south-central Washington 100 km long with no surface expression of faulting [Weaver et al., 1987]. Earthquakes in the SHZ have primarily right-lateral strike-slip focal mechanisms [Weaver and Smith, 1983]. Ma [1988] determined the mean orientation of the axes of principal stress for the SHZ based on 73 P-axes (Figure 4 shows the area from which earthquakes were used in calculating the direction and plunge of $\sigma_1$). For 55 P axes lying in the northern hemisphere of the focal sphere, $\sigma_1$ = N31°E, plunge 15°, and for 18 P axes lying in the southern hemisphere, $\sigma_1$ = S28°W, plunge 22°. In addition, a similar direction of $\sigma H_{max}$ is obtained from several late Quaternary vents in

Table 3: Stress data is sorted by latitude and corresponds to symbols in Figure 4. The latitude and longitude given for the St. Helens seismic zone corresponds to the location of the symbol shown in Figure 3. The type of indicator is denoted in column 3 [after Zoback and Zoback, 1980]: BO = Breakout; FM(S) = Focal mechanism (single); FM(A) = Focal Mechanism (average of several); G-VA = Geological indicator-volcanic vent alignment, G-FS = Geological indicator-fault slip. The stress regime is denoted in column 4 [after Zoback and Zoback, 1980]: N = Normal faulting ($\sigma_1$ vertical), SS = Strike-slip faulting ($\sigma_2$ vertical), T = Thrust or reverse faulting ($\sigma_3$ vertical). UCSS refers to University of California Seismographic Stations and the UCSS Bull. refers to the Bulletin of the Seismographic Stations of the University of California.

TABLE 3

| LATITUDE | LONGITUDE | sHmax | TYPE | COMMENTS | REFERENCES |
|---|---|---|---|---|---|
| 46.970 | -121.940 | 166° | FM (S) | Date 12/27/85, depth 7.02 km, magnitude 3.0 | Ma [1988] |
| 46.910 | -121.640 | 22° | FM (S) | Date 1/11/84, depth 5.94 km, magnitude 2.2 | Ma [1988] |
| 46.870 | -121.120 | 12° | FM (S) | Date 9/26/82, depth 3.25 km, magnitude 3.4 | Ma [1988] |
| 46.822 | -121.831 | 177° | FM (S) | Mt. Rainier, date 7/18/73, depth 10.9 km, magnitude 3.90 | Crosson and Frank [1975] |
| 46.761 | -121.519 | 159° | FM (S) | Mt. Rainier, date 4/20/74, depth 5.6 km, magnitude 4.80 | Crosson and Lin [1975] |
| 46.695 | -122.200 | 152° | FM (A) | Average of 2 earthquakes. Date 3/30/85, depths 15.98 km and 16.69 km, magnitudes 2.6 and 2.8 | Ma [1988] |
| 46.665 | -120.591 | 13° | FM (S) | Yakima, date 11/14/83, depth ?, magnitude 3.8 | Measured by S. D. Malone [Zoback and Zoback, 1989] |
| 46.574 | -121.408 | 3° | FM (A) | Average of 5 earthquakes. | Ma [1988], Zoback and Zoback [1989] |
| 46.540 | -122.730 | 18° | FM (S) | Date 6/5/83, depth 23.73 km, magnitude 2.3 | Ma [1988] |
| 46.375 | -122.380 | 31° | FM (A) | Average of 73 earthquakes in the St. Helens Seismic Zone. Primarily strike-slip focal mechanisms. | Ma [1988], Weaver and Smith [1983], Zoback and Zoback [1989], Grant and Weaver [1986] |
| 46.240 | -122.690 | 18° | FM (S) | Date 3/13/83, depth 15.40 km, magnitude 2.9 | Ma [1988] |
| 46.180 | -120.900 | 0° | G-VA | Quaternary. | Zoback and Zoback [1989] |
| 46.070 | -122.740 | 176° | FM (S) | Date 7/28/83, depth 15.65 km, magnitude 2.3 | Ma [1988] |
| 46.000 | -121.820 | 3° | G-VA | Quaternary. | Zoback and Zoback [1989] |
| 45.990 | -122.440 | 30° | FM (S) | Date 3/3/82, depth 11.78 km, magnitude 2.1 | Ma [1988] |
| 45.962 | -120.507 | 171° | FM (S) | Date 6/14/81, depth 13.58 km, magnitude 3.20 | S. D. Malone [unpub. data, 1988] |
| 45.942 | -122.411 | 45° | FM (S) | Date 3/11/86, depth 14.84 km, magnitude 3.10 | S. D. Malone [unpub. data, 1988] |
| 45.670 | -122.170 | 8° | G-VA | Quaternary. | Zoback and Zoback [1989] |
| 45.370 | -121.710 | 35° | FM (A) | Average of composites and single event solutions from Mt. Hood area. One normal event, largest event. 10 events total, mainly strike-slip, date 11/77-12/78, depth <15 km, magnitude <2.0 - 3.4 | Zoback and Zoback [1989], Weaver et al. [1982] |
| 45.154 | -120.861 | 18° | FM (S) | Composite focal mechanisms using foreshocks, mainshock and aftershocks from Deschutes Valley, date 4/12/76, depth 15 km, magnitude 4.80 | Couch et al. [1976] |
| 45.121 | -122.596 | 11° | FM (S) | Date 11/22/85, depth 22.89 km, magnitude 3.00 | S. D. Malone [unpub. data, 1988] |
| 44.880 | -123.740 | 3° | FM (S) | Date 3/7/63, depth >20 km, magnitude 5.40 | Bolt et al. [1968], UCSS Bull., 33, no. 1 [1965] |
| 44.350 | -121.930 | 177° | G-VA | North of Three Sisters. Quaternary. | Measured by M. Schiltz [Zoback and Zoback, 1989] |
| 43.900 | -121.600 | 165° | G-VA | South of Three Sisters. Quaternary. | Measured by M. Schiltz [Zoback and Zoback, 1989] |
| 43.500 | -120.700 | 168° | G-VA | Southwest of Newberry Crater. Quaternary. | Measured by M. Schiltz [Zoback and Zoback, 1989] |
| 42.317 | -121.800 | 140° | G-FS | Klamath Falls, Quaternary fault slip, 350 m long normal flt zone exposed in gravel quarry, small component right-lateral slip in addition to dip-slip, 23 striae measurements. | Measured by W. L. Power [Zoback and Zoback, 1989] |
| 42.133 | -121.683 | 167° | G-FS | Merrill, Quaternary fault slip, 100 m long normal fault with small component of right-lateral slip exposed in gravel pit, 4 striae measurements on main fault surface. | Measured by W. L. Power [Zoback and Zoback, 1989] |
| 41.850 | -124.330 | 161° | FM (S) | Date 8/23/62, depth 2.0 km, magnitude 5.60 | Bolt et al. [1968], UCSS Bull., 32, no. 3 [1964] |
| 41.000 | -124.400 | 0° | FM (S) | Date 9/4/62, depth ? km, magnitude 4.90 | Bolt et al. [1968], UCSS Bull., 35, no. 3 [1967] |
| 40.641 | -124.191 | 81° | BO | 'A' quality breakout, 14 elong with S.D.=12.1° Second subset of 4 nearly orthogonal elongations interpreted as drilling-induced hydrofracs with mean sHmax orientation of 45°. | Measured by V. Mount and J. Suppe [Zoback and Zoback, 1989] |
| 40.546 | -124.113 | 65° | BO | 'B' quality breakout, 8 elong with S.D.=20.7° Second subset of 4 nearly orthogonal elongations interpreted as drilling-induced hydrofracs with mean sHmax orientation of 48°. | Measured by V. Mount and J. Suppe [Zoback and Zoback, 1989] |
| 40.500 | -124.700 | 177° | FM (S) | Date 12/10/67, depth 10-20 km, magnitude 5.60 | Bolt et al. [1968], UCSS |
| 40.300 | -124.500 | 149° | FM (S) | Date 7/14/62, depth 10 km, magnitude 5.10 | Bolt et al. [1968], Relocation by UCSS |
| 40.101 | -122.212 | 44° | BO | 'A' quality breakout, 9 elongations with S.D.=12.9°. | Measured by V. Mount and J. Suppe [Zoback and Zoback, 1989] |
| 40.010 | -122.044 | 55° | BO | 'B' quality breakout, 6 elongations with S.D.=15.9°. | Measured by V. Mount and J. Suppe [Zoback and Zoback, 1989] |

the SHZ which are elongated approximately NE [Weaver et al., 1987; Luedke and Smith, 1982; and Evarts et al., 1987].

Weaver et al. [1982] located ten shallow earthquakes (<15 km depth) beneath the slopes of Mt. Hood (Figure 4). The earthquakes primarily had strike-slip focal-mechanism solutions except for one normal focal-mechanism solution, and the earthquake foci may lie along a common NNW-trending structure [Weaver et al., 1982]. The average direction of $\sigma H_{max}$ for the events was N35°E [Weaver et al., 1982].

The average P-axis directions for both the SHZ and Mt. Hood are rotated clockwise with respect to the rest of the Pacific Northwest. In both cases the rotation of P-axes appears to be related to NNW-trending structural zones of weakness, which may locally reorient the direction of $\sigma H_{max}$.

Alternatively, Ma [1988] suggests the direction of $\sigma H_{max}$ may change little through the SHZ or Mt. Hood. If this is the case, the rock in these areas is mainly failing along pre-existing zone of weakness not parallel to a plane of maximum shearing stress. In order to determine the direction of $\sigma H_{max}$, Ma [1988] determined the best-fit regional principal stress directions that are most nearly consistent with all of the observed focal mechanisms [Gephart and Forsyth, 1984; Ma, 1988]. For 73 focal mechanisms in the SHZ with a magnitude of 1.0 to 4.3, Ma [1988] found the best-fitting deviatoric stress tensor to be $\sigma_1$= N6°E, plunge 1°. However, this direction should be regarded with caution, as it differs substantially from the average P-axes direction.

## GEOLOGIC DATA

Two types of Quaternary geologic stress indicators --slickenside lineations and volcanic alignments-- are shown for the Pacific Northwest in Figure 4. The slickenside lineations (measured by W. L. Powers) are from two normal faults in the Oregon Basin and Range province. They indicate a NW to NNW direction of $\sigma H_{max}$ [Zoback and

Zoback, 1989]. The direction of $\sigma H_{max}$ from fault-slip data generally has a standard deviation of ±10°-15° [Zoback and Zoback, 1980].

Oregon and Washington volcanic alignments primarily lie in the Cascade province and are composed of cinder cones [MacLeod and Sherrod, 1986; Zoback and Zoback, 1989], which should reflect the trend of underlying feeder dikes or fissures [Figure 4; Zoback and Zoback, 1980]. Volcanic alignments have been shown to parallel the direction of $\sigma H_{max}$ rather than being controlled by pre-existing structure [Anderson, 1951; Nakamura, 1977; Zoback and Zoback, 1980]. All the alignments in Figure 4, reliable to ± 5°-10°, indicate a N-S direction of $\sigma H_{max}$ [Zoback and Zoback, 1980].

# DISCUSSION

The source for differential horizontal compression in the western United States, particularly the Pacific Northwest, is probably linked to plate interactions. Figure 5 shows the motion of the Pacific plate and Juan de Fuca plate system with respect to North America at 0.5 Ma [Riddihough, 1984]. The Cascadia subduction zone forms the Juan de Fuca system/North American plate boundary and extends from British Columbia to northern California (Figure 1). Scattered late Pleistocene-Holocene Cascade stratovolcanoes as well as Quaternary deformation at Coos Bay and on the Oregon shelf and slope are evidence of recently active subduction. However, there have been relatively few earthquakes in the Benioff zone, particularly beneath Oregon, and no historic low-angle thrust earthquakes between the North American and Juan de Fuca plates [Heaton and Hartzell, 1986; Weaver

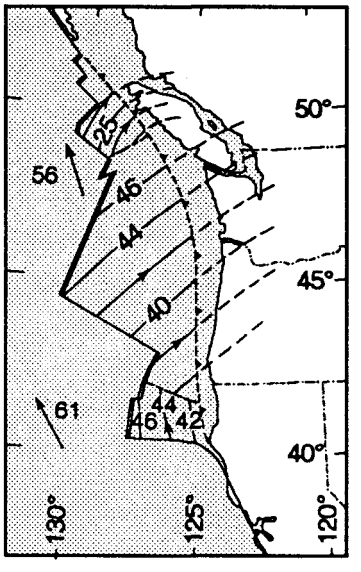


Figure 5: Pacific and Juan de Fuca plate motions relative to the North American plate. The arrows show the motion of the Pacific plate and Juan de Fuca plate system with respect to North America at 0.5 Ma. The motions are based on magnetic anomalies and global solutions for both Pacific/North America and "absolute" (relative to hotspot) motion. The velocities are in millimeters per year. Errors are at least ±7° and ±7 mm/yr [after Riddihough, 1984].

and Baker, 1988]. The relative lack of seismicity along the Cascadia subduction zone can be explained by (1) an unlocked or weakly coupled plate boundary which creeps aseismically, or (2) a locked or strongly coupled plate boundary which is either permanently locked or accumulates stress and fails periodically during great subduction earthquakes.

The direction of plate convergence between the Juan de Fuca and North American plates is approximately N50°E based on the orientation and spacing of 730 ka (Brunhes-Matuyama) and older magnetic-anomaly boundaries [Riddihough, 1977; 1984]. This convergence direction does not appear to have changed much between 6.5 to 0.5 Ma, although the Juan de Fuca's absolute subduction rate decreased 60% [Riddihough, 1984; Spence, 1989]. Typically, in the frontal zones of convergent plate boundaries, the direction of $\sigma H_{max}$ in the overriding plate is parallel to the direction of plate convergence [Nakamura and Uyeda, 1980]. However, the Cascadia subduction appears to be anomalous; the direction of $\sigma H_{max}$ in the overriding plate is generally NNW-NNE rather than N50°E.

To the north and south of the Cascadia subduction zone respectively, the Queen Charlotte and San Andreas faults form the plate boundary between the North American and Pacific plates (Figure 1). These faults play an important role in determining the direction $\sigma H_{max}$ in North America as they comprise >60% of the length of the western North American plate boundary between Mexico and Alaska [Zoback and Zoback, 1989]. The direction of $\sigma H_{max}$ along the San Andreas fault in central California is fairly well constrained by borehole breakouts, earthquake focal mechanisms, hydraulic fracturing in situ stress measurements, and young volcanic alignments. The near-field (within ≈ 100 km of the fault) direction of $\sigma H_{max}$ appears to be controlled by the strength of the fault and is NE, but the far-field direction of $\sigma H_{max}$ is NNE due to the right-lateral shear of the Pacific plate relative to the North American plate [Zoback and Zoback, 1987]. Similarly, the average NNE direction of $\sigma H_{max}$ determined from borehole breakouts in western

Oregon may be due to the right-lateral shear of the Pacific plate relative to the North American plate [Crosson, 1972; Sbar, 1982]. Decoupling of stress across the Cascadia subduction zone may explain the dominant role of right-lateral shear of the Pacific plate relative to the North American plate.

However, several lines of evidence indicate the Cascadia subduction zone is currently locked [Heaton and Hartzell, 1987; Spence, 1989]. Assuming a locked boundary, Spence [1989] argues that the direction of $\sigma H_{max}$ in western Oregon and Washington is due to the northwestward-moving Pacific plate driving into the Gorda and Juan de Fuca plates at the Mendocino and Blanco fracture zones (Figure 1). The westward component of the Pacific plate's motion is accommodated largely by right-lateral strike-slip faulting while the N-S component of compression is transmitted across the fracture zones into the Gorda and Juan de Fuca plates. The N-S direction of $\sigma H_{max}$ is then transmitted from the Juan de Fuca plate across the Cascadia subduction zone into the overriding North American plate. A problem with Spence's [1989] model is the inconsistency between N-S compression in the Juan de Fuca plate, which remains to be shown due to a relative lack of seismicity, and the N50°E convergence direction.

Alternatively, the predominant NNW to NNE orientation of $\sigma H_{max}$ in western Oregon may be due to the landward counterclockwise rotation of $\sigma H_{max}$. The rotation would occur primarily along the boundary between less competent Pliocene-Quaternary sediments of the shelf and slope and competent basement rock of the Oregon Coast Range. E-W shortening along the Oregon and Washington continental shelf and slope (and in Coos Bay) may serve to dampen the E-W component of stress. Most of the shortening occurs in the westernmost 40 km (on the slope and shelf) and rapidly dies out farther east [Adams, 1984]. A N-S direction of $\sigma H_{max}$ would thus characterize the more competent rocks of the plate interior, as indicated by the borehole breakouts and earthquake focal mechanisms in the Oregon Coast Range. Similarly, Nakamura and Uyeda [1980] have suggested that the

compressive stress in arc fronts of other convergent margins may change direction towards the plate interior due in part to internal deformation of the overriding plate.

## CONCLUSIONS

1. Borehole-breakout data in western Oregon are generally consistent with a regional NNW to NNE $\sigma H_{max}$. The NNW orientation of $\sigma H_{max}$ in central western Oregon seems to rotate to NNE in northwestern Oregon and southern Washington, based on borehole breakouts as well as focal mechanisms and volcanic alignments. The mean frequency-weighted azimuth of $\sigma H_{max}$ for all borehole breakouts is 9.7° with a standard deviation of 32.8°. The mean cumulative-length-weighted azimuth of $\sigma H_{max}$ is 13.0° with a standard deviation of 27.8°.

2. The orientation of slickenside lineations on strike-slip faults in the Coast Range of western Oregon is consistent with N-S shortening, whereas the Coos Bay synclinorium and its offshore extension suggest at least some E-W shortening.

3. Focal mechanisms, alignments of volcanic centers, and slickenside lineations in the Pacific Northwest are generally consistent with a regional NNW to NNE direction of $\sigma H_{max}$ with the exception of the Mt. St. Helens seismic zone and Mt. Hood focal mechanisms. The rotation of the average P-axis direction may indicate failure along pre-existing zone of weakness not parallel to a plane of maximum shearing stress or a local reorientation in the direction of $\sigma H_{max}$.

4. Two alternative explanations for the NNW to NNE compression are: (a) the NW-moving Pacific plate drives into the Juan de Fuca plate system and indirectly transmits NNW to NNE compression across a strongly coupled plate boundary into the overriding North American plate [Spence, 1989]; (b) landward counterclockwise rotation of the direction of $\sigma H_{max}$.

# II. STRUCTURE AND TECTONICS OF THE NORTHERN WILLAMETTE VALLEY

## ABSTRACT

The northern Willamette Valley lies on the eastern flank of the broad north-northeast-trending Coast Range structural arch. Eocene to Oligocene marine sedimentary rocks crop out along the western side of the northern Willamette Valley and form a gently eastward dipping homocline. However, beneath the center of the Willamette Valley, Eocene to Oligocene strata are structurally warped up.

During the Late Eocene several major volcanic centers subdivided the Coast Range forearc region into shallow to deep marine basins. Several such volcanic centers occur adjacent to the northern Willamette Valley and are associated with residual gravity anomaly highs and lineations.

The top of basalt in the northern Willamette Valley (middle Miocene Columbia River basalt except near the valley margins) is contoured based on petroleum exploration wells, water wells, and seismic-reflection data. It is structurally downwarped to an altitude of less than -500 m just north of Woodburn. The downwarp is bounded to the south by the NE-trending Waldo Hills range-front fault and in part to the north by the NE-trending Yamhill River-Sherwood fault zone.

The NW-trending Mt. Angel fault extends across the northern Willamette Valley between Mt. Angel and Woodburn and deforms Columbia River basalt and overlying Pliocene and Miocene fluvial and lacustrine deposits. The top of Columbia River basalt is vertically separated, NE side up, roughly 100 m based on seismic-reflection data near Woodburn, and 250+ m based on water-well data near Mt. Angel. The Mt. Angel fault is part of a NW-trending structural zone that includes the Gales Creek fault west of the

Tualatin basin; however, a connection between the Gales Creek and Mt. Angel faults does not occur through Willamette River alluvial deposits.

A series of small earthquakes (6 events with $m_C$ = 2.0, 2.5, 2.4, 2.2, 2.4, 1.4) occurred on August 14, 22, and 23, 1990 with epicenters near the northwest end of the Mt. Angel fault. Routine locations indicate a depth of about 30 km. The preferred composite focal mechanism is a right-lateral strike-slip fault with a small normal component on a plane striking north and dipping steeply to the west.

Both recent mapping of the Mt. Angel fault and the recent seismicity suggest that the Gales Creek-Mt. Angel lineament is similar to the Portland Hills-Clackamas River lineament found to the north. Together, these two lineaments may take up right-lateral strike-slip motions imposed on the upper plate by oblique subduction.

Boring Lava appears to occur extensively in the subsurface of the northeastern portion of the northern Willamette Valley based on seismic data. Many of the faults in the area are interpreted to be largely caused by doming from influx of Boring magma or subsidence associated with evacuation of Boring magma. Such faults occur at Petes Mountain, at Parrett Mountain, along the Molalla River, and possibly near Curtis. The fault along the Molalla River offsets the Pleistocene (?) Rowland Formation 1 m (Glenn, 1965).

# INTRODUCTION

## GEOLOGIC SETTING

The northern Willamette Valley is located in northwestern Oregon between Salem and Portland (Figures 6 and 7). It is part of a N-S trending linear depression, the Willamette-Puget lowland, which extends from Georgia Strait, Washington to Eugene, Oregon (Figure 6). The lowland is bounded on the west by the Oregon Coast Range and on the east by the Cascade mountains.

The Willamette-Puget Lowland has been part of a forearc basin which existed during much of Cenozoic time [Niem and Niem, 1984]. The forearc basin formed in the early middle Eocene, when the Cascadia subduction zone moved from its previous inboard position east of the Coast Range to its current location offshore [Snavely et al., 1968; Niem and Niem, 1984].

## OBJECTIVES

The purpose of the thesis is to:

(1.) Identify structures which may be potential seismic hazards. This thesis represents part of the effort by the Oregon Department of Geology and Mineral Industries (DOGAMI) and the United States Geological Survey (USGS) to evaluate the seismic risk from subduction-zone and intraplate earthquakes in the more populated part of Oregon. Several metropolitan centers including the state capital (Salem) lie within the study area.

(2.) Determine the general structure of the northern Willamette Valley by integrating surface and subsurface data, collected largely during oil and gas exploration in the 1970's and 1980's. The distribution of older structures and strata is important in controlling recent deformation.

(3.) Establish a geologic framework for analyzing ground shaking potential from either subduction zone earthquakes or intraplate earthquakes. The shaking potential should

depend in part on the thickness of unconsolidated sediments overlying Columbia River basalt because the sediment/basalt contact corresponds to a large acoustic impedance contrast.

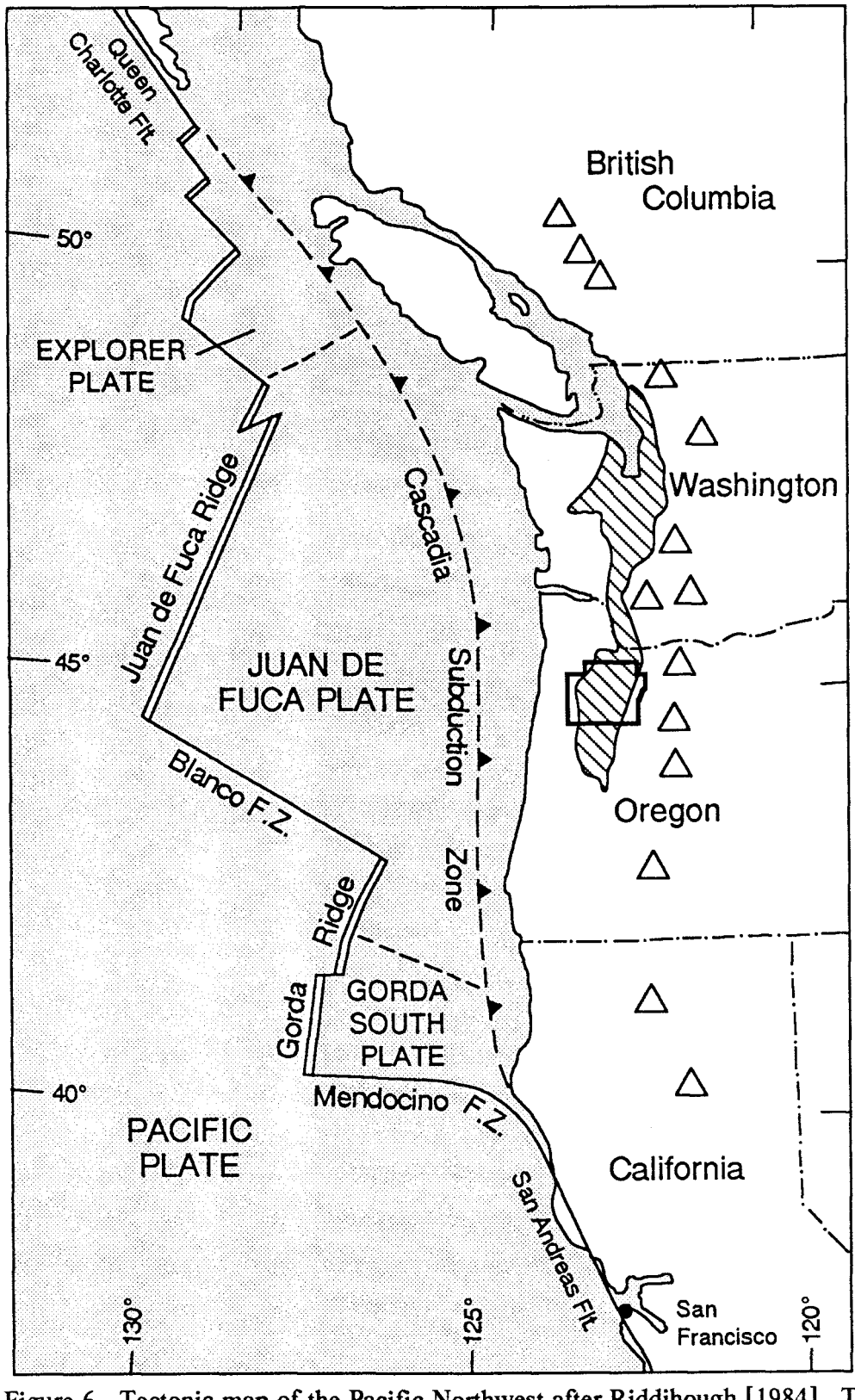


Figure 6. Tectonic map of the Pacific Northwest after Riddihough [1984]. The Willamette-Puget lowland corresponds to the hachured pattern [after Niem and Niem, 1984]. The location of the study area is outlined. Major stratovolcanoes are shown by open triangles.

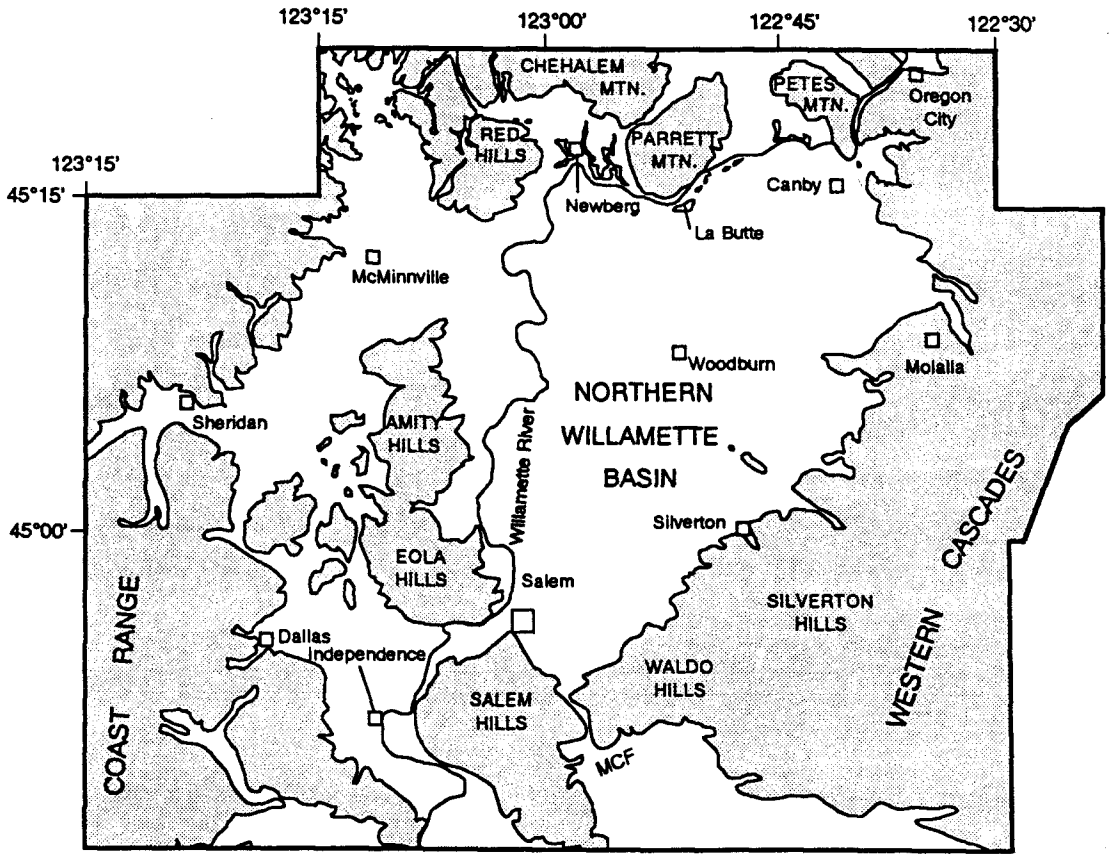


**Figure 7. Map showing the location of the thesis area in northwestern Oregon. Shaded areas correspond to geologic units older than Quaternary.**

# METHODS

## GENERAL STATEMENT

The structure of the northern Willamette Valley was determined using surface and subsurface data. The main contribution of this thesis is the incorporation of subsurface data, which includes previously unreleased seismic-reflection data (interpreted using synthetic seismograms), petroleum exploration wells, and water-well data. In addition, gravity data was filtered to generate residual and regional gravity anomaly maps, which are discussed in the gravity section.

## COMPILATION OF GEOLOGIC MAP

Plates I and II are compilations of geologic source maps onto four U.S. Geological Survey 1:100,000 metric-series maps of the northern Willamette Valley and surrounding area; the description of units, explanation, and index maps are shown in Plate III. The author's contribution extends between the Salem Hills to the south and Oregon City to the north. The Tualatin Valley area of Plate I was compiled by T. Popowski and the southern Willamette Valley area of Plate II was compiled by E. Graven. Air photos and field checking were used to resolve differences in the location of contacts between different source maps. Geologic units are labelled based on age and environment of deposition or lithology to avoid nomenclature problems (i.e. **OEm** = Oligocene and Eocene marine sedimentary rock), although nomenclature has been included as subscripts where unambiguous (i.e. $\mathbf{Mb_{cg}}$ = Miocene basalt; Columbia River Basalt Group, Grande Ronde Basalt). In addition to geologic units, the map shows formation tops in petroleum wells, contours of the altitude of the top of Columbia River basalt, and radiometric age dates from Fiebelkorn et al. [1983] and N. MacLeod [personal communication, 1990].

## SYNTHETIC SEISMOGRAMS

Synthetic seismograms were generated using a program written by J. Shay for the Sun computer system at the Geophysics branch of the College of Oceanography. A synthetic seismogram is an artificial seismic reflection record created by convolving a reflectivity series with a source wavelet. It is used to correlate known horizons in petroleum exploration wells to reflections on seismic reflection lines as shown in Figures 8, 12, and 17.

The reflectivity series for each petroleum exploration well was generated using a sonic log. The sonic log, which measures depth versus slowness of the rock (microseconds per foot), was digitized and converted to depth versus velocity (Figures 8, 12, and 17). Depth versus velocity was in turn converted to a reflectivity series (time versus reflection coefficient), where the reflection coefficient = $(\rho_2V_2-\rho_1V_1)/(\rho_2V_2+\rho_1V_1)$. A density of 2.67 gm/cc was used in determining reflection coefficients for all synthetic seismograms.

Because the energy source for almost all of the seismic reflection lines was Vibroseis, the reflectivity series was convolved with a zero phase source wavelet (0.25 sec. long). A frequency content of 10-55 Hz was used for the zero phase source wavelet, which generally corresponds to the frequency content of the shallow portion of the filtered seismic reflection lines. Synthetic seismograms for each well were also generated using automatic gain control and variable frequency content to allow the best correlation with seismic reflection lines.

## STRUCTURE CONTOUR MAP ON TOP OF BASALT

The structure contour map on the top of basalt is constrained by seismic reflection lines, petroleum wells, water wells, and field mapping of the $Mb_C$/Mu contact (Plates I and II). The map primarily shows the altitude of the top of Columbia River basalt, however,

locally the basalt may be Boring Lava (i.e. near La Butte, Aurora, and Curtis), basalt of Waverly Heights, or Miocene and Oligocene basalt (i.e. north of Marquam).

**Seismic Reflection Control**

Portions of proprietary multichannel seismic reflection lines used to constrain the top of Columbia River basalt are located in Plates I and II and in Figure 9. These seismic reflection lines were collected in the search for petroleum during the 1970's and 1980's. The source used for the seismic lines is generally Vibroseis, although dynamite was used for minor sections of two seismic lines. The seismic lines were generally migrated.

The reflector corresponding to the top of Columbia River basalt was picked using the synthetic seismogram from the DeShazer well, the only well for which the sonic velocity was logged shallow enough in the hole (Figure 8). However, the top of Columbia River basalt can easily be extrapolated from synthetic seismograms of the DeShazer, Werner 34-21, Werner 14-21, and Bagdanoff wells. The reflector corresponding to the top of Columbia River basalt was fairly apparent on all of the seismic lines due to the large acoustic impedance contrast generated by the increase in sonic velocity from Pliocene and Miocene fluvial and lacustrine sediments into underlying Columbia River basalt (Figure 8).

The reflector corresponding to the top of Columbia River basalt was converted from two-way time to depth using an average velocity derived from well control. The average velocity to the top of Columbia River basalt was calculated in six locations where both wells and seismic lines are in close proximity using the following formula:

$$V_a = 2 * D / (T_{2d} \pm (2*d/V_d))$$

D = depth from the ground to the top of Columbia River basalt; $T_{2d}$ = two-way time from the datum (independent for each seismic line) to the reflector; d = the elevation between the datum and ground level; $V_d$ = datum velocity. The average velocity was then contoured for the remaining area of seismic-line coverage (Figure 9). The contour map of average

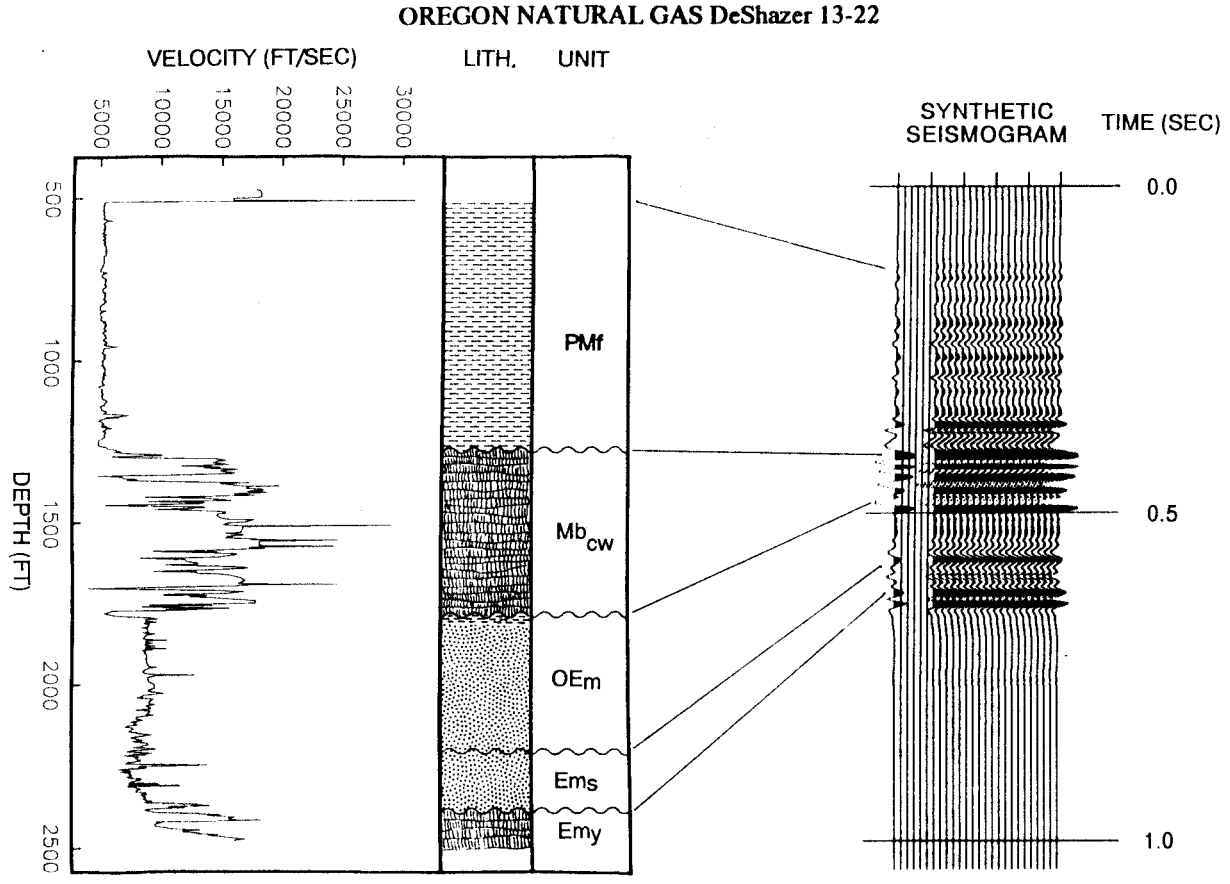


Figure 8. Synthetic seismogram of the DeShazer 13-22 well. The high velocity interval at the top is due to the casing, and was removed for the synthetic seismogram. PMf = Pliocene and Miocene fluvial and lacustrine sediments; $Mb_{cw}$ = Miocene Columbia River Basalt Group, Wanapum Basalt; OEm = Oligocene and Eocene marine strata; $Em_s$ = Eocene marine Spencer Formation; $Em_y$ = Eocene marine Yamhill Formation.

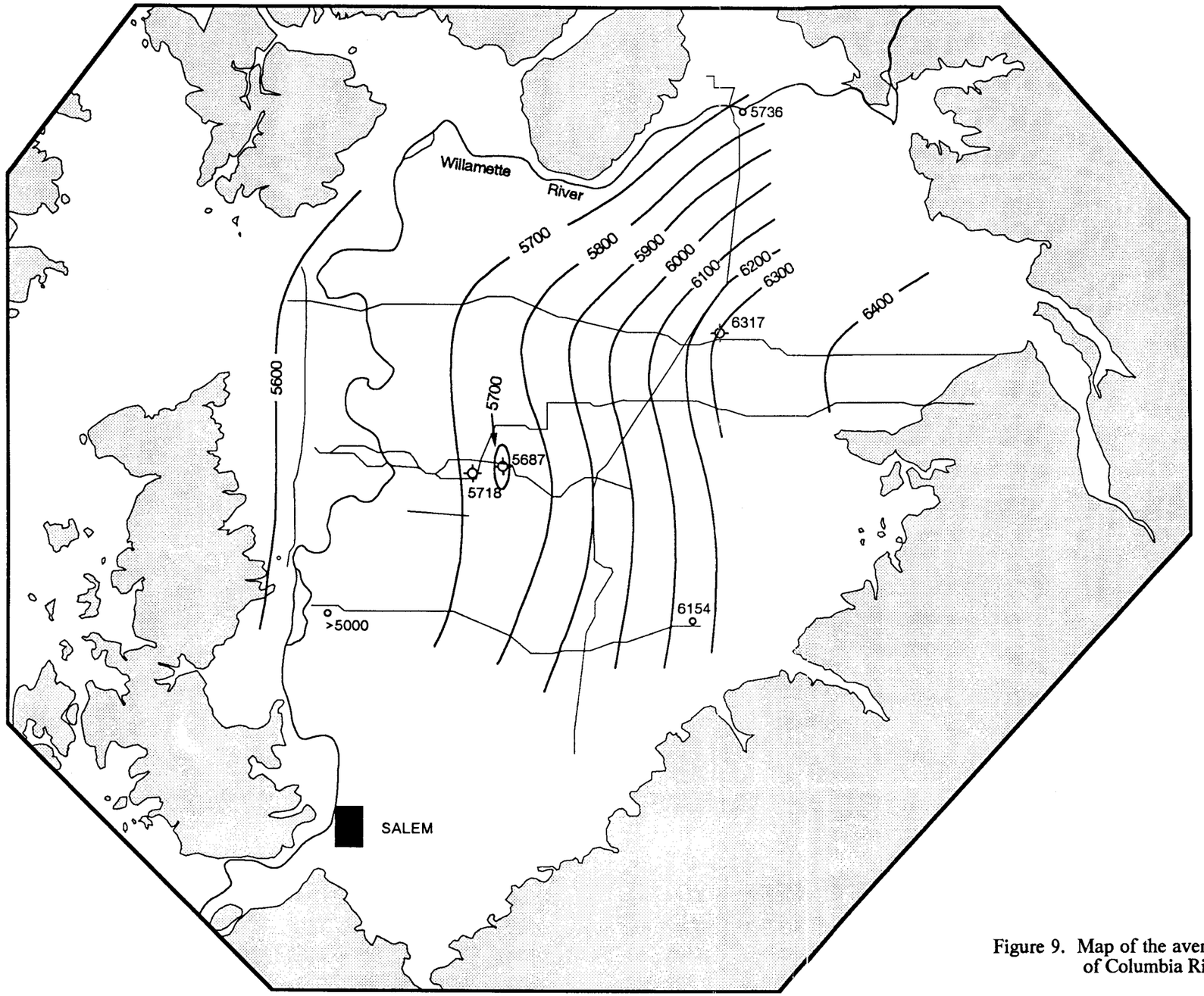


EXPLANATION

- Contact between Quaternary alluvium or terraces and shaded bedrock
- Contoured average velocity to the top of Columbia River Basalt in ft/sec.
- Seismic reflection line
- Petroleum exploration well
- Water well

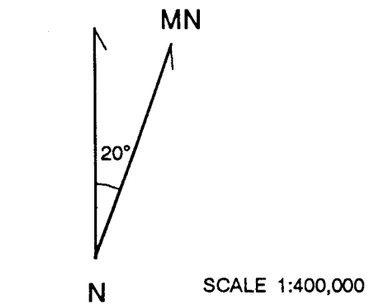


SCALE 1:400,000

0 10

Kilometers

Figure 9. Map of the average velocity from ground level to the top of Columbia River basalt. Refer to text for explanation.

velocity is poorly constrained, but the average velocity appears to increase eastward towards the Cascades and towards the center of the northern Willamette basin (due in part to thicker Pliocene and Miocene sediments which should be more compacted towards the base).

The one-way time from the ground to the reflector corresponding to the top of Columbia River basalt was determined using the following formula:

$$T_{1g} = [\, T_{2d} - (2 * d / V_d)] / 2$$

The altitude to the top of Columbia River basalt was then determined using the following formula:

$$A_{Mb_c} = A_s - (T_{1g} * V_a)$$

where As = altitude of the surface of the earth.

**Water-Well Data**

Water-well data were used to determine the altitude of the top of Columbia River basalt near the margins of the northern Willamette basin. The source for water-well data is either ground-water reports from the Oregon Water Resource Department or individual water-well reports (Plates I and II).

The ground-water reports used in this study include Price [1961], Hampton [1963], Price and Johnson [1965], Price [1967a, b], Frank and Collins [1978], and Leonard and Collins [1983]. Well locations based on ground-water reports have been field checked by the Oregon Water Resource Department. Altitudes for a given well were determined from the appropriate ground-water report.

Individual water-well reports are available at the Water Resources Division in Salem. Only those water wells located to the quarter-quarter section were used as data

points, except for a few wells in flat areas. Well locations were not field checked. Altitudes were determined from 7 1/2' quadrangle topographic sheets.

The top of basalt was picked in water wells based on the occurrence of hard rock, i.e. "basalt", "black rock", "hard rock", "broken rock", or "decomposed rock". Therefore, the top Columbia River basalt determined from water-well data should roughly correspond to the acoustic impedance contrast on seismic reflection lines. However, the true top of weathered Columbia River basalt (or base of overlying fluvial and lacustrine sediments), which commonly corresponds to the top of a "red clay" or "sandstone", may actually occur at a higher altitude.

**Contact Between $Mb_C$ and Mu**

In the Waldo and Silverton Hills, the contact between Columbia River basalt ($Mb_C$) and overlying Miocene units (Mu) which cap high ridges was used to contour the top of Columbia River basalt. The contours reflect the eroded top of Columbia River basalt prior to deposition of Neogene formations, but do not reflect Quaternary downcutting by streams. The contact between Columbia River basalt and the overlying Miocene unit has an angular discordance of 2°-4° in places [Hampton, 1972].

In the southwestern Waldo Hills, contours were inferred by assuming a thickness of Columbia River basalt of 70 m and extrapolating upward from the altitude of the base of Columbia River basalt. Because of variation in thickness of Columbia River basalt, contours are poorly constrained in that area.

# STRATIGRAPHY

Simplified stratigraphic sections for the western and eastern portions of the northern Willamette Valley are shown in Figure 10. The discussion of stratigraphy follows the time scale of Salvador [1981] and Armentrout et al. [1983].

Subsurface well correlations are based largely on electric logs, mud logs, and the biostratigraphic reports of McKeel [1984; 1985]; dipmeter and sonic logs were also consulted. The biostratigraphic reports of McKeel [1984; 1985] contain information on age and paleobathymetry determined using foraminiferal assemblages found in well cuttings. McKeel [1984; 1985] and McWilliams [1968, 1973] assigned benthic foraminiferal assemblages (a few planktonic fossil occurrences were also used) to the California stages of Kleinpell [1938], Schenck and Kleinpell [1936], and Mallory [1959]. The absolute age range of each benthic foraminiferal stage shown in Figure 10 is based on Armentrout et al. [1981]. However, because the foraminifera may be time-transgressive between California and Oregon, the absolute ages assigned to each benthic foraminiferal stage in Figure 10 are not well constrained. McKeel [1984, 1985] classified the paleobathymetry using the benthic marine zones shown in Figure 11.

## SILETZ RIVER VOLCANICS

The Siletz River Volcanics were first named and described by Snavely and Baldwin [1948] based on exposures along Siletz River and its tributaries in the central Oregon Coast Range. The volcanics form the basement rock of the Oregon Coast Range, reaching a thickness of 3,660+ m [Armentrout et al., 1983], and they extend eastward beneath the Willamette Valley [Niem and Niem, 1984; Keach, 1986; EMSLAB, 1988]. They consist largely of tholeiitic submarine pillow lava and breccia, locally capped by alkalic basalt [Snavely et al., 1968]. In the Sheridan-McMinnville area, the Siletz River Volcanics are composed of vesicular basalt flows and pillow basalt, flow-breccia, and tuff breccia with

A.

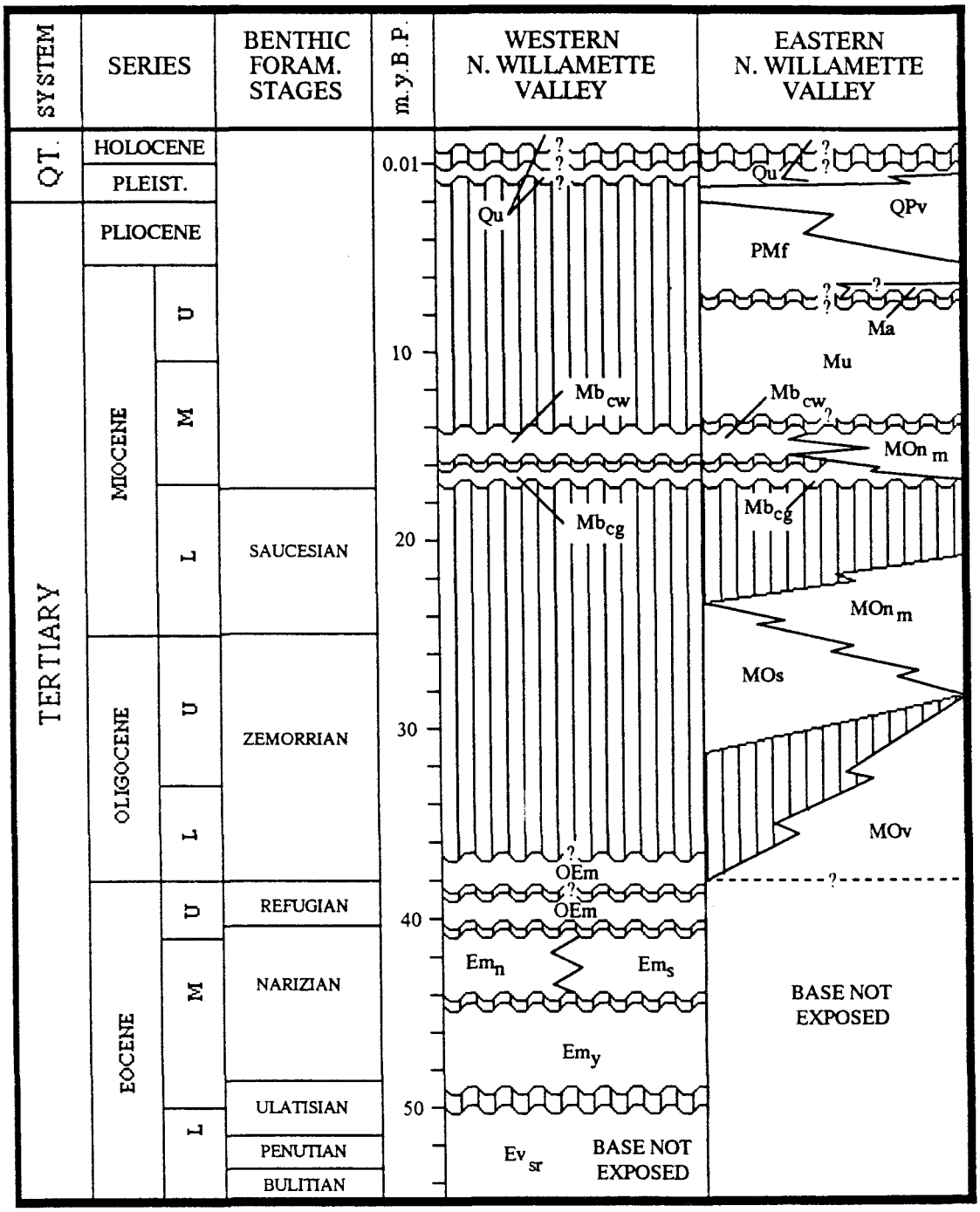


Figure 10. Generalized stratigraphic column for the western and eastern portions of the northern Willamette Valley. Portions of the stratigraphic column are after Armentrout et al. [1983] and Miller and Orr [1988]. A.) Stratigraphic column shows unit abbreviations as on Plates 1, 2, and 3. B.) Stratigraphic column shows commonly used unit names.

B.

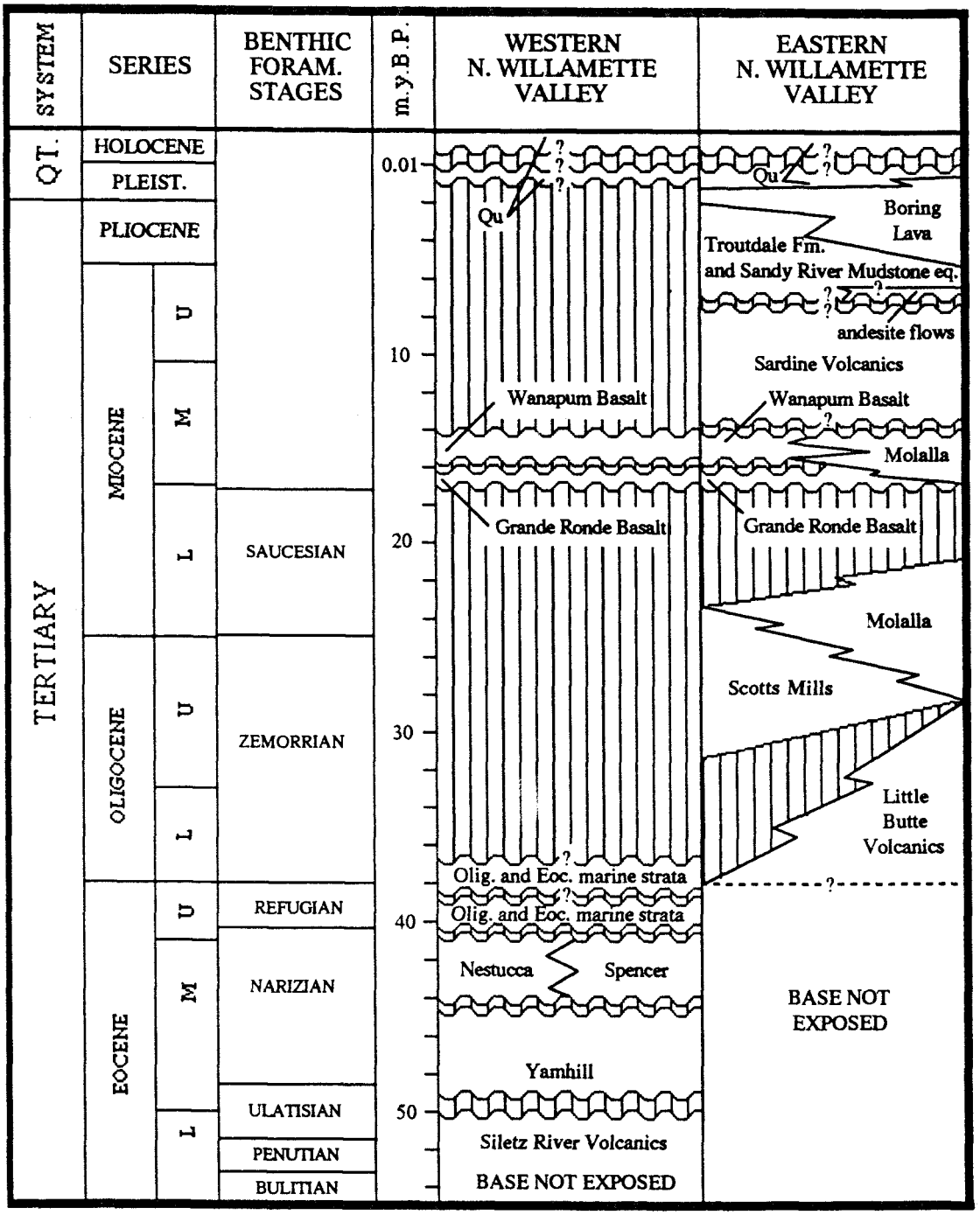


Figure 10 continued

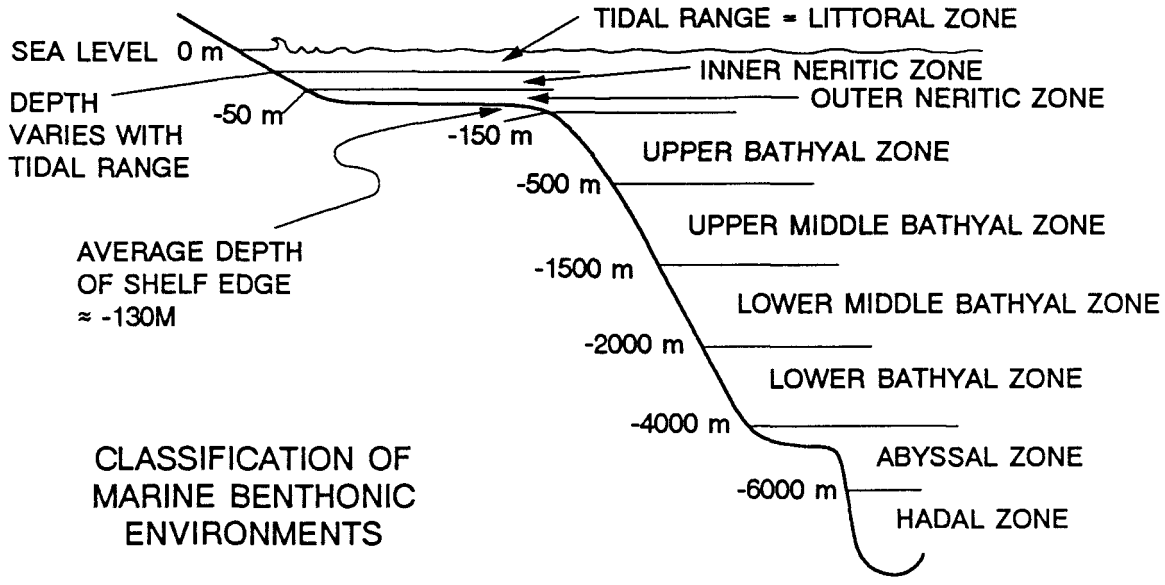


Figure 11: Classification of marine benthonic environments in terms of maximum depth of each benthonic marine zone in the modern ocean. Modified after Ingle [1980].

red to green calcareous sandy tuff [Baldwin et al., 1955; Brownfield, 1982a]. The unit is pervasively zeolitized and veined with calcite [Wells et al., 1983]. Intercalated sedimentary rock, in part correlative to the Kings Valley Siltstone, is included in the upper Siletz River Volcanics. The sedimentary rock is composed of medium- to dark-gray, calcareous tuffaceous shale, siltstone, and sandstone [Baldwin et al., 1955; Brownfield and Schlicker, 1981a; Brownfield, 1982a].

The Siletz River Volcanics are thought to be part of a seamount chain generated on the Farallon plate by the Yellowstone hotspot or along leaky transform faults and then accreted to the North American continent prior to deposition of the Tyee Formation of middle Eocene age [Snavely and MacLeod, 1977; Duncan, 1982; Wells et al., 1984]. Alternatively, they may have erupted during oblique rifting of the continental margin possibly related to the Yellowstone hotspot [Wells et al., 1984]. The oblique rifting model is currently favored because of the chemical character of the basalts, the North American provenance of intercalated sedimentary rock including conglomerates, and field relations suggesting the Coast Range province was connected to North America at its southern and northern ends during deposition of the Siletz River Volcanics [Parrish et al., 1990].

The age of crystallization of the Siletz River Volcanics, based on K-Ar dates, ranges between 50.7±3.1 to 58.1±1.5 Ma [Duncan, 1982]. The age of outcropping, intercalated sedimentary rock included within the upper Siletz River Volcanics is estimated as Penutian and Ulatisian as defined by Mallory [1959] [Snavely et al., 1968; McWilliams, 1980].

**Subsurface Data**

In the northern Willamette Valley, only the Bruer and Finn wells appear to have drilled into the upper portion of the Siletz River Volcanics (Plate 1; Figure 14). The Siletz River Volcanics in the Bruer well consist of 300+ m (977+ ft) of "volcaniclastics", volcanic breccia, and red and green tuff. The Siletz River Volcanics in the Finn well

consist of 1,110+ m (3,651+ ft) of gray tuffs and tuffaceous shale, siltstone, and sandstone.

Foraminiferal assemblages from well cuttings indicate the intercalated sedimentary strata is lower Narizian to Ulatisian. However, the two lower Narizian picks from the Bruer well are questionable. No lower Narizian foraminifera are reported in outcrops of the Siletz River Volcanics. The lower Narizian picks may be the result of downhole sloughing from the overlying Yamhill Formation. The foraminiferal assemblages from the Finn well range in age from Ulatisian (undifferentiated) to upper Ulatisian, and range in paleodepth from lower middle bathyal to tropical inner neritic [McKeel, 1984].

Figure 12 shows a synthetic seismogram for the Siletz River Volcanics in the Bruer well. The sonic velocity increases downward at the top of the Siletz River Volcanic sedimentary rock (4550 ft) and again sharply at the top a the "volcanic breccia" (4690-4755 ft). The synthetic seismogram shows a medium-amplitude reflection corresponding to the top of the Siletz River Volcanic sedimentary rock, and a high positive/negative amplitude couple associated with the volcanic breccia.

Figure 13 shows an E-W trending seismic line along the west side of the Willamette Valley (refer to Figure 14 for its location). Intercalated volcanic and sedimentary rock at the top of Siletz River Volcanics appears to correspond to a series of high-amplitude, discontinuous reflectors. Based on field observations, Brownfield [1982a] notes that the upper surface of the Siletz River Volcanic sequence appears "irregular" due to volcanism, tectonism, and erosion. Similarly, offset seismic reflectors suggest a laterally discontinuous distribution of volcanics and sedimentary rock, faulting, and/or erosion.

## YAMHILL FORMATION

The Yamhill Formation ($Em_y$) was first named by Baldwin et al. [1955] for exposures at its type locality along Mill Creek, a tributary of the Yamhill River (Plate I). The Yamhill Formation disconformably overlies the Siletz River Volcanic sequence

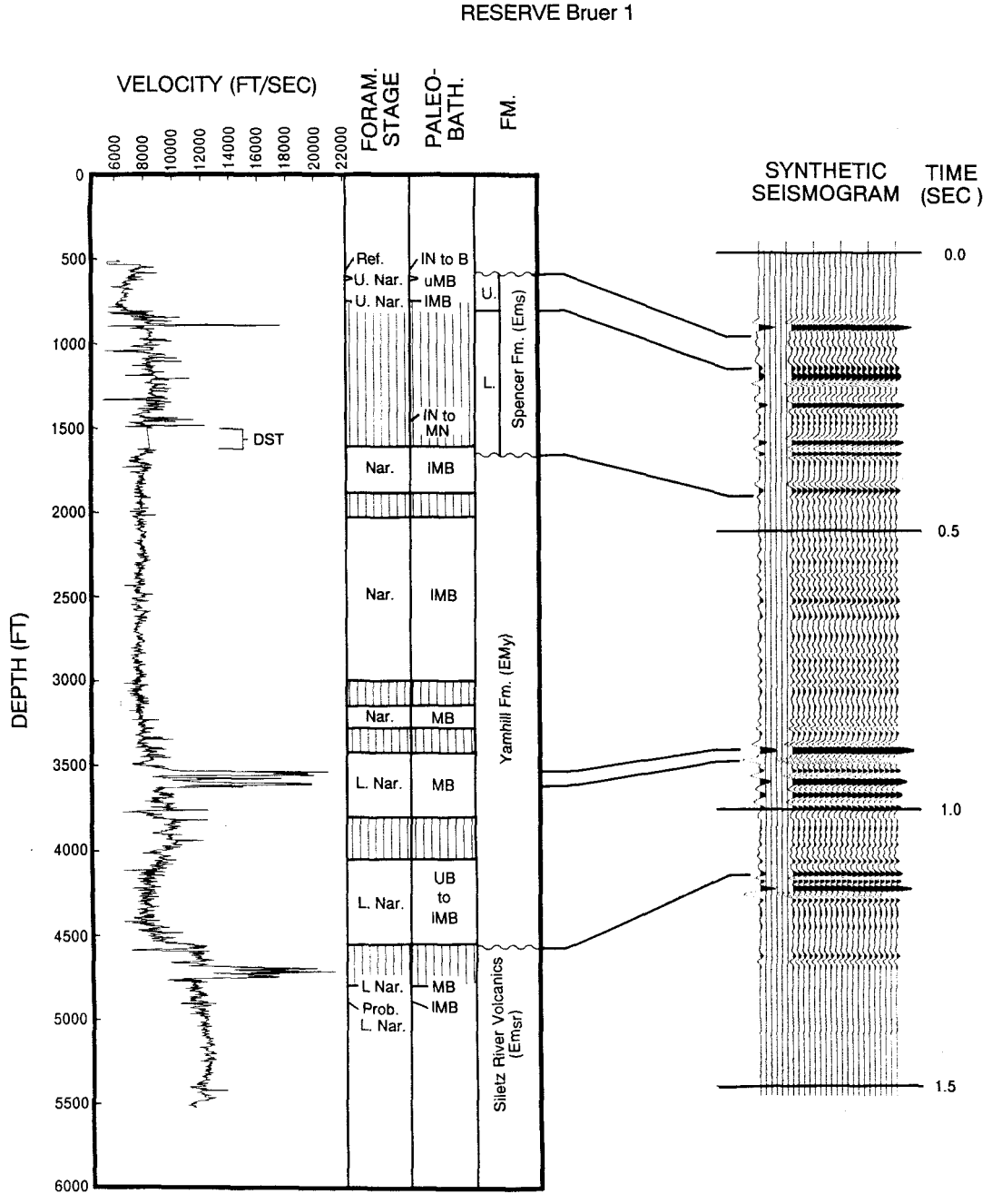


Figure 12. Synthetic seismogram of the Bruer 1 well. The drill stem test (DST) washes out the borehole resulting in very low sonic velocities. In order to avoid producing a reflection corresponding to the drill stem test interval, the velocity was kept constant. The high velocity between 3530-3630 ft corresponds to "basalt", ie. a flow or sill. The foraminiferal stages are abbreviated as follows: Ref. = Refugian; U. Nar. = upper Narizian; Nar. = Narizian, undifferentiated; L. Nar. = lower Narizian; Prob. L. Nar. = probable lower Narizian. The paleobathymetry is abbreviated as follows: IN = inner neritic; MN = middle neritic; B = bathyal; uMB = upper middle bathyal; lMB = lower middle bathyal. The biostratigraphy is from McKeel [1984].

A.

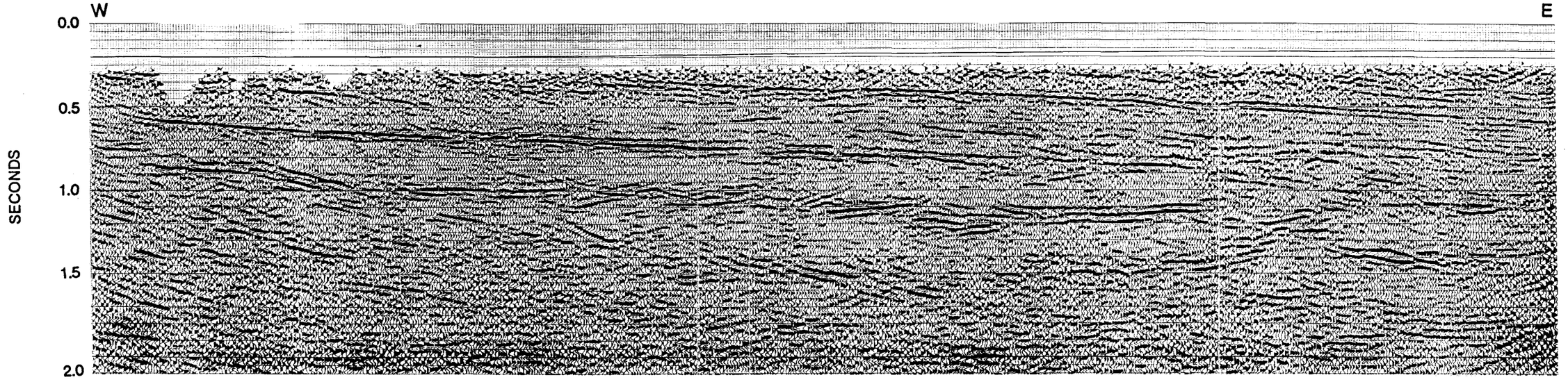


B.

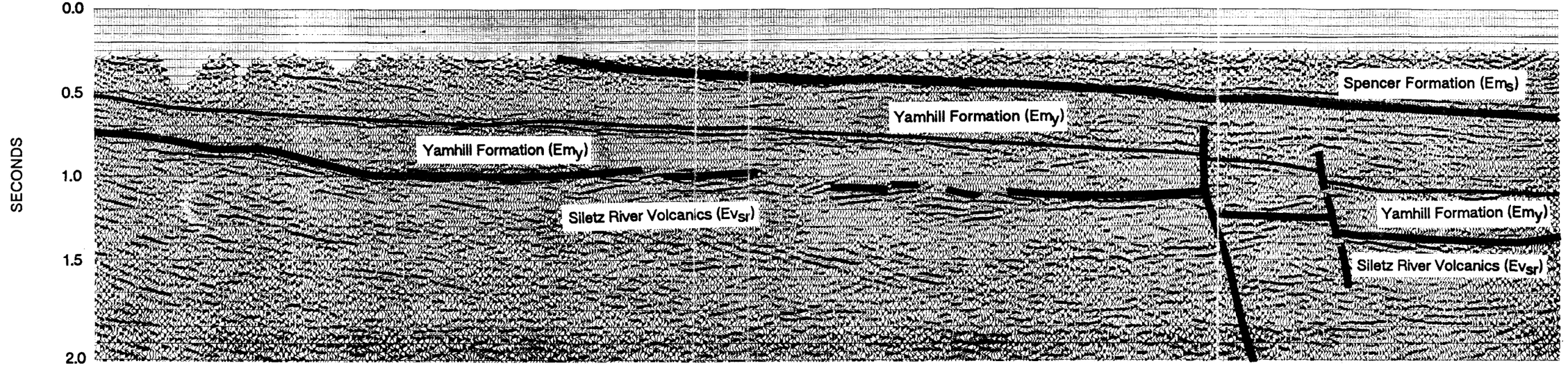


Figure 13. E-W seismic reflection line across the Amity Hills. Location of line shown in Figure 14. The reflections above the Spencer/Yamhill Formation contact do not correspond entirely to Spencer Formation, but also include Oligocene and Eocene sedimentary rock and perhaps some Columbia River basalt.

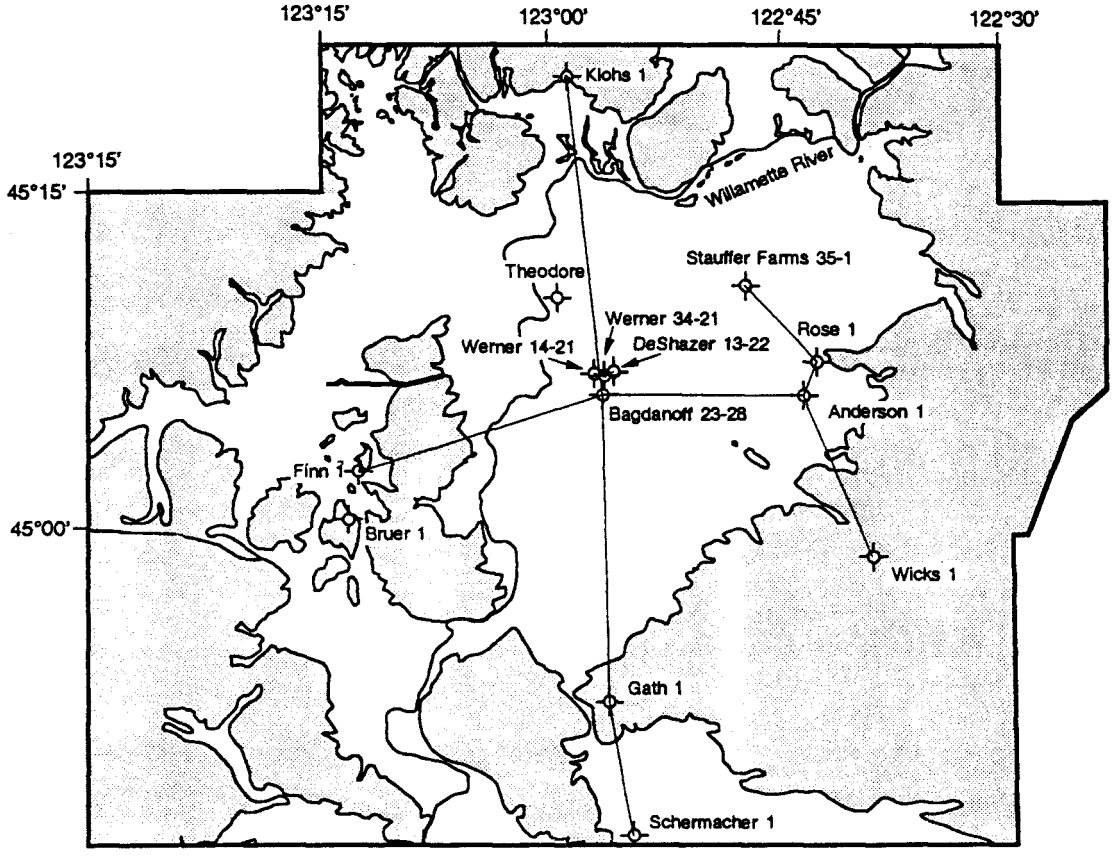


**Figure 14. Location map for seismic line (thick line) shown in Figure 13 and well correlation sections.**

[Armentrout et al., 1983]. The bulk of the Yamhill Formation in the northern Willamette Valley is composed of micaceous, carbonaceous, tuffaceous mudstones and siltstones [Brownfield, 1982a], and is a possible source rock for hydrocarbons [Armentrout and Suek, 1985]. The Yamhill Formation has been divided into several members in the subsurface of the southern Willamette Valley, however, it remains undifferentiated in the northern Willamette Valley due to the lack of the coarser grained middle member (refer to following Subsurface Data section).

Molluscan fauna of the Yamhill Formation are late Eocene in age [Baldwin et al., 1955]. The Yamhill Formation contains abundant foraminifera, and it has been assigned to the Ulatisian to upper Narizian based on foraminiferal assemblages collected along its type section [D. McKeel, personal communication to T. Berkman, 1987]. The Yamhill does not appear to be age equivalent to the upper Narizian Hamlet formation in Clatsop and Tillamook counties, although they are lithologically similar. The Hamlet formation is a 200-900 m thick marine sequence of *upper Narizian* mudstone, siltstone, sandstone, and basal basaltic conglomerate underlying the Cowlitz Formation [Rarey, 1986; Berkman, 1990]. The Cowlitz Formation correlates to the Spencer Formation of the northern Willamette Valley. The upper Yamhill Formation does not appear to correlate to the Hamlet Formation based on stratigraphic relationships to the Tillamook Volcanics in addition to limited biostratigraphic data. The Hamlet Formation overlies Tillamook Volcanics (which are dated at about 44 Ma [Wells et al., 1984]) [Berkman, 1990], whereas the Yamhill Formation appears to underlie the Tillamook Volcanics in the McMinnville-Sheridan area [Wells et al., 1984]. Furthermore, benthic foraminiferal age control in the Bagdanoff well indicates the upper Yamhill Formation is lower Narizian, not upper Narizian.

**Subsurface Data**

The Yamhill Formation thickens eastward from 885 m in the Bruer well and 830 m in the Finn well to 932+ m in the Bagdanoff well (Figure 15). Much of the eastward thickening occurs across NNE(?)-trending normal faults discussed in the structure section.

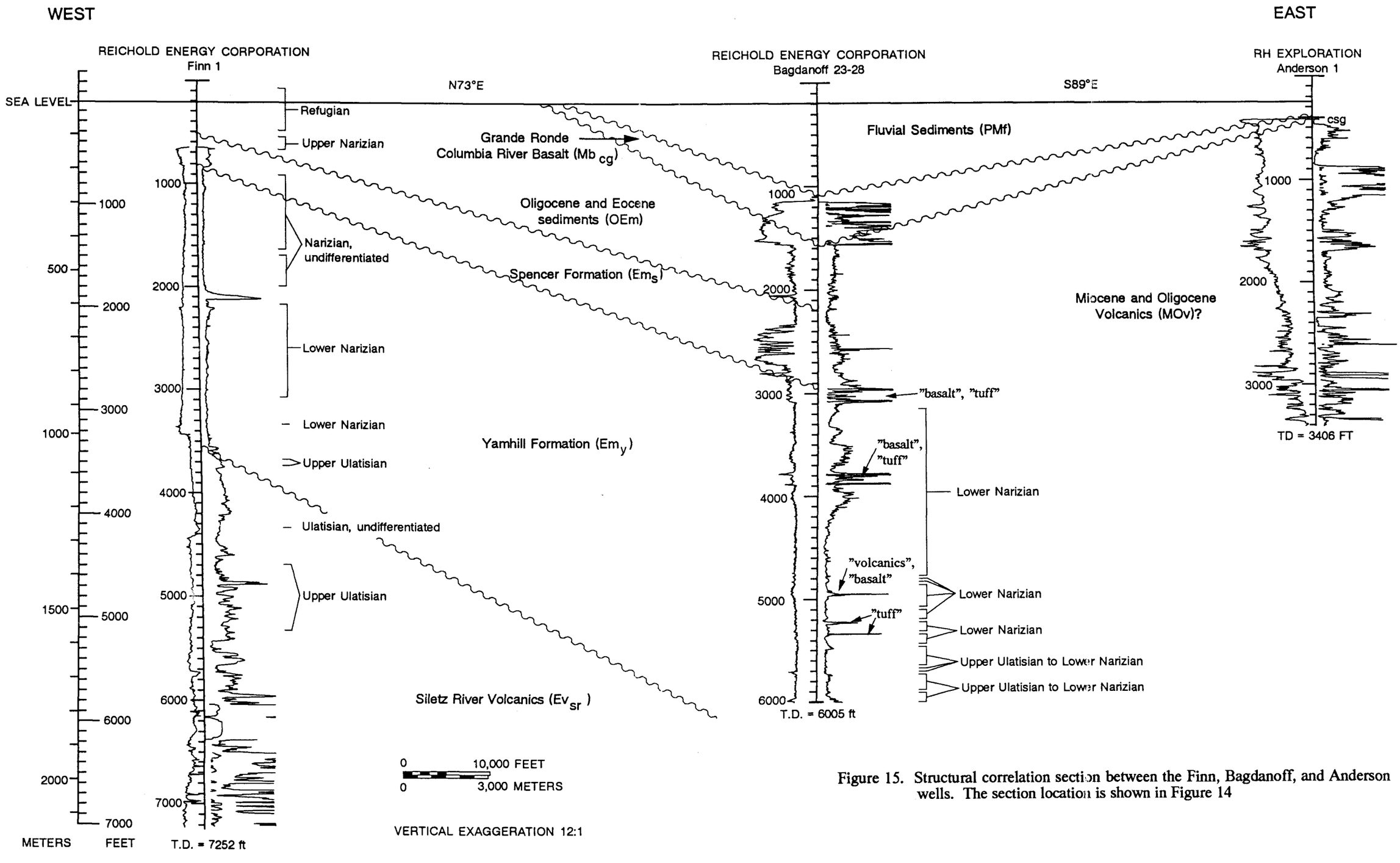


Figure 15. Structural correlation section between the Finn, Bagdanoff, and Anderson wells. The section location is shown in Figure 14

The Klohs, Bagdanoff, and Gath wells all reach the Yamhill Formation, but not the underlying Siletz River Volcanics (Figure 16). In the Bruer and Finn wells located along the western side of the valley, the Yamhill Formation is composed largely of claystone and siltstone with minor fine-grained sandstone and tuffaceous sedimentary rock. The Bruer well also has a 9 m-thick basalt sill (?) (at 3530 ft) and a 9 m thick volcaniclastic bed (at 3600 ft). To the east, the Bagdanoff well encountered several sills or volcanic and volcaniclastic layers.

In the subsurface of the southern Willamette Valley, the Yamhill Formation is composed of upper and lower mudstone units separated by the Miller sandstone, which is composed of interbedded sandstone and siltstone [Bruer et al., 1984; Baker, 1988; Graven, 1991]. However, the Miller sandstone is absent in the subsurface of the northern Willamette Valley, although locally interbedded calcareous, fossiliferous, basaltic sandstone is present [Brownfield, 1982a]. The Miller sandstone largely pinches out into Yamhill siltstone and mudstone north of the Merrill and Gath wells [Figure 16; Baker, 1988]. The northwestward abrupt decrease in thickness of the Miller Sandstone appears to be controlled by the Corvallis fault and possibly the Waldo Hills lineation (refer to Structure section).

Volcanics interfinger with the Yamhill Formation to the east as seen in wells located near Woodburn. The volcanics consist of basalt and tuff, and they are the earliest indication from wells in the northern Willamette Valley of possible western Cascade calcalkaline volcanism. Alternatively, the volcanics may be coming from the Challis volcanic arc. The age of the lowest basalt and tuff unit in the Bagdanoff well (3780 ft to 3885 ft) is lower Narizian as constrained by bracketing foraminiferal assemblages (Figure 15). Larger amounts of volcaniclastic and volcanic rock of Yamhill age are present in the southern Willamette Valley indicating that volcanism in the western Cascade calcalkaline arc may have started by 45-48 Ma [Baker, 1988; Graven, 1991]. Previously, Lux [1982]

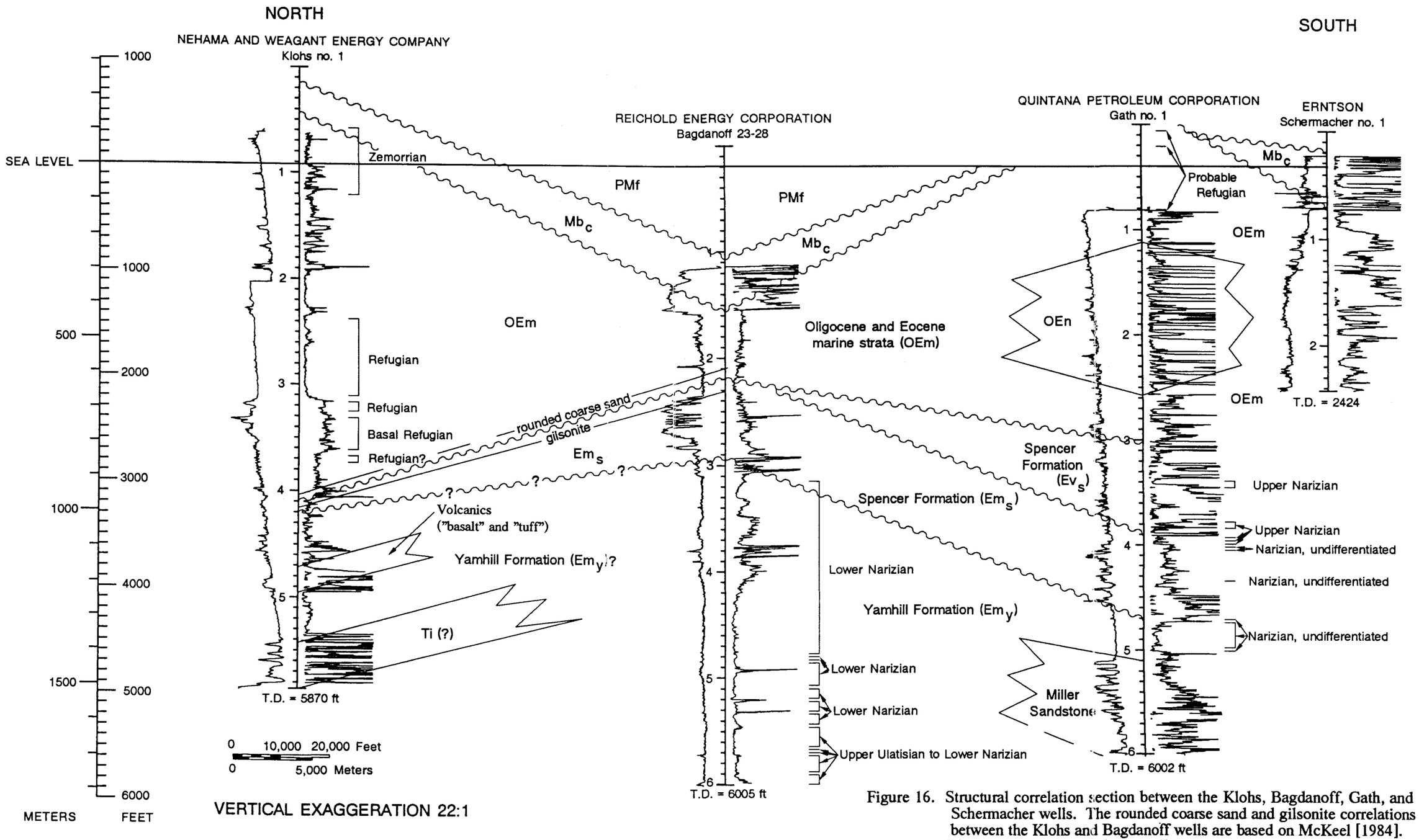


Figure 16. Structural correlation section between the Klohs, Bagdanoff, Gath, and Schermacher wells. The rounded coarse sand and gilsonite correlations between the Klohs and Bagdanoff wells are based on McKeel [1984]. The section location is shown in Figure 14.

concluded that volcanism in the Cascade Range started at roughly 42 Ma, based only on surface exposures.

Foraminiferal assemblages from well cuttings indicate a lower Narizian to upper Ulatisian-lower Narizian age for the Yamhill Formation. The Bagdanoff well in the center of the northern Willamette Valley has the older (?) lower Narizian to upper Ulatisian Foraminiferal assemblage.

The beginning of Yamhill deposition corresponded to a drastic change in the paleobathymetry from shallow marine faunas to bathyal water depths [McKeel, 1985]. Most of the Yamhill Formation in the northern Willamette Valley was deposited in bathyal marine water depths [McKeel, 1984; 1985]. The Yamhill Formation shallows upward from middle bathyal to outer neritic depths in the Bagdanoff well. Further west, the Yamhill Formation is middle to upper bathyal in the Bruer well and lower to middle bathyal in the Finn well [McKeel, 1984].

The Yamhill Formation can be divided into two seismic facies at the Bruer and Finn wells. The lower facies of the Yamhill Formation is characterized by low-amplitude reflectors (due to a homogeneous lithology and constant sonic velocity) (Figures 12 and 17). High-amplitude reflections correspond to intercalated volcanics in the Bruer well or a well-cemented sandstone (?) in the Finn well (Figure 17). The upper facies of the Yamhill Formation is characterized by medium-amplitude reflections. Low velocity tuffaceous sedimentary rock in the upper Yamhill Formation tends to have low sonic velocities which probably results in the medium-amplitude reflections.

The seismic line in Figure 13 (and an unpublished synthetic seismogram by the author for the Bagdanoff well) indicate that both seismic facies of the Yamhill Formation are characterized by higher amplitude reflectors to the east. Increasing amplitude may be due to an increasing number of coarser-grained volcaniclastic interbeds as well as more intercalated volcanics. Both coarsening sediment and more volcanics are evident in Figure

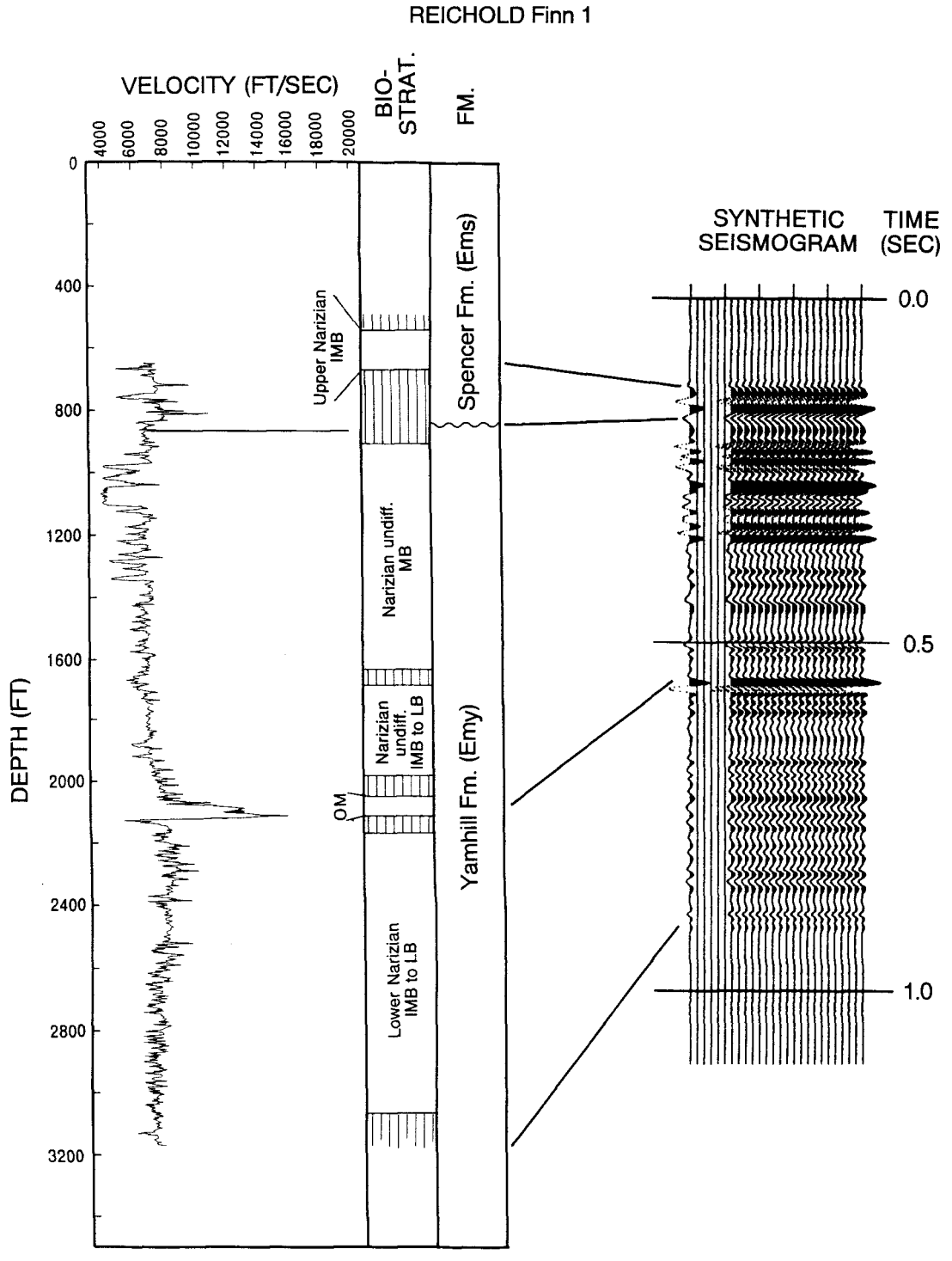


Figure 17. Synthetic seismogram of the Finn 1 well. The Spencer Formation extends up to 515 ft. The paleobathymetry is abbreviated as follows: OM = open marine; MB = middle bathyal; lMB = lower middle bathyal; LB = lower bathyal. The biostratigraphy is from McKeel [1984].

15, which shows generally higher resistivities in the upper Yamhill Formation at the Bagdanoff well than in the Finn well.

The transgressive lower Yamhill Formation onlaps the Siletz River Volcanics in a westerly direction (left side of Figure 13). The onlapping relationship of lower Yamhill bathyal mudstone and siltstone indicates a relative submarine high of Siletz River Volcanics (and possibly Tillamook Volcanics) to the west during the lower Narizian. Furthermore, the upper portion of the Yamhill Formation downlaps eastward onto the volcanic (?) unit. The downlap is consistent with eastward progradation of basaltic terrigenous sediments from a western highland. The western source must have been a volcanic high of Siletz River Volcanics and/or Tillamook Volcanics. Several subaerial highlands in the Coast Range were present by late Eocene time [Snavely and Wagner, 1963].

## EOCENE BASALT OF WAVERLY HEIGHTS AND ASSOCIATED UNDIFFERENTIATED SEDIMENTARY ROCKS

The Eocene basalt of Waverly Heights and associated undifferentiated sedimentary rocks ($Ev_{wh}$), was originally included by Trimble [1963] as part of the Skamania Volcanic Series. Recently, Beeson et al. [1989b] renamed the unit based on exposures at Waverly Heights in the Portland metropolitan area. Exposure in Plate I is restricted to a small area along the Willamette River near Oregon City. In this area, the basalt (subaerial) and associated undifferentiated sedimentary rocks dip 35° to the east, whereas the overlying Columbia River basalt dips only 9° [Schlicker, 1953; Schlicker and Finlayson, 1979]. As suggested by Trimble [1963] and Beeson et al. [1989b] and supported by the presence of a large gravity high, the Waverly Heights basalt unit is probably quite thick and may represent part of an oceanic island (analogous to the Siletz River Volcanics). Two flows of the Waverly Heights Basalt have K-Ar ages of approximately 40 Ma [R. Duncan, personal communication, 1982, to Beeson, 1989].

## NESTUCCA FORMATION

The Eocene Nestucca Formation ($Em_n$) was originally named and described by Snavely and Vokes [1949]. It appears to overlie the Yamhill Formation and Siletz River Volcanics with angular unconformity [Snavely and Vokes, 1949; Baldwin et al., 1955; and Armentrout et al., 1983]. In addition, Wells et al. [1983] indicate the presence of possible Tillamook Volcanics underlying the Nestucca Formation north of Sheridan. The Nestucca Formation is correlative to the Hamlet formation [Wells et al., 1983; Berkman, 1990], and is partially a correlative, but deeper water facies, of the Spencer Formation [Baldwin, 1981; Armentrout et al., 1983].

The Nestucca Formation is composed of thin bedded tuffaceous mudstone and siltstone and thin-bedded basaltic sandstone intercalated with basaltic debris flows, pillow basalt, breccia, and tuff [Baldwin et al., 1955]. It was deposited in a basin which extended west from McMinnville. The Nestucca Formation is 610+ m (2000+ ft) thick in the Sheridan-McMinnville area [Baldwin et al., 1955], whereas the shallow water equivalent Spencer Formation is 100 m thick in the Finn well. The basin possibly formed in part due to structural control involving downdropping along the Yamhill River fault.

W. Rau [written communication to Wells et al., 1983] assigned foraminiferal assemblages in siltstone of the Nestucca Formation to the upper Narizian Stage of Mallory [1955]. The Nestucca Formation does not occur in any petroleum exploration wells in the Willamette Valley.

## SPENCER FORMATION

The Eocene Spencer Formation ($Em_S$) was named by Turner [1938] for beds along Spencer Creek west of Eugene. It has been mapped along the western side of the Willamette Valley from Eugene northward to Gales Creek and is the southern equivalent of the Cowlitz Formation [Baker, 1988]. The Spencer Formation overlies the Yamhill

Formation with angular unconformity. It consists of two members: a lower member composed primarily of micaceous arkosic sandstone, and an upper member composed of deeper marine siltstone and mudstone [Baker, 1988]. The sandstones in the Spencer Formation are a potential reservoir for oil and gas. American Quasar briefly produced gas from the Spencer Formation in the Hickey 9-12 well in the southern Willamette Valley.

The lower member of the Spencer Formation was deposited in a shelf to nearshore environment [Baker, 1988] and formed a strandline-deltaic unit in the Willamette Valley [Snavely and Wagner, 1964; Niem and Niem, 1984]. Locally, coals occur in the Spencer Formation [Al-Azzaby, 1980]. Foraminiferal assemblages from the Spencer Formation correspond to the upper Narizian stage [McWilliams, 1968, 1973; McKeel, 1980, 1984].

**Subsurface Data**

The thickness of the Spencer Formation is highly variable due largely to an overlying angular unconformity (Figure 18). Based on surface outcrops, the Spencer Formation thins northward from 760 m near Dallas to 490 m in Yamhill and Washington counties [Baker, 1988]. Similarly, in the subsurface the Spencer Formation appears to thin northward from 525 m in the Gath well to 30 m in the Klohs well (age control is poor, Figure 16). It appears to thin eastward from 325 m thick in the Bruer well, to 230 m thick in the Bagdanoff well, and 45 m thick in the DeShazer well. Minor pyroclastics and sills or basalt flows interfinger with the Spencer Formation to the southeast. The Gath well contains a large section of Eocene volcanics of Spencer age.

The Eola-Amity hills area appears to have been a relative high during deposition of the Spencer Formation. In the Bruer well, the Spencer Formation is coarser grained than in wells to the east and southeast, indicating uplift [Baker, 1988]. The Spencer Formation in the Bruer well is also coarser grained (and thinner) than equivalent Nestucca Formation to the north.

Several petroleum exploration wells were drilled in the center of the basin targeting a pinchout of the Spencer Formation. The Werner 34-21 well showed gas in the lower

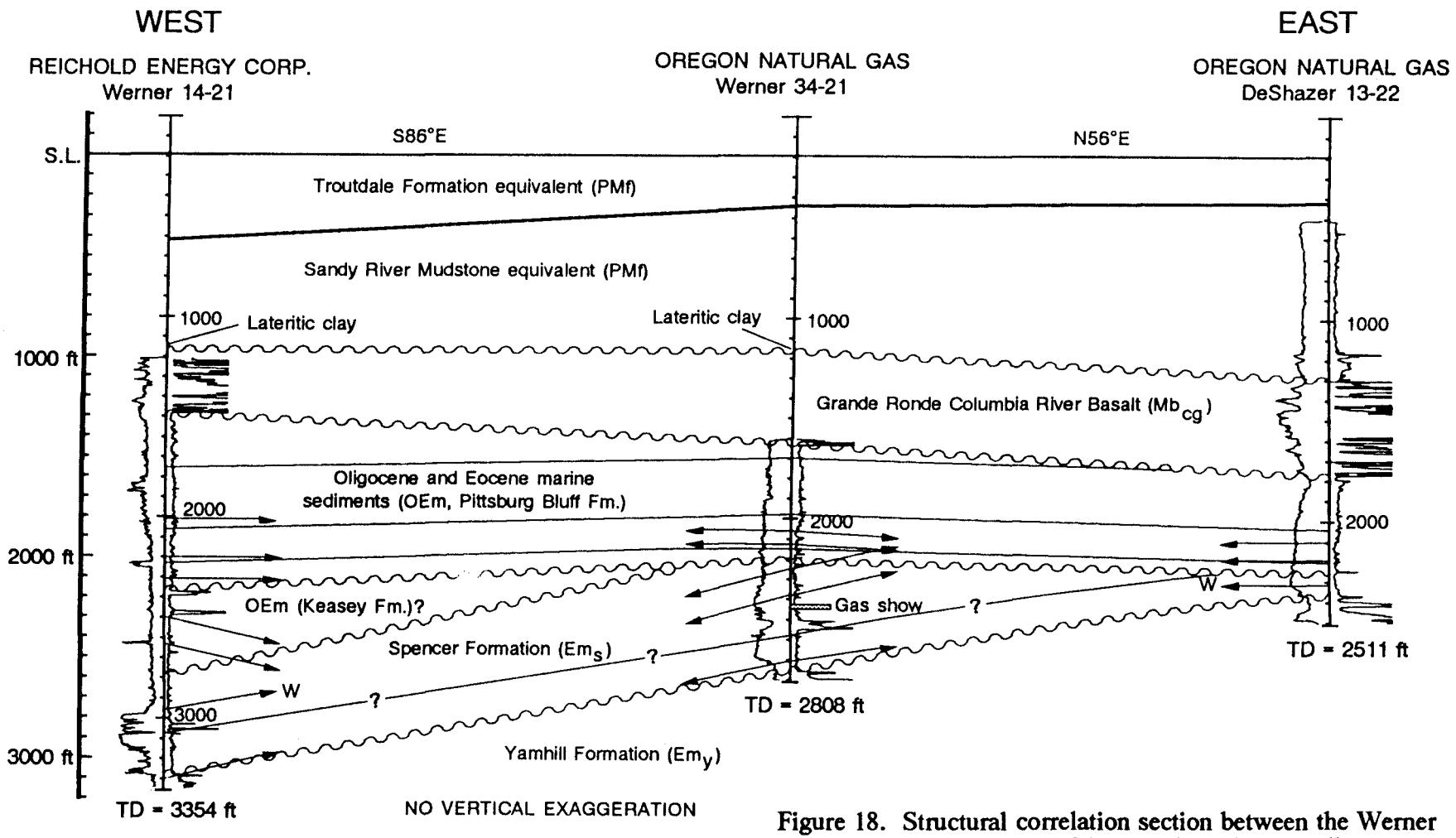


Figure 18. Structural correlation section between the Werner 14-21, Werner 34-21, and DeShazer wells. W indicates a weak dip determination. The section location is shown in Figure 14.

sandstone member of the Spencer Formation (Figure 18). The angular unconformity between the sandstone member of the Spencer and overlying clay of OEm appears to have formed the seal.

Foraminiferal assemblages from the Spencer Formation in the Finn, Bruer, and Gath wells indicate an upper Narizian age (almost all of the constraining fossil assemblages occurred in the upper Spencer member). The lower member was deposited in a neritic to marginal marine-nonmarine setting based on foraminiferal assemblages from the Bruer and Bagdanoff wells [McKeel, 1984]. The upper member was deposited at middle to upper bathyal depths based on foraminiferal assemblages in the Finn, Bruer, and Gath wells [McKeel, 1984].

The synthetic seismogram from the Bruer well indicates the upper member of the Spencer Formation in that area is fairly homogeneous and has only low-amplitude reflectors (Figure 12). The lower member of the Spencer Formation is characterized by several medium- to high-amplitude reflectors, which correspond to contacts between interbedded sandstone and siltstone.

## OLIGOCENE-EOCENE MARINE SEDIMENTARY ROCKS

Oligocene and Eocene marine strata (OEm) unconformably overlie the Spencer Formation. In the southern Willamette Valley, OEm corresponds to the Eugene Formation. To the north, OEm can be divided into two units, although they remain undifferentiated along the Amity and Eola Hills due to poor exposure [Baldwin et al., 1955; Brownfield and Schlicker, 1981a; Bela, 1981]. Both units contain abundant volcanic clasts consistent with the presence of an active calcalkaline volcanic Cascade arc to the east.

The lower unit is a sandy, tuffaceous siltstone correlated to the Keasey Formation to the north [Brownfield and Schlicker, 1981a, b]. McWilliams [1968, 1973] assigned the foraminiferal assemblage in this unit to the Refugian and the upper Narizian stages [McWilliams, 1968, 1973; Brownfield and Schlicker, 1981a]. Baldwin et al. [1955] noted

an angular unconformity along the Eola-Amity Hills between strata of middle and early Oligocene age. Similarly, Van Atta [personal communication, 1989] believes the contact between the Keasey Formation and overlying shallower marine Pittsburg Bluff Formation to the north is slightly unconformable.

The upper unit is correlated to the Pittsburg Bluff Formation. The Pittsburg Bluff Formation, late Eocene-Oligocene in age, extends as far south as the Sheridan-McMinnville area along the base of the Amity Hills and Chehalem Mountains [Beaulieu, 1971; Baldwin, 1981]. The upper unit may correlate in part to the middle Oligocene Illahe formation of Brown [1951]. The upper unit is composed of fine- to coarse-grained, tuffaceous sandstone and siltstone [Brownfield and Schlicker, 1981a, b], and was probably deposited in a shallow embayment sheltered by the Coast Range to the west [Baker, 1988]. Marine deposition shifted northward during Oligocene (Zemorrian) to early Miocene (Saucisian) time [Snavely and Wagner, 1963; Peck et al., 1964].

**Subsurface Data**

Oligocene-Eocene marine sedimentary strata reach a thickness of about 715 m (2350 ft) in the Amity-Eola Hills based on mapping [Brownfield, 1981a]. The Bruer and Finn wells spud in OEm and fail to constrain its thickness. In the center of the northern Willamette Valley, the thickness of OEm is highly variable due largely to an angular unconformity within the formation as well that with the overlying Columbia River basalt (Figure 18).

Well log correlations in the center of the Willamette Valley appear to confirm the presence of an angular unconformity within OEm (Figure 18). In the Woodburn area, the upper unit is characterized by well-defined shallow dips, and is relatively easy to correlate using resistivity curves, which indicates the beds are laterally continuous. The upper unit appears to have a lignite or coal bed at its base in the DeShazer well. The lower unit dips as much as 15° and is missing from the DeShazer well.

Age constraints based on benthic foraminifera from the Gath and Schermacher wells indicate that some of the strata previously mapped as MOs (Scotts Mills Formation) in the western Waldo Hills are actually OEm (Plate II). The Gath well has probable Refugian age determinations as shallow as 15 m below ground level (Figure 16, Mckeel [1984]). Microfauna in the Schermacher well were possibly lower-middle Oligocene based on work done by the Gulf Oil Corporation. The thickness of OEm in these two wells is 915 m and >520 m respectively. A 440 m thick volcanic unit bracketed by upper Narizian and Refugian foraminiferal assemblages is present in the Gath well (Figure 16) and may be equivalent to the Fisher Formation in the southern Willamette Valley. The thickness of volcanics relative to nearby wells suggests a possible nearby source (i.e. vent complex) generated in late Eocene time (refer to Gravity section).

## TERTIARY INTRUSIVE ROCKS

Numerous intrusions occur in the Coast Range west of the northern Willamette Valley, some associated with faults. They occur in every unit cropping out along the western Willamette Valley (from $Ev_{Sr}$ to OEm), and are particularly abundant west of McMinnville within the Nestucca and Yamhill Formations. Intrusions are largely absent between Sheridan and Dallas (they do not occur in the Finn or Bruer wells), which indicates the intrusive rocks south of Dallas probably have a different source. The intrusive rocks north of Sheridan, primarily sills and some dikes, are composed of aphanitic to coarse-grained basalt and diabase [Wells et al., 1983; Brownfield,1982a, b]. They range in age from middle Eocene to middle Miocene [Wells et al., 1983].

Large bodies of intrusive rocks in the Coast Range obtain thicknesses of 150+ m [Baldwin et al., 1955]. Further east, the Klohs well drilled through 135+ m of basalt/gabbro in the Nestucca Formation, which may be a sill (Figure 16). A gravity high associated with the outcropping intrusive rocks suggests a possible source body at depth (refer to Residual Gravity Anomaly Highs).

Small intrusions occur east of the northern Willamette Valley along Butte Creek in Miocene and Oligocene sedimentary strata (Scotts Mills Formation; Plate 1). These intrusions are composed of fine- to medium-grained basalt and deuterically altered basaltic andesite [Miller and Orr, 1984a]. The intrusive rocks appear to be Miocene in age [Hampton, 1972; Miller and Orr, 1984a]

## MIOCENE AND OLIGOCENE VOLCANIC AND SEDIMENTARY ROCK

Miocene and Oligocene undifferentiated volcanic and sedimentary rocks (MOu) are the oldest exposed in the Western Cascades (Figure 10). MOu corresponds to the Little Butte Volcanics of Peck et al. [1964] and Hampton [1972], excluding the Molalla Formation or tuffs of the Molalla River area. The Little Butte Volcanic Series was first mapped by Wells [1956] in the Medford quadrangle and extended northward by Peck et al. [1964]. It is chiefly composed of ash-flow tuffs, debris flows, lava flows, and epiclastic mudstone and volcaniclastic sandstone, with some distinctive siliceous, iron-rich tholeiitic lavas interbedded in the upper part [Priest et al., 1983]. In the study area it includes the Breitenbush Series of Thayer [1939], and the pre-Butte Creek lavas of Harper [1946]. Based on mapping by Hampton [1972], MOu has been differentiated into a porphyritic andesite unit (MOa) and an olivine basalt, basaltic andesite, and volcanic breccia unit (MOb). MOu contains volcanic and sedimentary facies which appear to have complex overlapping and intertonguing relationships as shown schematically by Sherrod and Smith [1989] in Figure 19.

The location of vents indicates that the Oligocene to middle Miocene axis of volcanism was probably in the western Cascade physiographic province, although some vents may lie farther east beneath the cover of High Cascade lavas [Priest et al., 1983]. One Oligocene to middle Miocene vent lies within the study area roughly 5 km south of Molalla based on the local abundance of dikes and coarse rubble breccia [Peck et al.,1964].

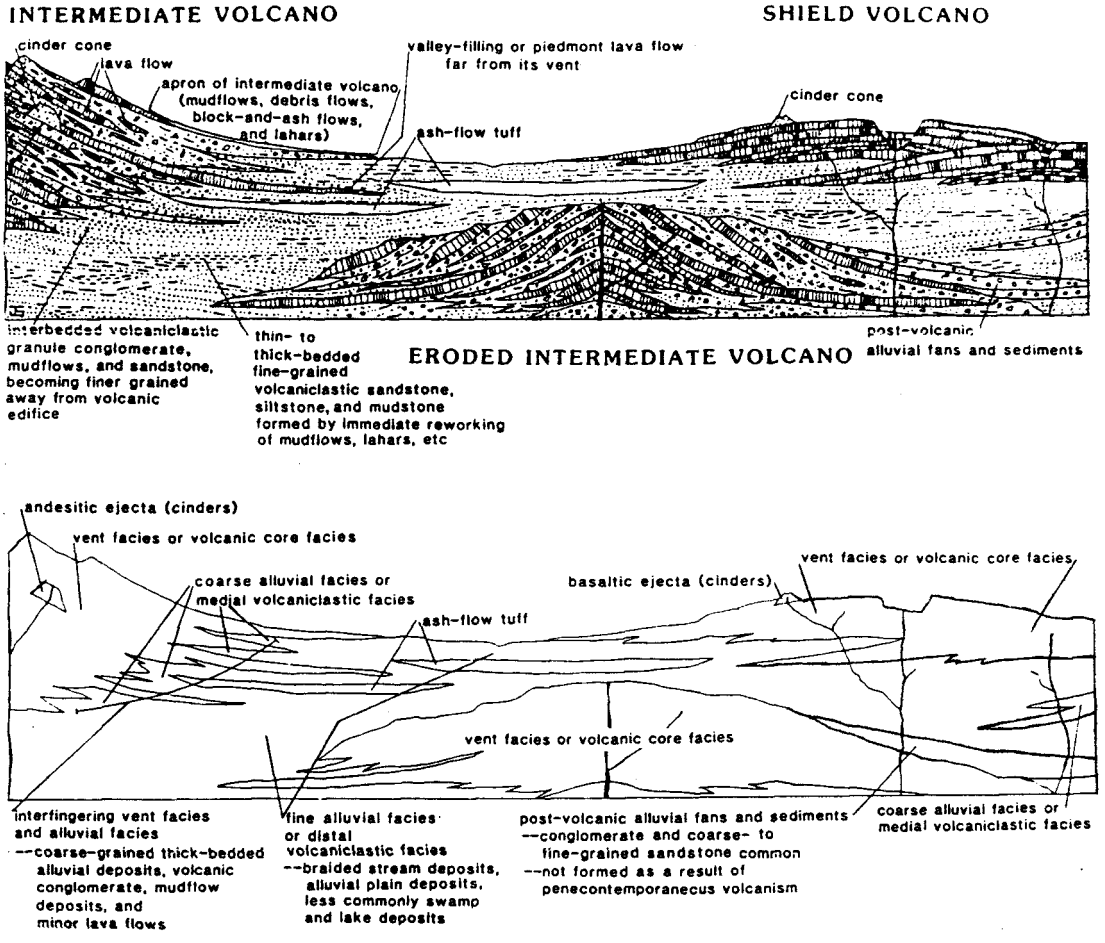


Figure 19. Schematic diagram showing relationship between volcanic and sedimentary facies [from Sherrod and Smith, 1989]. Note that sedimentary facies in the northern Willamette Valley would include marine facies.

Age control on MOu adjacent to the northern Willamette Valley is poor, and has largely been extrapolated from K-Ar age determinations further south. The closest K-Ar age determination for MOu is a 22.8±0.3 Ma date near Jordan by Verplanck [1985] (Plate II). MOu may be Eocene in part as suggested by Armentrout et al. [1983] and Miller and Orr [1986]; however, Peck et al. [1964] originally defined the Little Butte Volcanics as Oligocene to early Miocene. In addition, Sherrod and Smith [1989] recently mapped the volcanics adjacent to the northern Willamette Valley as Oligocene (corresponds to their 25-35 Ma age range). Volcanic rocks constrained as Eocene in petroleum wells (i.e. the Gath well) have been included as part of the Fisher Formation (OEn), which crops out east of the southern Willamette Valley, or the Spencer Formation.

### Subsurface Data

MOu is present in three petroleum exploration wells: the Rose, Anderson, and Wicks wells (Figure 20). It is typically described in mudlogs as basalt, andesite, and tuff (or "volcanics") with some intercalated sandstone and clay.

## SCOTTS MILLS FORMATION

MOu is unconformably overlain by Miocene and Oligocene sedimentary strata (MOs), which corresponds to the recently-proposed Scotts Mills Formation of Miller and Orr [1986]. The sedimentary rock of the Scotts Mills Formation was previously called the Butte Creek beds by Harper [1946], and unnamed marine rocks by Hampton [1972]. It is restricted to the Waldo and Silverton Hills, and the type section is located along Butte Creek.

The Scotts Mills Formation was deposited in an upper bathyal to terrestrial environment along a rockbound volcanic coastline [Orr and Miller, 1984c]. It is made up of three members that reach a combined thickness of 1000 m: the Marquam, Abiqua, and Crooked Finger Members [Miller and Orr, 1988]. The 500 m thick Marquam Member is composed of marine immature to mature litharenite conglomerate, sandstone, and

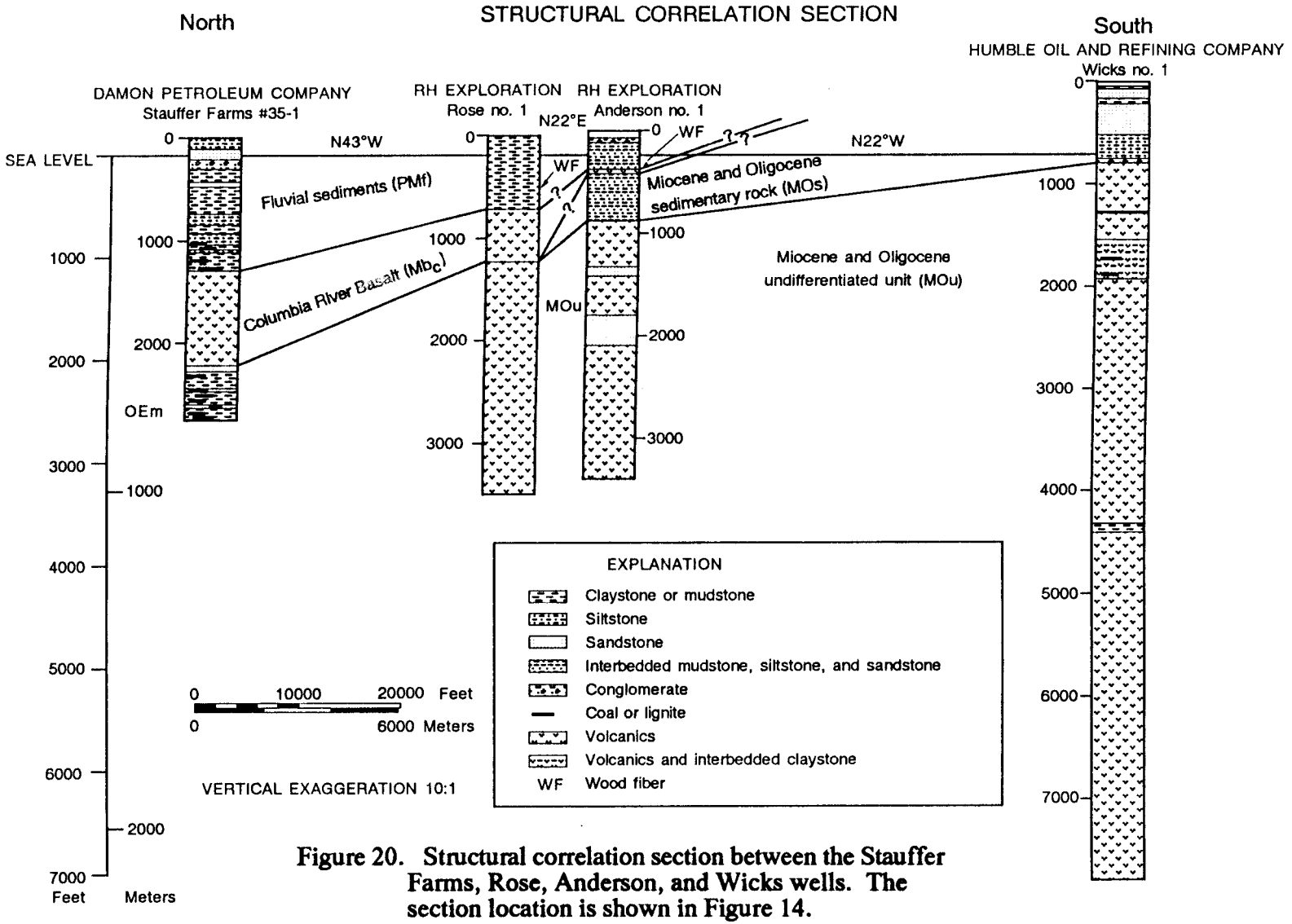


**Figure 20. Structural correlation section between the Stauffer Farms, Rose, Anderson, and Wicks wells. The section location is shown in Figure 14.**

tuffaceous or zeolitic claystone [Orr and Miller, 1986a, b; Miller and Orr, 1984a, b]. Plagioclase and volcanic rock fragments were derived from adjacent exposures of Oligocene volcanic rocks located to the northeast [Miller and Orr, 1986]. The Marquam member was deposited by storm-dominated waves as the Cascades underwent transgression [Miller and Orr, 1988]. The overlying 300 m thick Abiqua Member is composed of tuffaceous and arkosic sandstone and gravel conglomerate deposited from beach-ridge accretion [Miller and Orr, 1986; 1988]. It was deposited during a period of regression along the Cascade arc [Miller and Orr, 1988]. The uppermost 200 m thick Crooked Finger Member consists of fluvial volcanic conglomerate, mudstone, and interbedded coal primarily of nonmarine origin [Miller and Orr, 1986]. The Scotts Mills Formation is the youngest marine sedimentary rock in the northern Willamette Valley, and it appears to have been deposited in a marine embayment which extended southward from the Portland area [Peck et al., 1964; Snavely and Wagner, 1964].

The Scotts Mills Formation has been dated as upper Oligocene to lower Miocene based on molluscs, barnacles, vertebrate fossils, and echinoderms, in addition to its interfingering relationship with the overlying Molalla Formation [Peck et al., 1964; Hampton, 1972; Miller and Orr, 1986; Orr and Miller, 1986a, b].

**Subsurface Data**

Only the Wicks and Anderson wells appear to penetrate the Scotts Mills Formation. The Scotts Mills Formation thins rapidly north of the Anderson well and is absent in the Rose well (Figure 20). The Wicks well spuds in the bottom portion of the Abiqua Member. It penetrates 239 m (from +214 MSL to -25 MSL) of volcanic rock, claystone, sandstone, volcanic siltstone, and a minor volcanic conglomerate overlying Miocene and Oligocene volcanics. The Anderson well appears to penetrate 140 m (from -52 MSL to -192 MSL) of Scotts Mills Formation, dependent on the interpretation that the overlying thin basalt flow is Columbia River basalt. The Scotts Mills Formation in the Anderson well is

composed of a generally upward-coarsening sequence of sandstone, siltstone, and claystone containing volcanic fragments overlying Miocene and Oligocene volcanics.

The wells in Figure 21 are hung on the top of Columbia River basalt, showing the restored geology at the end of middle Miocene time. The rapid northward thinning of Scotts Mills Formation and concurrent thickening of Columbia River basalt is probably due to erosion of Scotts Mills Formation to the north before emplacement of overlying Columbia River basalt. Miller and Orr [1988] estimate the relief on the Miocene and Oligocene volcanic surface to be on the order of 10 m locally and as high as 100 m regionally. Figure 21 shows 385 m relief on the top of Miocene and Oligocene volcanics at the end of Columbia River basalt emplacement, part of which may be due to previous folding rather than erosion.

## MOLALLA FORMATION

The Miocene and Oligocene nonmarine sedimentary rock ($MOn_m$) corresponds to the Molalla Formation of Miller and Orr [1984a, b] and Orr and Miller [1986a, b]. Hampton [1972] mapped the sedimentary rock as tuffs of the Molalla River area and included them in the Little Butte Volcanic Series. The Molalla Formation is 300 m thick and is composed of pumiceous volcanic conglomerate and aquagene tuff with tuffaceous paleosols [Miller and Orr, 1988]. Miller and Orr [1986] concluded that the Molalla Formation actually includes two distinct depositional episodes separated by an unconformity (Figure 10). The lower Molalla Formation interfingers with the Scotts Mills Formation, while the upper Molalla Formation interfingers with Columbia River basalt [Miller and Orr, 1988].

Two reliable radiometric ages of 15.9 ± 1.0 Ma and 15.0 ± 0.7 Ma or middle Miocene were determined by Fiebelkorn et al. [1983] for tuffs in the Molalla Formation near Shady Dell. In addition, relative age dates by J. A. Wolfe [personal communication to D. L. Peck, 1962] based on fossil leaves are early Miocene.

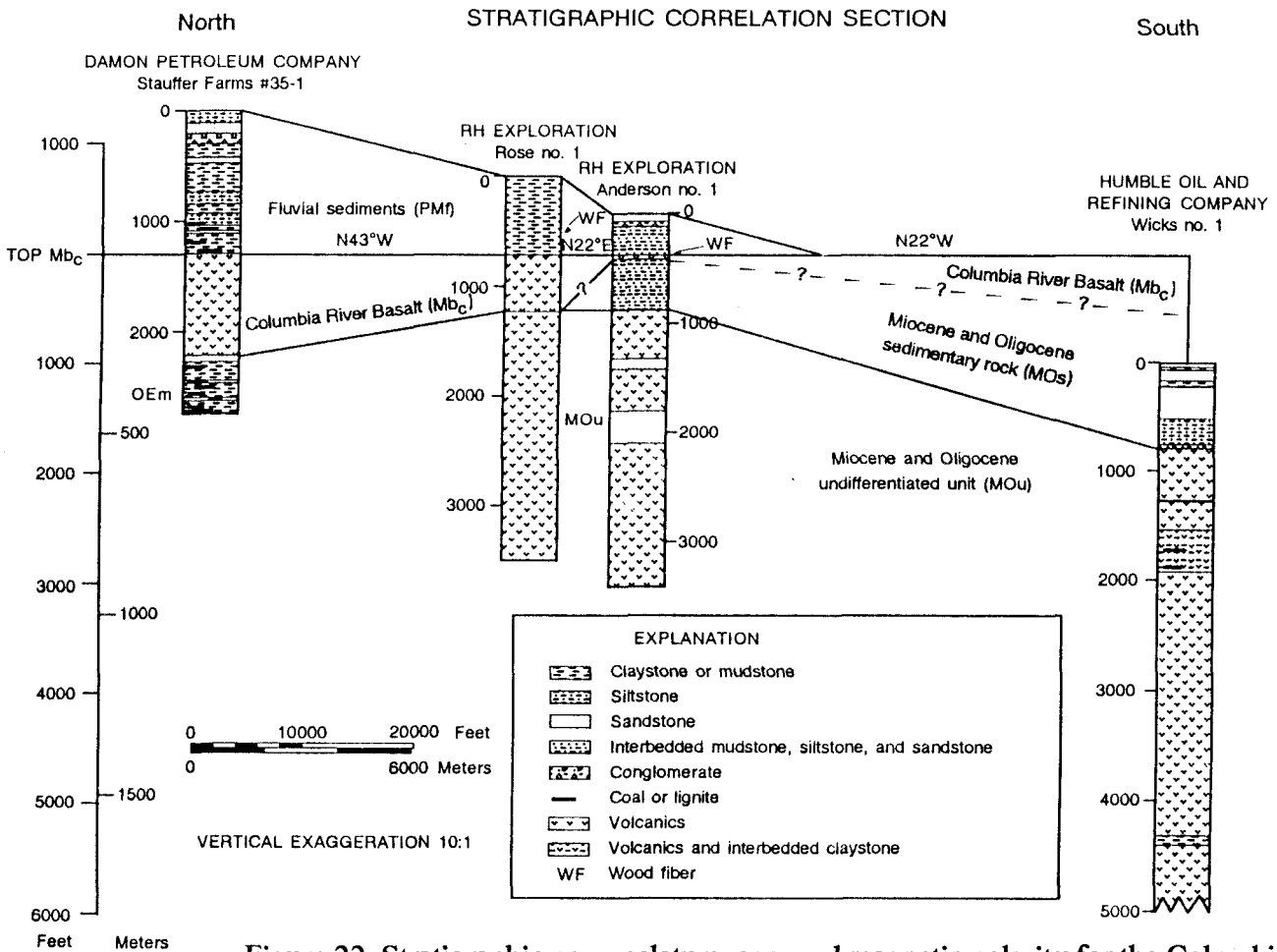


Figure 22. Stratigraphic nomenclature, age, and magnetic polarity for the Columbia River Basalt Group as revised by Swanson et al. [1979] and modified by Beeson et al. [1985]. Flows that cross the Portland Hills - Clackamas River structural zone into the northern Willamette Valley are indicated by a triangle. N = normal magnetic polarity; R = reversed magnetic polarity; T = transitional magnetic polarity; E = excursional magnetic polarity.

## COLUMBIA RIVER BASALT

Columbia River basalt ($Mb_C$) in the northern Willamette Valley was extruded on a slightly folded and eroded surface as indicated by a local basal conglomerate [Baldwin, 1981]. It unconformably overlies OEm, MOu, MOs, and $MOn_m$ (Plates I and II). The Columbia River Basalt Group is a sequence of subaerial tholeiitic flood basalt flows (covering an area of approximately 163,700 ± 5,000 $km^2$) extruded from fissures in eastern Oregon, eastern Washington, and western Idaho [Tolan et al., 1989]. The stratigraphic nomenclature for the Columbia River basalt as revised by Swanson et al. [1979] and modified by Beeson et al. [1985] is shown in Figure 22. Only the Grande Ronde Basalt ($Mb_{Cg}$) and the Frenchman Springs Member of the Wanapum Basalt ($Mb_{CW}$) reached the northern Willamette Valley [Beeson and Moran, 1979]. They are separated by a distinctive weathering surface and interbed of carbonaceous material referred to as the Vantage horizon [Beeson and Moran, 1979].

The Grande Ronde Basalt and the Frenchman Springs Member flowed westward through a N60°-80°E trending "Columbia Trans-arc Lowland" (apparent on aeromagnetic maps of the northern Cascades [Couch et al., 1985]), which crossed the Cascades between Mt. Hood and the Clackamas River [Beeson and Tolan, 1989]. The distribution of flows that crossed the Portland Hills-Clackamas River structural zone into the Willamette Valley and as far south as Scio (Plate II) is shown in Figure 23 [Beeson and Tolan, 1989]. The earlier Grande Ronde Basalt R2 and N2 flows are more widespread than the later Frenchman Springs flows. Flows from the Frenchman Springs Member appear to be restricted to the hills surrounding the Willamette valley. Flows of the Grande Ronde Basalt appear to have initially filled a broad low; subsequently, streams eroded deep canyons around the margin of the resistant Grande Ronde Basalt as indicated by the distribution of Frenchman Springs intracanyon flows [Figure 23, after Beeson et al., 1989].

The top of Columbia River basalt commonly contains ferruginous bauxite deposits or high-iron, high-aluminum laterites (a highly weathered, red subsoil). The bauxite

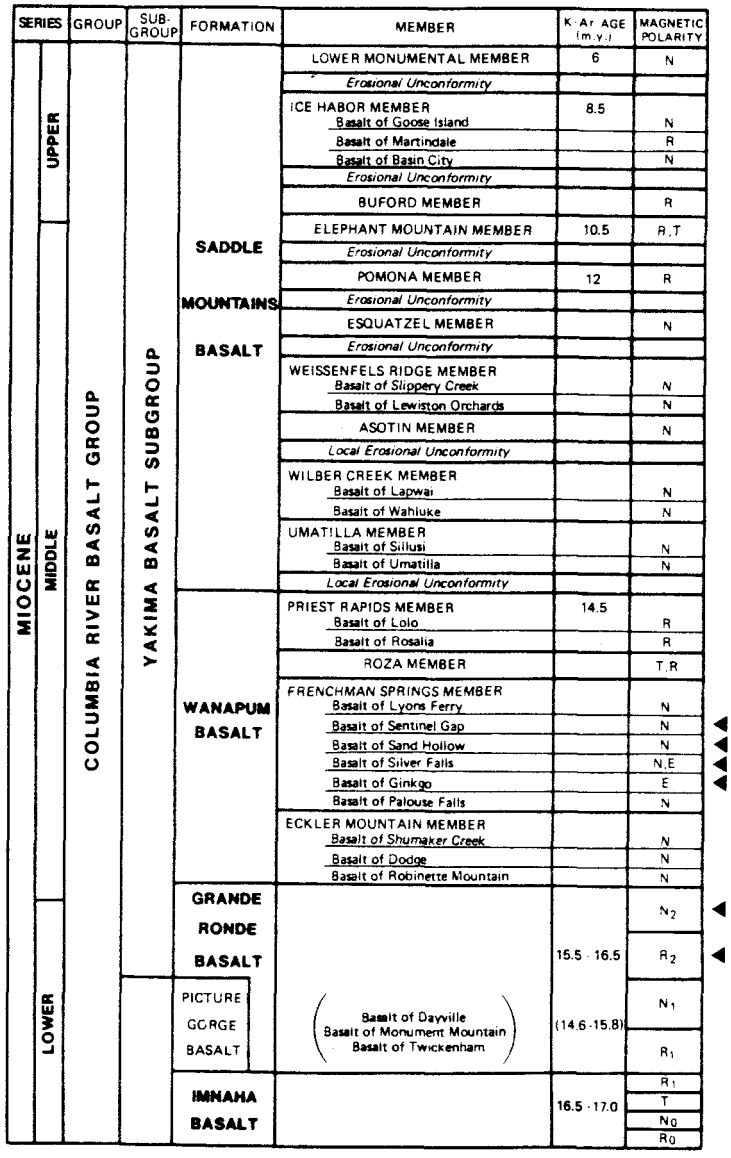


Figure 22. Stratigraphic nomenclature, age, and magnetic polarity for the Columbia River Basalt Group as revised by Swanson et al. [1979] and modified by Beeson et al. [1985]. Flows that cross the Portland Hills - Clackamas River structural zone into the northern Willamette Valley are indicated by a triangle. N = normal magnetic polarity; R = reversed magnetic polarity; T = transitional magnetic polarity; E = excursional magnetic polarity.

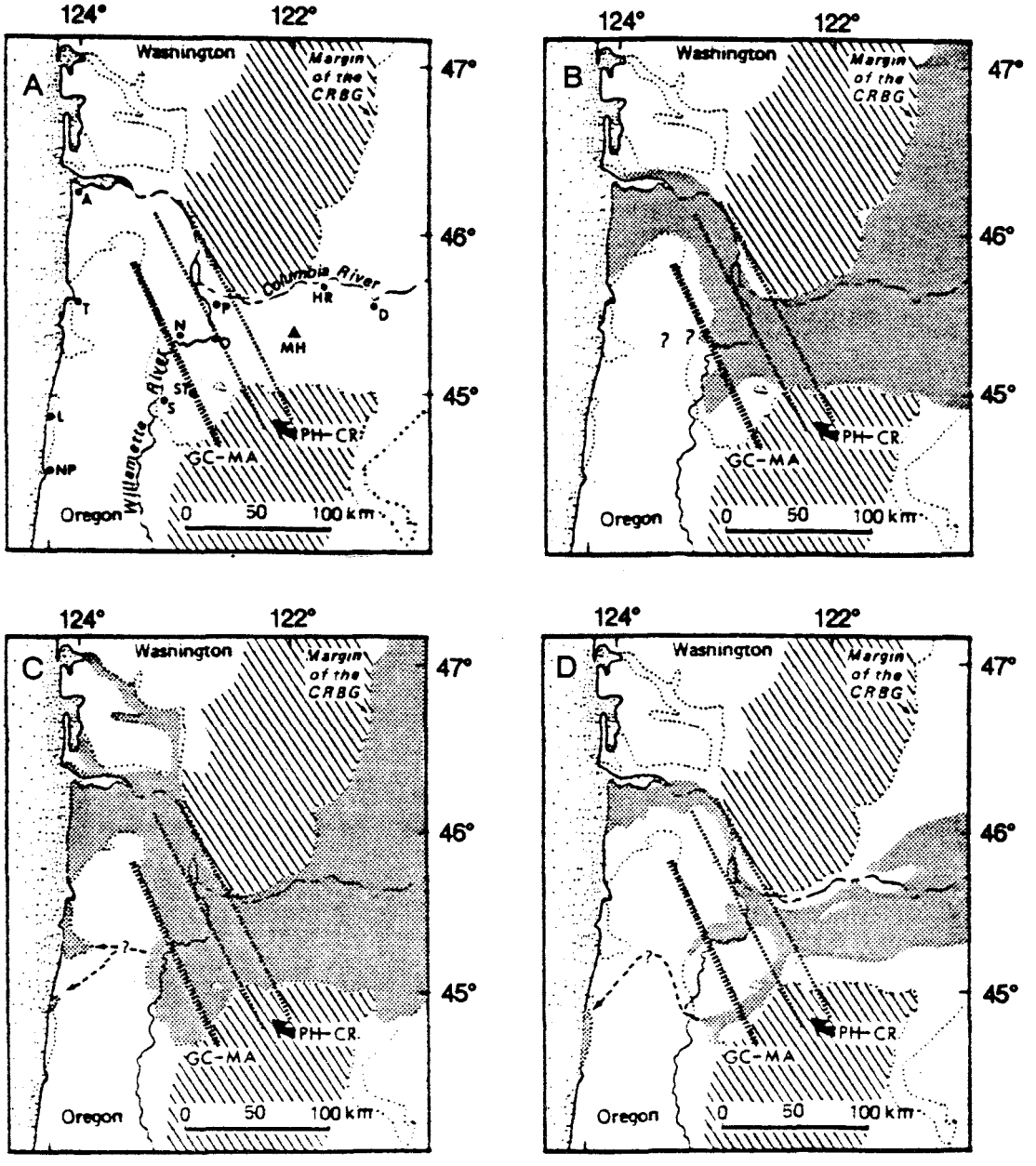


Figure 23. Distribution of Columbia River basalt flows that cross the Portland Hills - Clackamas River structural zone into the northern Willamette Valley from Beeson and Tolan [1989]. The dotted line indicates the maximum extent of the Columbia River Basalt Group. a.) Base map showing cities, and geographic features: A = Astoria, HR = Hood River, P = Portland, D = The Dalles, T = Tillamook, MH = Mt. Hood, N = Newberg, O = Oregon City, ST = Silverton, S = Salem, L= Lincoln City, NP = Newport, GC-MA = Gales Creek - Mt. Angel structural zone, PH-CR = Portland Hills - Clackamas River structural zone. b.) $R_2$ Grande Ronde Basalt; c.) $N_2$ Grande Ronde Basalt; d.) Basalt of Ginkgo flow, dashed line shows inferred path of Ginkgo across Coast Range; e.) Basalt of Silver Falls; f.) Basalt of Sand Hollow flow; g.) Basalt of Sentinal Gap flow.

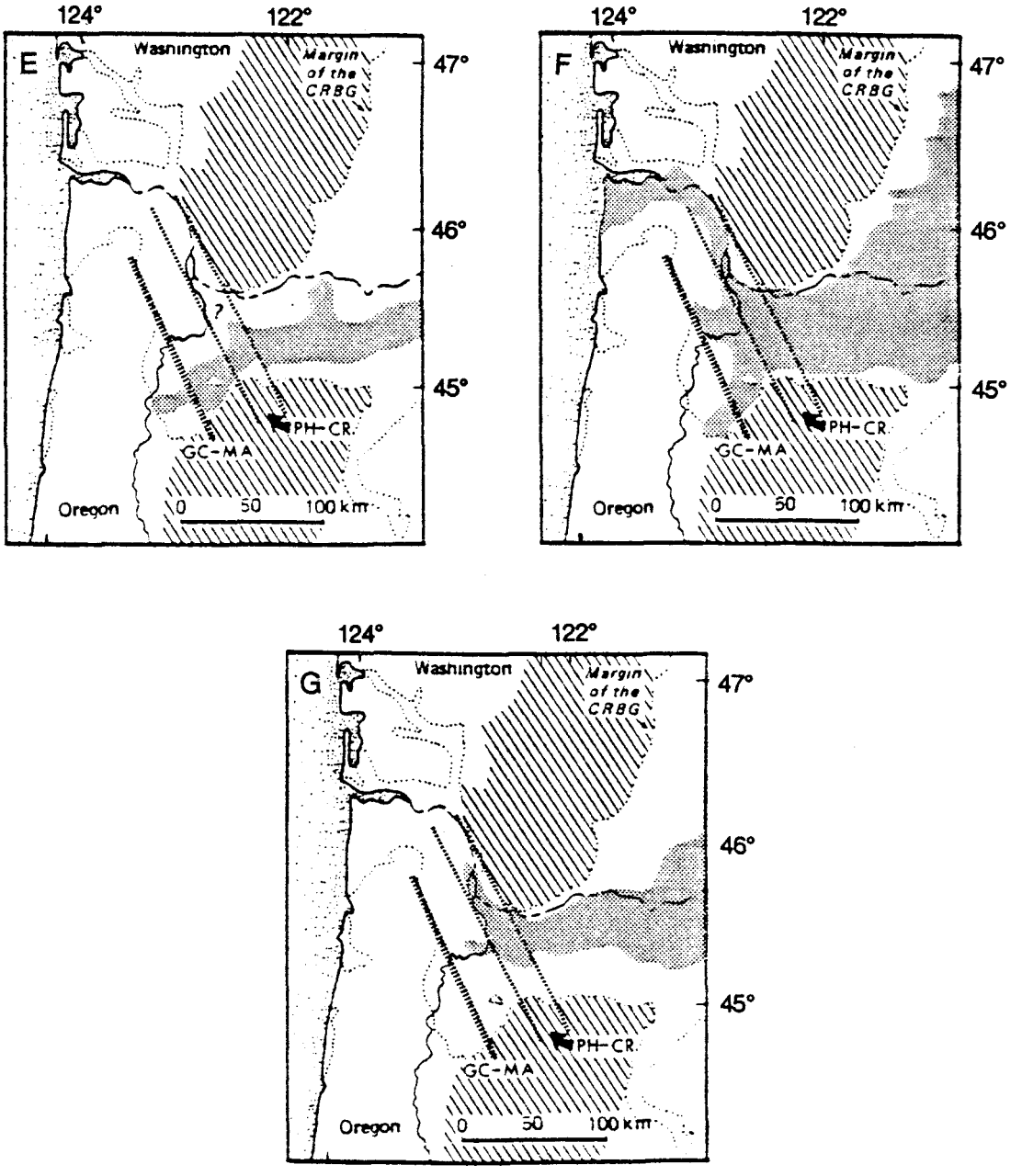


Figure 23 continued

deposits occur primarily in the Salem Hills, although lesser amounts are present in the Waldo, Eola, and Amity Hills, and Red Hills of Dundee. They are apparently related to topography, as the depth of laterization increases down valley [Hoffman, 1981]. A strong correlation exists between the distribution of the ferruginous bauxite deposits and the Kelley Hollow flow (a Silver Falls flow) of the Frenchman Springs Member of the Wanapum Basalt [Hoffman, 1981].

Several radiometric ages have been determined for the Columbia River basalt and are shown in Plates I and II. All of the age dates range from 14.6±0.4 Ma to 15.9±1.0 Ma, except for one inconsistent date of 19.2±0.6 Ma [Sutter, 1978; Lux, 1982; Fiebelkorn et al., 1983; Verplanck, 1985].

**Subsurface Data**

The thickness of Columbia River basalt varies greatly throughout the northern Willamette Valley. Columbia River basalt thins westward from 280 m in the Stauffer Farms well to 100-151 m near Gervais. In the Eola-Amity Hills, it varies in thickness from 0-305 m [Brownfield and Schlicker, 1981a, b]. The average thickness in the Salem Hills is approximately 125 m [Hoffman, 1981]. To the north at Parrett Mountain, Columbia River basalt is greater than 275+ m thick based on water wells. The increased thickness at Parrett Mountain corresponds to the presence of a paleotrough near Sherwood (possibly an extension of the Columbia trans-arc lowland), which funneled Columbia River basalt to the southwest [Beeson et al., 1989a]. In the Waldo and Silverton Hills the Columbia River basalt varies from 190+ m in water wells to 0 m where it locally pinches out along Molalla River and upper Drift Creek as indicated by middle to late Miocene units directly overlying MOs and the $MOn_m$.

The Columbia River basalt present in the Klohs, Werner 14-21, Werner 34-21, Bagdanoff, DeShazer, and Rose wells is all Grande Ronde Basalt [M. Beeson, personal communication, 1990]. The lack of Wanapum Basalt in those wells suggests the northern Willamette basin had not yet begun subsiding during Wanapum time [Beeson et al.,

1989a]. In addition, a lateritic clay or paleosol is present at the top of the Grande Ronde Basalt in several of the wells suggesting weathering of the Grande Ronde Basalt before deposition of overlying Pliocene and Miocene fluvial and lacustrine sediments. I have interpreted the basalt in the Anderson well from 385-420 ft to be Columbia River basalt based on its appropriate stratigraphic position. Well cuttings of the basalt were not available to M. Beeson for examination.

## MIDDLE TO LATE MIOCENE UNITS

Middle to Late Miocene units (Mu, Ma, Mv, Mn) on Plates 1 and 2 correspond to the Sardine Volcanics of Peck et al. [1964]. They unconformably overlie Columbia River basalt and older formations [Hampton, 1972]. They are primarily intermediate volcanic rocks with common interbedded dacite tuffs [Priest et al., 1983], which originated from at least a dozen vents in the Western Cascades [Peck et al., 1964]. Adjacent to the northern Willamette Valley, the Miocene units have been mapped and subdivided by Hampton [1972] as follows: capping pyroxene andesite flows (Ma); volcanic mudflow breccia, water-laid tuff, and tuff corresponding to the Rhododendron Formation of Hodge [1933] (Mv); and massive pumice tuff, basaltic andesite flows, and some agglomerate-conglomerate beds corresponding to the Fern Ridge Tuffs of Thayer [1939] (Mn). The Rhododendron equivalent (Mv) and capping pyroxene andesite flows (Ma) appear to be separated by an unconformity based on the presence of a laterite at the top of the older Rhododendron equivalent (Mv) (Figure 10). Hampton [1972] concluded the pyroxene andesite subunit (Ma) is intercalated with Pliocene and Miocene fluvial and lacustrine sediments in water wells in the northern Willamette Valley. However, where the capping pyroxene andesite flows are absent, the overlying Pliocene and Miocene fluvial and lacustrine sediments unconformably overlie the Rhododendron equivalent [Trimble, 1963].

Priest [1989] estimates that the volcanism related to Mu, Ma, Mv, and Mn (corresponding to his late western Cascade volcanism) occurred from 13-14 Ma to 7.5 Ma.

K-Ar ages of 15-17 Ma for the Miocene and Pliocene unit were determined by Fiebelkorn et al. [1983] at sample locations just east of the map boundary; however, these older ages appear to be inaccurate due to weathering or alteration at sample locations [Priest, 1989]. In the northern Willamette Valley, Mu, Ma, Mv, and Mn do not occur in any petroleum exploration wells.

## PLIOCENE AND MIOCENE FLUVIAL AND LACUSTRINE SEDIMENTS

Pliocene and Miocene fluvial and lacustrine sediments (PMf) unconformably overlie the Columbia River basalt and Rhododendron equivalent (Mv) in the northern Willamette basin. The unconformable contact is indicated by a laterite both at the top of Columbia River basalt and the top of the Miocene Rhododendron equivalent (Mv). However, Hampton [1972] concluded that younger pyroxene andesite flows (Ma), included in his Sardine Formation, are intercalated with Pliocene and Miocene fluvial and lacustrine sediments.

The Pliocene and Miocene fluvial and lacustrine sediments correlate to the Troutdale Formation of Hodge [1933], which is named for exposures near the town of Troutdale, Oregon (adjacent to the Columbia River) (Figure 24). The Troutdale Formation of Hodge [1933] was later divided by Trimble [1963] into an upper Troutdale Formation and lower Sandy River Mudstone. The nomenclature of Trimble [1963] has been applied by several workers to similar Pliocene and Miocene nonmarine sediments of the northern Willamette Valley (i.e. Price [1967a, 1967b], Hampton [1972], and Leonard and Collins [1983]). However, the type sections of the Troutdale Formation and Sandy River Mudstone in the Portland area were deposited primarily by the Columbia River [Swanson, 1986]. The "Troutdale Formation" and "Sandy River Mudstone" in the northern Willamette Valley were deposited primarily by the Willamette River (and other rivers draining the southern Willamette Valley), minor rivers draining the Western Cascades, and the Yamhill River draining the Coast Range.

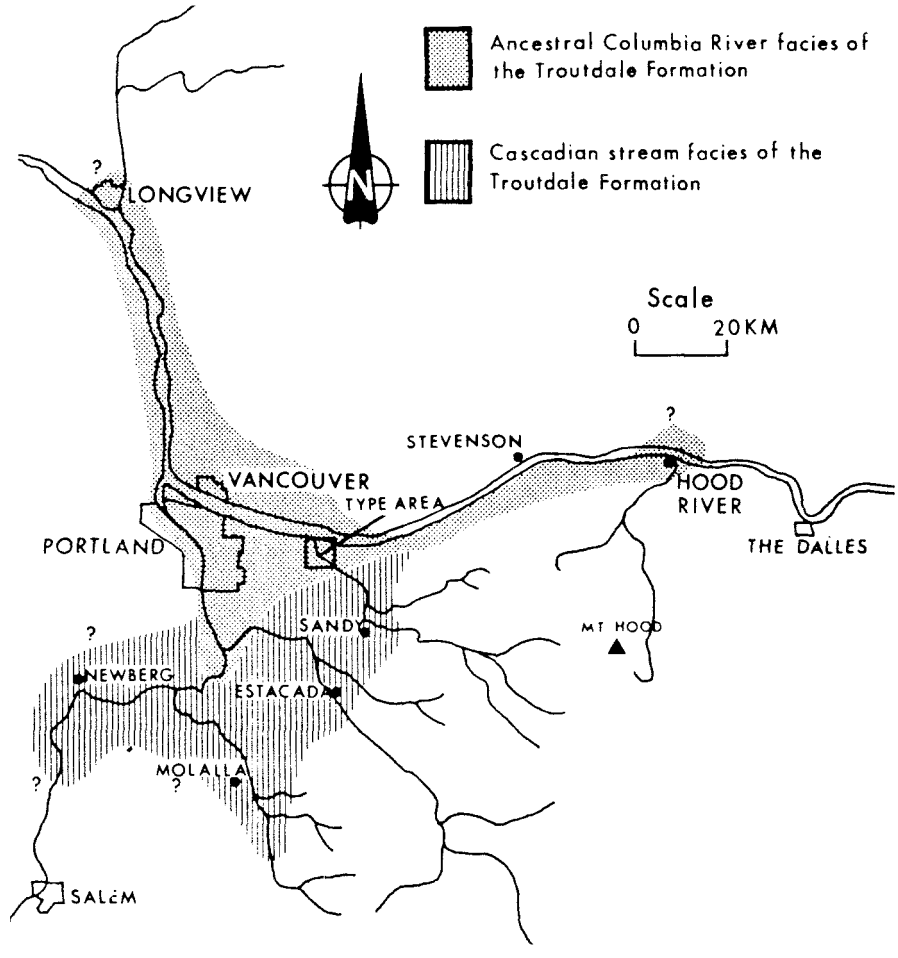


Figure 24. Troutdale Formation facies map [from Tolan and Beeson, 1984].

The Sandy River Mudstone is exposed along the Sandy and Clackamas Rivers, where it consists of claystone, siltstone, and fine grained sandstone [Trimble, 1963]. Similarly, in petroleum exploration wells of the northern Willamette Valley, the lower portion of Pliocene and Miocene fluvial and lacustrine sediments is composed of blue, gray, and green claystone with minor silt, sand, and gravel. These fine-grained sediments may also correlate to the late Miocene to Pliocene (?) Monroe Formation of the southern Willamette Valley [Roberts and Whitehead, 1984].

Trimble [1963] originally suggested that the Sandy River Mudstone was all lacustrine. However, A. R. Niem and C. D. Peterson [personal communication to I. Madin, 1989] have recently suggested based on a quick reconnaissance that the Sandy River Mudstone along the Clackamas River is in part fluvial rather than lacustrine as it interfingers with gravels and contains massive rootlets in growth position. In addition, the Monroe clay in the southern Willamette Valley largely consists of overbank deposits based on the presence of rootlets in growth position, paleosols, and lack of laminations. The presence of coal in the Stauffer Farms well (Figure 20) suggests swamp-like conditions at least locally.

The Troutdale Formation has been separated into two informal members by Tolan and Beeson [1984]. The lower member contains far-derived fluvial deposits of the ancestral Columbia River (includes foreign clasts of quartzite, schist, granite, and rhyolite), and is generally restricted to an older channel adjacent to the modern course of the Columbia River (Figure 24) [Tolan and Beeson, 1984]. It is largely composed of quartzite-bearing, basaltic gravels and micaceous arkosic sand beds [Tolan and Beeson, 1984].

The upper member of the Troutdale Formation is characterized by fluvial vitric-lithic sandstones (hyaloclastites) with minor basaltic conglomerates in the Portland area [Tolan and Beeson, 1984; Swanson, 1986]. It extends into the northern Willamette Valley, where it is largely composed of lithic sand and basaltic gravel with minor clay. The

Troutdale Formation equivalent in the DeShazer, Werner 34-21, and Werner 14-21 wells contains some quartz pebbles. The quartz pebbles suggest a possible contribution from the Columbia River at least as far south as Gervais. Hampton [1972] observed a gradual transition from >25% quartzite pebbles at the type section on the lower Sandy River to no quartzite pebbles in the Salem area, where rocks are derived only from the nearby Cascades and Coast Ranges.

The age of the Miocene and Pliocene fluvial and lacustrine sediments is constrained by fossil leaves and overlying volcanic rock. The lower bound for the age of Sandy River Mudstone is late Miocene by present standards of dating [Baldwin, 1981] based on examination of leaves by Chaney [1944]. Tolan and Beeson [1984] assigned an upper age limit of 2 Ma for the Troutdale Formation in the Portland area based on a K-Ar date of 1.56 ± 0.2 Ma for an overlying flow of Boring Lava.

**Subsurface Data**

The Pliocene and Miocene fluvial and lacustrine sediments are present in petroleum exploration wells and on seismic reflection lines. Based on petroleum exploration wells, the lower fine-grained portion of the Pliocene and Miocene fluvial and lacustrine sediments, equivalent to the Sandy River Mudstone, thickens northeastward. It is 160 m thick in the Bagdanoff and Werner 14-21 wells, 265 m thick in the DeShazer well, and 300 m thick in the Stauffer Farms well (Figures 14 and 18).

The Pliocene and Miocene fluvial and lacustrine sediments are characterized by a lower and upper seismic facies, possibly corresponding to the Sandy River Mudstone and Troutdale Formation equivalents, respectively. The lower seismic facies generally contains low-amplitude (transparent) reflectors, while the upper seismic facies contains high- to medium-amplitude reflectors (Figure 25). The low-amplitude reflectors are consistent with a relatively homogeneous mudstone (equivalent to the Sandy River Mudstone), whereas the higher amplitude reflectors indicate internal density contrasts possibly between the interbedded conglomerate, sandstone, siltstone and mudstone (equivalent to the Troutdale

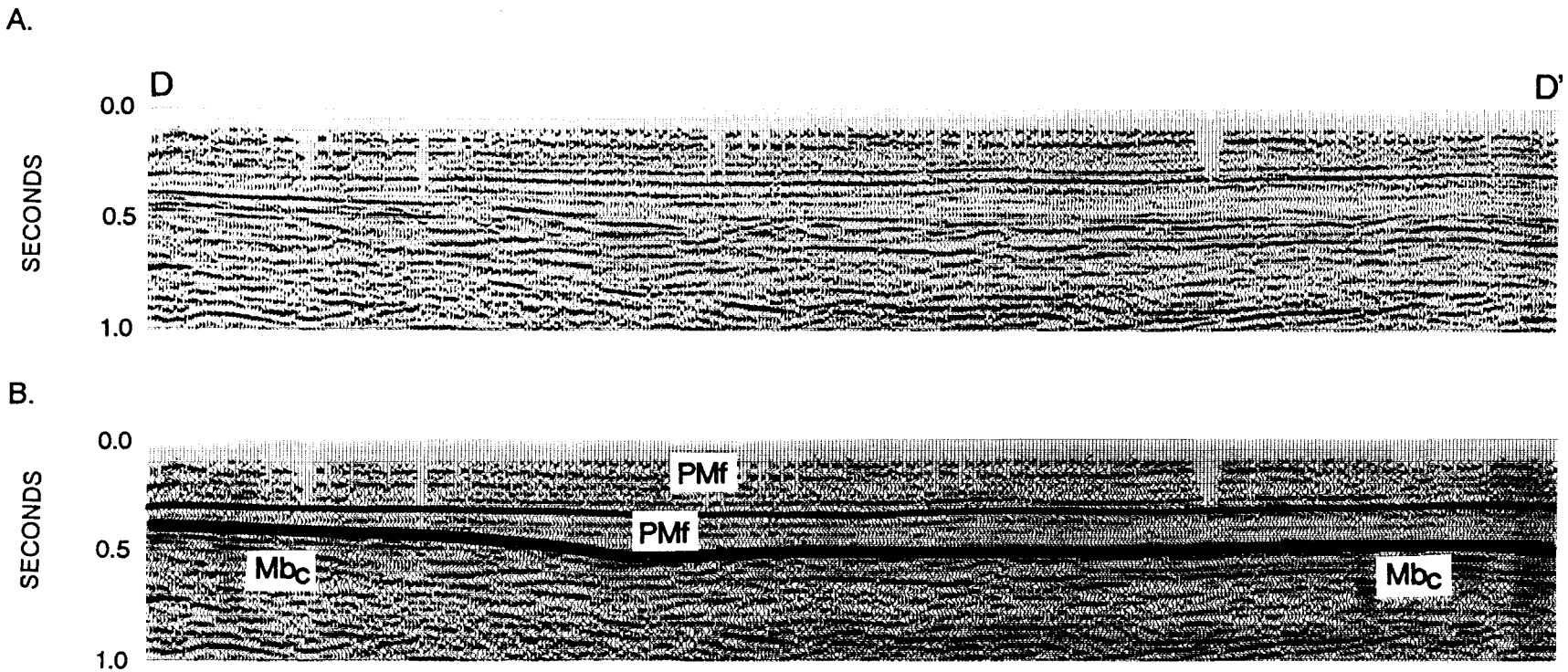


Figure 25. Seismic section D-D'. PMf = Pliocene and Miocene fluvial and lacustrine sediment, $Mb_C$ = Miocene Columbia River basalt. Location of seismic section shown in Figure 32.

Formation). The reflectors are surprisingly continuous particularly in the upper facies considering the fluvial nature of the sediments.

## QUATERNARY AND PLIOCENE VOLCANICS

Except for volcanics at Snow Peak, the Quaternary and Pliocene volcanics correspond to Boring Lava. Boring Lava was originally described by Treasher [1942] based on exposures at the Boring Hills to the north. Within the study area, outcropping Boring Lava had previously been restricted to the Oregon City plateau, south of Oregon City (Plate 1). However, M. Beeson [personal communication, 1989] has recently determined, based on geochemistry, that the basalt or andesite at La Butte is not Columbia River basalt as previously mapped, but probably Boring Lava. La Butte thus becomes the westernmost outcrop of Boring Lava currently mapped.

Boring Lava is composed of olivine basalt and basaltic andesite, and some pyroclastic material of local extent [Hampton, 1972; Schlicker and Finlayson, 1979]. It is probably a westward extension of Cascade Range volcanism [Baldwin, 1981]. Over 90 vents of Boring Lava have been mapped based on topography in the greater Portland area [Allen, 1975]. Most of the lava which is exposed at the Oregon City plateau originated from vents at Highland Butte [Trimble, 1963; Allen, 1975]. The Boring Lava at La Butte and possibly the newly mapped "intrusion(s)" near Aurora correspond to more vents.

Based on K-Ar dating, Boring Lava ranges in age from 5 Ma to as young as 612 ± 23 ka [Luedke and Smith, 1982; Swanson, 1986; and R. Duncan, personal communication to I. Madin, 1990]. Boring Lava of the Oregon City plateau yielded a K-Ar date of 2.6 Ma [MacLeod, personal communication, 1990].

### Subsurface Data

Leonard and Collins [1983] evaluated data from 260 drilled wells in a 16 square mile area just northwest of Highland Butte (T. 3 S., R. 2 E., secs. 14-16, 20-29, 33-35) and determined the thickness of Boring Lava ranges from 5 to 155 m (averaging 55 m).

Boring Lava appears to occur in the subsurface of the northeastern Willamette valley both near Aurora and Curtis based on seismic reflection and water-well data (refer to Structure section). Chaotic reflections on seismic reflection lines are interpreted as corresponding to Boring Lava.

## QUATERNARY TERRACE GRAVELS

Pleistocene gravels in the Willamette Valley form a series of progressively younger and lower cut and fill terraces [McDowell and Roberts, 1987]. The Pleistocene gravels were deposited due to the decreasing stream gradient of the Willamette River and its tributaries. No comprehensive mapping of the gravels has been done in the northern Willamette Valley except for the study of Piper [1942], which included all terrace deposits in one unit. The following discussion will rely on the nomenclature of Allison [1953], Allison and Felts [1957], and Balster and Parsons [1969], who mapped the Lacomb, Leffler, and Linn gravels (the last, renamed the Rowland Formation; Figure 26), along the northern and southern Santiam Rivers. These three gravel units may be correlative to the Springwater, Gresham, and Estacada Formations along the Clackamas and Sandy Rivers mapped by Trimble [1963], although recent mapping of the Estacada Formation by Madin [1990] has cast doubt on Trimble's nomenclature in the Portland area.

The high terrace gravels (Qt) shown on Plates I and II appear to correlate to the older Lacomb and Leffler gravels. The high terrace deposits are generally composed of weathered clay, silt, sand, and basaltic gravel [Baldwin et al., 1955; Brownfield, 1982a; Bela, 1981; Hampton, 1972]. They range in altitude from 120-320 m along tributaries of the Willamette River (the Yamhill and Molalla Rivers) and from 43-91 m along the Willamette River west of Salem. They vary in thickness from 0-30 m along tributaries and 1-5 m along the Willamette River west of Salem [Hampton, 1972; Bela, 1981; and Brownfield, 1982a]. Terrace deposits in the unglaciated Coast Range (such as those adjacent to the Yamhill River) are probably fluvial in origin while those along the eastern

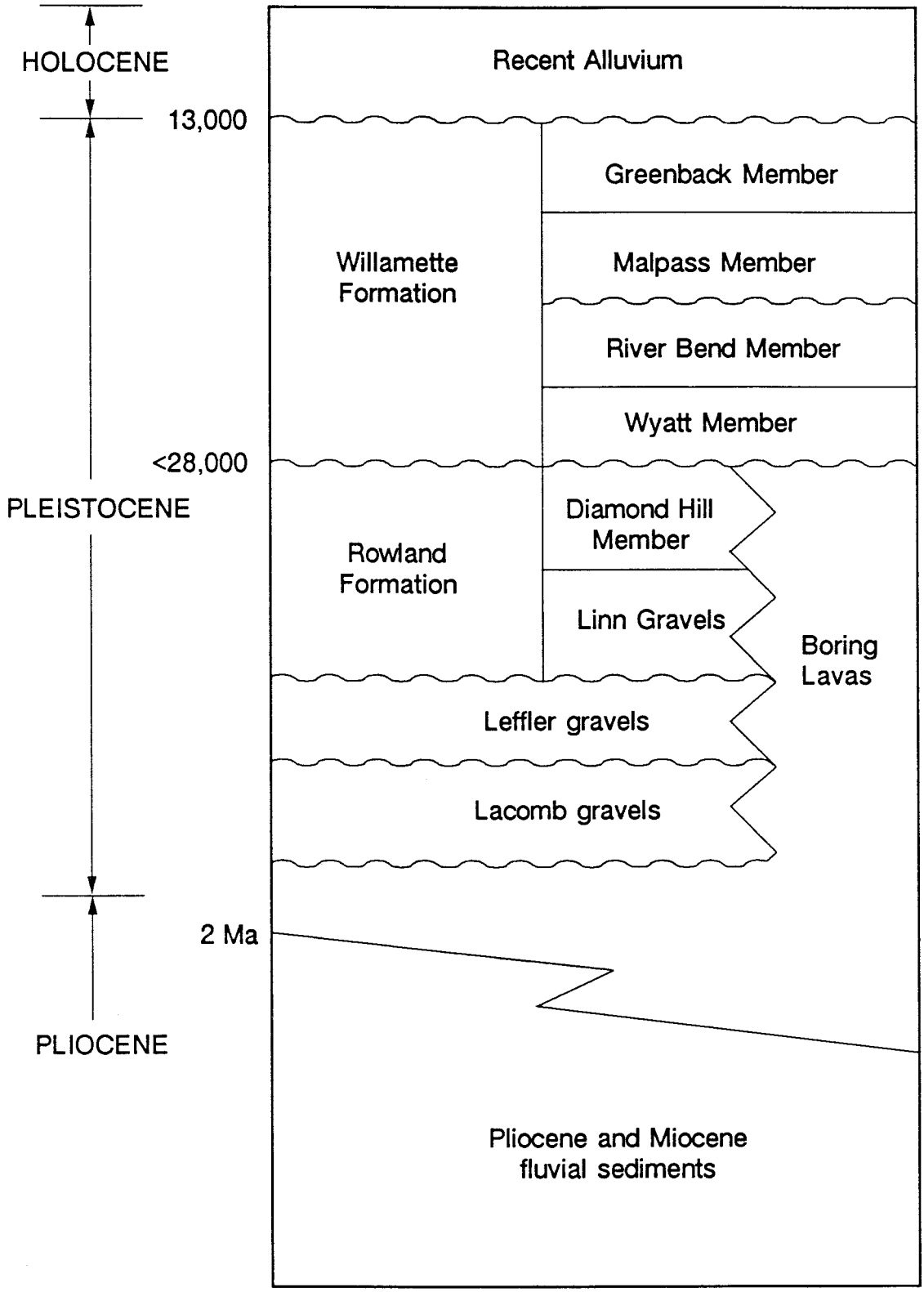


Figure 26. Pliocene and Quaternary stratigraphy. After Roberts [1984] and Trimble [1963]

margin of the Willamette Valley (such as those along the Molalla River) are probably glaciofluvial in origin [McDowell, in press].

The younger Rowland Formation occurs below the Willamette Formation (mapped as Qu), and includes the Linn Gravels and Diamond Back member [Balster and Parsons, 1969]. The Linn Gravels unconformably overlie the Troutdale Formation and Boring Lava. In the southern Willamette Valley, the Linn Gravels are composed of sand and cross-bedded gravel of intermediate and basic igneous rocks [Balster and Parsons, 1969]. The Linn gravels generally vary from 5-20 m in thickness in the southern Willamette Valley [Graven, 1991].

The Diamond Hill Formation is composed of sand. Clastic dikes were noted in the Diamond Hill member by Glenn [1965], most likely related to later flooding (or sudden loading) associated with deposition of the overlying Willamette Formation, but possibly related to earthquake shaking. A paleosol commonly occurs at the top of the Diamond Back member due to extensive weathering (Figure 27); in isolated areas erosion has removed the entire member [Balster and Parsons, 1969].

The Mill Creek-North Santiam Valley fan gravels are correlative to the low Molalla fan gravels, and probably both were deposited during alpine glaciation associated with the advance of the Okanogan lobe of the Cordilleran Glacier complex [Glenn, 1965].

The terrace gravels are mid-late Pleistocene in age (Figure 26), and appear to correspond to the pre-Kansan, Kansan, and Illinoin or early Wisconsin glaciations respectively [Allison, 1936; 1953; McDowell, in press]. Radiocarbon dates on the Diamond Hill member in the southern Willamette Valley indicate deposition ranged from >36,000 yr B.P. until <28,500 yr. B.P. [McDowell, in press].

## QUATERNARY UNDIFFERENTIATED SEDIMENTS

Quaternary undifferentiated sediments cover most of the northern Willamette Valley floor below an altitude of 100 m. The sediments include the Willamette Formation,

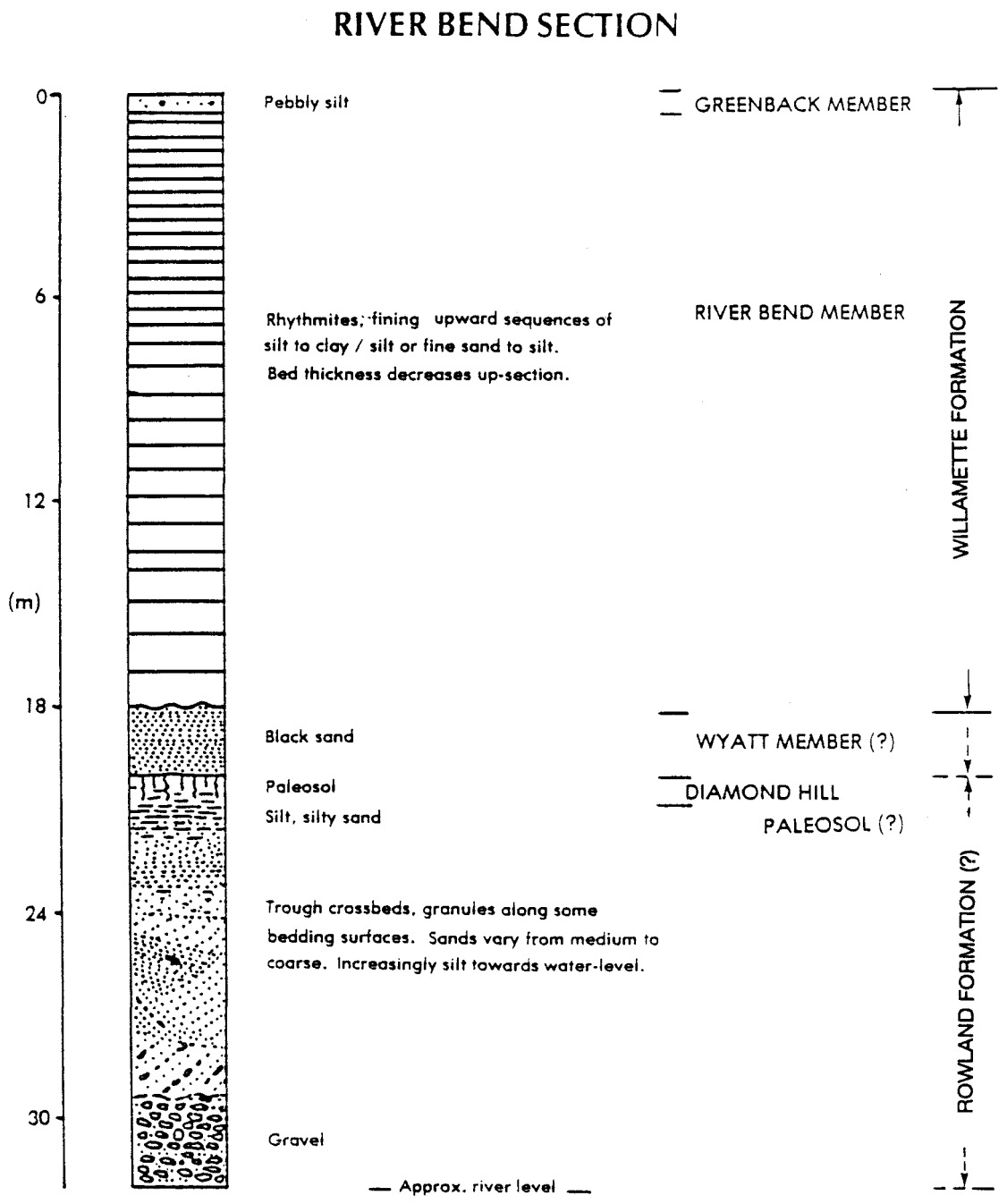


Figure 27. Type section of the River Bend member of the Willamette Formation from McDowell and Roberts [1987]. The section is located along the eastern bank of the Willamette River, T5S, R3W, section 1 (SSW of St. Paul).

originally named the Willamette Silt by Allison [1932, 1936, 1953, 1978], and overlying Holocene valley alluvium (restricted to stream channels). The Willamette Formation unconformably overlies the Rowland Formation and older units. Balster and Parsons [1969] divided the Willamette Formation into four members based on mapping in the southern Willamette Valley in addition to reconnaissance mapping in the northern Willamette Valley. The four members are the Wyatt, River Bend, Malpass, and Greenback members (Figure 26).

The lower Wyatt member is locally present in channels, and is composed of locally derived sandy and silty alluvium, typically composed of basaltic rocks [Balster and Parsons, 1969]. The black sand in the River Bend section probably corresponds to the Wyatt member (Figure 27; McDowell and Roberts [1987]).

The overlying River Bend member, named for exposures at River Bend, comprises the bulk of the formation (Figure 27). It is the coarser grained equivalent of the Irish Bend member in the southern Willamette Valley [Roberts, 1984; McDowell and Roberts, 1987]. The River Bend member is composed of at least 40 distinct parallel, nearly-horizontal beds of silt and fine sand [Glenn, 1965], but includes pebbles and boulders of ice-rafted debris (including granite, granodiorite, quartzite, gneiss, and slate) [Allison, 1936, 1953; McDowell, in press]. The River Bend member becomes coarser, containing intercalated coarse sands and even gravels, towards the the north [Glenn, 1965]. It is topped by a paleosol where it has not been eroded.

Assuming each bed represents a flooding event, the River Bend member was deposited by at least 40 rapidly-recurring, large, turbulent floods [Allison, 1932, 1978, Glenn, 1965]. The floods probably occurred due to repeated failures of lake Missoula dams, seasonally supplemented by floods due to icejams [Glenn, 1965]. The seasonal floods from the Columbia River would have backed up into the tributary Willamette Valley due to damning along the Columbia River Gorge below Portland, Oregon [Allison, 1935]. The sediment for the River Bend member was probably supplied from the scablands in

eastern Washington by erosion of the Palouse Formation (eolian silts and fine sands) [Glenn, 1965].

The overlying Malpass and Greenback members unconformably overlie the River bend member and are much more areally extensive [Balster and Parsons, 1969]. The Malpass member is a discontinuous massive gray clay locally deposited in swales by the Willamette River system [Balster and Parsons, 1969; McDowell and Roberts, 1987]. It is less than 1 m thick in the southern Willamette Valley [McDowell and Roberts, 1987]. Its distribution and thickness in the northern Willamette Valley have not been studied.

The upper Greenback member is composed of silt-size quartz and feldspar with coarse and sand-size iron manganese oxide concretions [Balster and Parsons, 1969]. It was deposited by the largest glacial outburst flood, the "Spokane flood". The Spokane flood spilled from the Tualatin Valley into the northern Willamette Valley across the divide between Sherwood and Norwood resulting in local scabland topography [Glenn, 1965; Allison, 1978]. Spokane flood water also flowed southward through the Oregon City water gap. Glacial erratics (iceberg-borne debris) associated with the flood are present at elevations as high as 120 m above sea level (as much as 75 m above the valley floor) [Allison, 1935]. The Greenback member is less than 1 m thick in the southern Willamette Valley [McDowell and Roberts, 1987]. Its distribution and thickness in the northern Willamette Valley have not been studied.

The lower age of the Willamette Formation is constrained by sands of the Diamond Hill member of the Linn Formation, which are dated as 28,480 ± 1810 yr B.P. [Roberts, 1984; McDowell and Roberts, 1987]. Several of the floods within the River Bend member appear to be associated with Wisconsin glaciation [McDowell and Roberts, 1987]. The upper age limit of the Willamette Formation is 13,080 ± 300 yr B.P. based on dated bog deposits in the Portland area deposited after the "Spokane flood" [Mullineaux et al., 1978].

The proto-Willamette River flowed through the Labish Channel northeastward across the northern Willamette Valley, but abandoned the channel 11,000 ± 230 years before present based on a dated peat at the base of the channel [Glenn, 1965].

**Subsurface Data**

The thickness and distribution of the Wyatt, Malpass, and Greenback members in the northern Willamette Valley are poorly known. The thickness of the River Bend member typically varies from 10-20 m in the northern Willamette Valley based on exposures measured by Glenn [1965] at Needy, Canby, and River Bend (just west of St. Paul). The maximum observed thickness is 23 m as measured by McDowell and Roberts [1987] in a water test well in Woodburn. The River Bend member is thicker on the flanks of the Western Cascades than on the flanks of the Coast Range. It appears to pinch out above an altitude of 100 m [Glenn, 1965].

# STRUCTURE

The northern Willamette Valley lies on the eastern flank of the broad north-northeast-trending Coast Range structural arch which is underlain by Siletz River Volcanics and Tillamook Volcanics [Bromery and Snavely, 1964; Wells et al., 1983]. Middle Eocene to late Oligocene sedimentary rocks crop out along the western side of the northern Willamette Valley and form a gently eastward dipping homocline (Figure 13 or Plate IV). However, beneath the center of the Willamette Valley, Eocene to Oligocene strata are structurally warped up as shown in Figure 18, and Plate IV. Oligocene to Miocene rocks in the western Cascades also appear to dip gently to the east, but north of 44°30' the homoclinal map pattern is obscured by unconformably overlying Pliocene and Miocene rocks. South of 44°N latitude, Oligocene to Miocene rocks regionally dip about 5° eastward [Sherrod and Smith, 1989]. The northern Willamette basin is formed by structurally downwarped Columbia River basalt unconformably overlain by younger sediments. The first-order downwarping as well as faults, secondary folds, and intrusion of Quaternary and Pliocene magma, are shown in Figure 28.

## FAULTS

### Eola-Amity Hills Subsurface Normal Faults

Two synthetic normal faults occur only in the subsurface beneath the Eola-Amity Hills (Figure 13 or Plate IV). The strike of the faults is poorly constrained, however, the Amity lineation, which is based on residual gravity contours and corresponds to the faults, trends NNE (refer to Gravity section). Both faults appear to dip steeply to the east. They offset the Eocene Siletz River Volcanics and Yamhill Formation down to the east. The Eocene Yamhill Formation thickens from 950 m to 1450 m, a total of 500 m, across both faults based on stacking velocities.

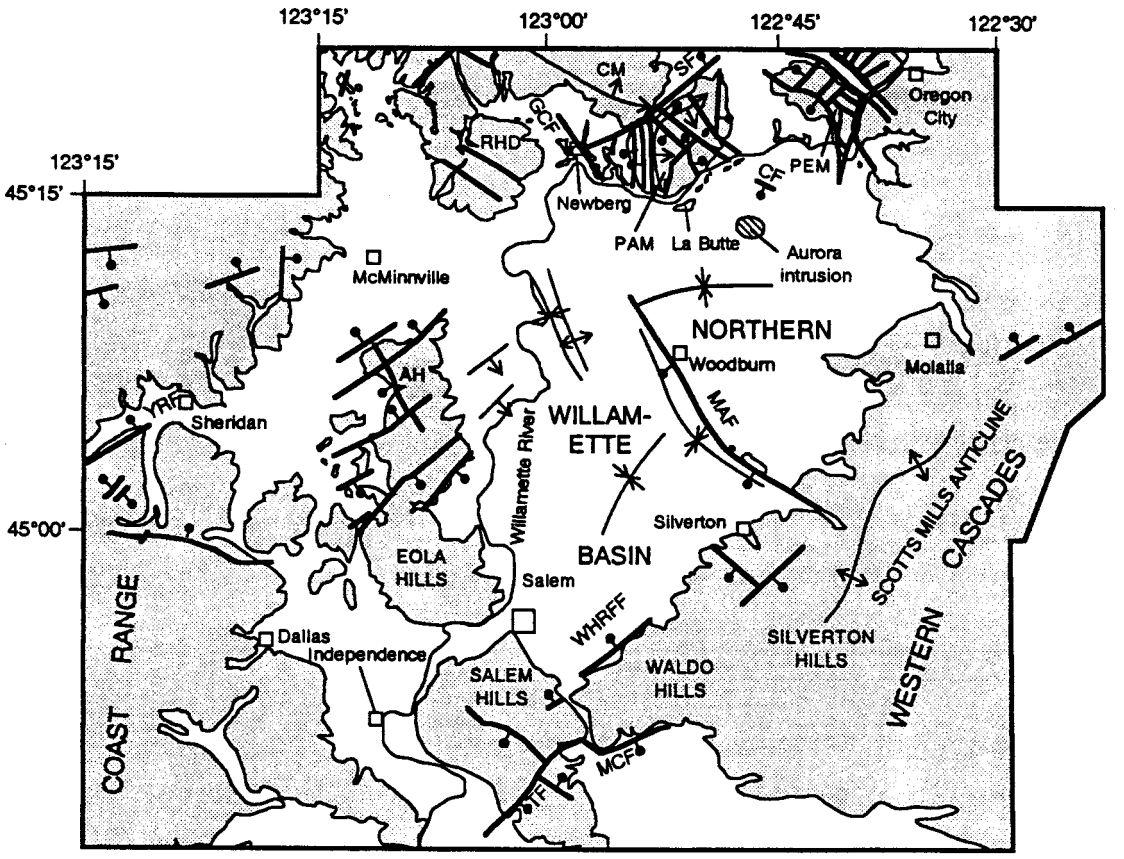


Figure 28. Tectonic map showing faults, fold axes in bedrock (lines with one arrow correspond to homoclines), and contact between bedrock and Quaternary and Pliocene sediments. Hills and mountains are abbreviated as follows: AH = Amity Hills; CM = Chehalem Mountains; PAM = Parrett Mountain; PEM = Petes Mountain; and RHD = Red Hills of Dundee. Faults are abbreviated as follows: CF = Curtis fault; GCF = Gales Creek fault; SF = Sherwood fault; TF = Turner fault; WHRFF = Waldo Hills range-front fault; and YRF = Yamhill River fault.

The two faults were active before and during deposition of the the Yamhill Formation based on differential offset of reflectors within the underlying upper Siletz River Volcanics and lower part of the Yamhill Formation. Overlying reflectors are interpreted as corresponding to the upper Yamhill and lower Spencer formations. Slight warping of the reflectors directly above the westernmost fault indicates that deformation appears to have continued until part of the overlying Spencer Formation had been deposited (Figure 13).

**Waldo Hills Range-Front Fault**

Information about the northeast-trending Waldo Hills range-front fault is based largely on the linearity of the Waldo Hills range front, geologic mapping by Hampton [1972], and water-well data (Plate IV, Figure 28 and 29). Side-looking radar images show a prominent lineation along the Waldo Hills range-front which corresponds to the fault and suggest that it may extend along a greater portion of the range front than shown in Figure 28. The north side of the Waldo Hills range-front fault is downthrown.

The lineation continues northeast of the Waldo Hills and corresponds to faults mapped east of Molalla. The faults east of Molalla, north side downthrown, are based largely on a break in slope that corresponds to the northwest limit of middle and upper (?) Miocene andesite (included in PMu on Plate I) [written communication, Sherrod, 1990]. Goldfinger [1990] also suggested a possible connection of the Waldo Hills range-front fault to the Corvallis fault, which lies further southwest along the same lineation.

Hampton's [1972] mapping indicates that sedimentary rock, which appears to be Oligocene and Eocene (refer to Stratigraphy section) along the base of the Waldo Hills, crops out below Columbia River basalt (Plate II). Two deep water wells southeast of the fault penetrate Columbia River basalt and reach "gray clay" and "blue" or "gray shale" interpreted to be Oligocene and Eocene sediments (Figure 29). Northwest of the fault, water wells indicate the altitude of the top of Columbia River basalt is lower than the altitude of the base of the Columbia River basalt in the Waldo Hills (Figure 29). However, some apparent offset may be from erosion of Oligocene and Eocene strata north of the fault

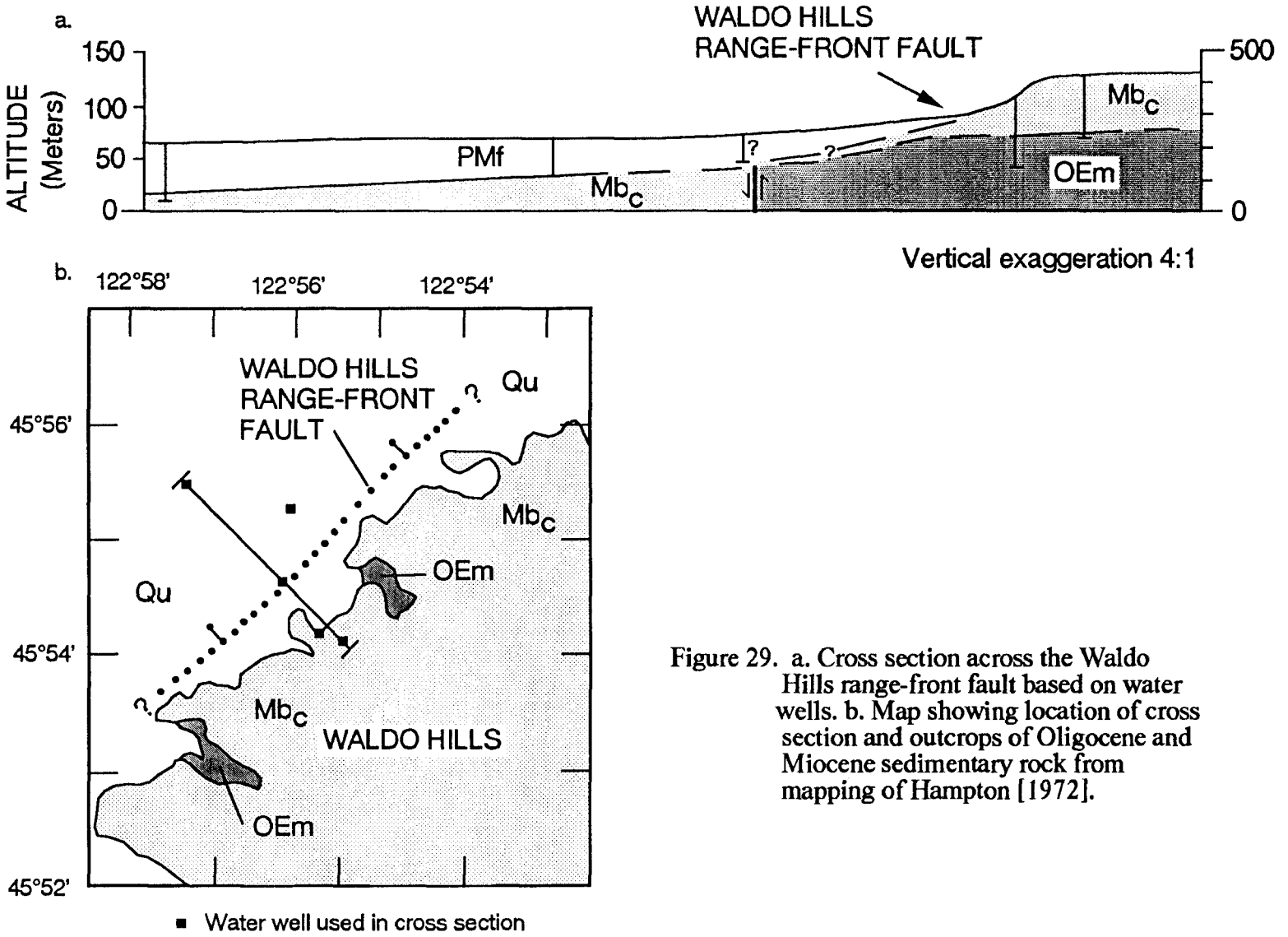


Figure 29. a. Cross section across the Waldo Hills range-front fault based on water wells. b. Map showing location of cross section and outcrops of Oligocene and Miocene sedimentary rock from mapping of Hampton [1972].

before emplacement of Columbia River basalt. The age of faulting is at least mid-Miocene or younger based on offset of the top of Columbia River basalt. It is not known if the fault deforms younger sediments.

### Yamhill River-Sherwood Structural Zone

The Yamhill River-Sherwood structural zone trends northeast and appears to include the Yamhill River and Sherwood faults (Plate I). A lineation on the residual gravity anomaly map corresponds to the Yamhill River-Sherwood structural zone southwest of Willamina and northeast of Newberg, but not in the McMinnville area presumably due to the lack of a large density contrast.

The Yamhill River fault was mapped by Baldwin et al. [1955] and Brownfield [1982a, b] along the Yamhill River. It extends approximately 24 km west of Plate I [MacLeod, 1969], and appears to continue northeastward along the northern end of the Amity Hills based on proprietary seismic data. The fault vertically separates Eocene Yamhill strata down to the northwest. Baldwin et al. [1955] estimate the maximum vertical separation is greater than 300 m.

The Sherwood fault is a major fault between the Parrett and Chehalem Mountains that has 100-150 m of vertical separation [Hart and Newcomb, 1965; Beeson et al., 1989a]. Beeson et al. [1989a] have suggested that it corresponds to the northern boundary of the Sherwood trough through which Columbia River basalt flowed to the coast.

### Salem and Eola-Amity Hills Northwest and Northeast Striking Faults

The conjugate faults located in the Eola-Amity and Salem Hills were mapped by Brownfield and Schlicker [1981a, b] and Hoffman [1981], respectively (Plate I). Some faults in the Eola-Amity Hills were inferred from aerial photos [Brownfield and Schlicker, 1981a, b]. They predominantly strike N35°E to N65°E except for one fault striking N27°W to N40°W.

The western extent of several NE-striking faults in the Eola and Amity Hills has been lengthened and new faults added based on a proprietary seismic reflection line west of

the Eola and Amity Hills. Faults on the seismic reflection line are consistent in location and sense of offset with the mapping of Brownfield and Schlicker [1981a, b].

The NW-striking fault in the Eola-Amity Hills, down to the southwest, is not evident on the east-west seismic line, which crosses the Amity Hills (Figure 14). The lack of offset reflectors on the seismic line corresponding to the mapped fault indicates either that vertical separation is minor and not resolvable, or the fault does not exist.

The faults in the Salem Hills are based on offset of Columbia River basalt flows, and the vertical separation across the faults ranges from 15 to 30 m [Hoffman,1981]. The Mill Creek fault may be offset from the Turner fault. It appears to form a northern basin bounding fault for the Stayton basin and is largely based on Oligocene and Eocene strata cropping out below Columbia River basalt similar to the Waldo Hills range-front fault.

**Gales Creek-Mt. Angel Structural Zone**

The Gales Creek-Mt. Angel structural zone consists of the NW-trending Mt. Angel and Gales Creek faults [Beeson et al., 1985] which extend across much of northwestern Oregon. An intervening seismic reflection line across the northern Willamette Valley indicates that the two faults are not continuous in strata younger than Columbia River basalt.

The Gales Creek fault, or a fault en echelon to it, extends southeastward to Newberg (Plate I and Figure 30). In the Newberg area, the southwest side of the fault is downthrown based on geologic mapping and water wells. This sense of offset contradicts the sense of motion further northwest where Columbia River basalt northeast of the fault is downthrown relative to Tillamook volcanics southwest of the fault [Jackson, 1983].

In the Newberg area the base of Columbia River basalt north of the fault occurs along the base of the Chehalem Mountains and dips northeastward (Figure 30). On the south side of the fault, Columbia River basalt occurs in the Red Hills of Dundee and also dips northeastward (Figure 30). This geometry results in the juxtaposition of Columbia River basalt on the south side of the fault against Oligocene and Eocene marine strata on the north side. Several deep water wells north of the fault drill through a thick section of blue

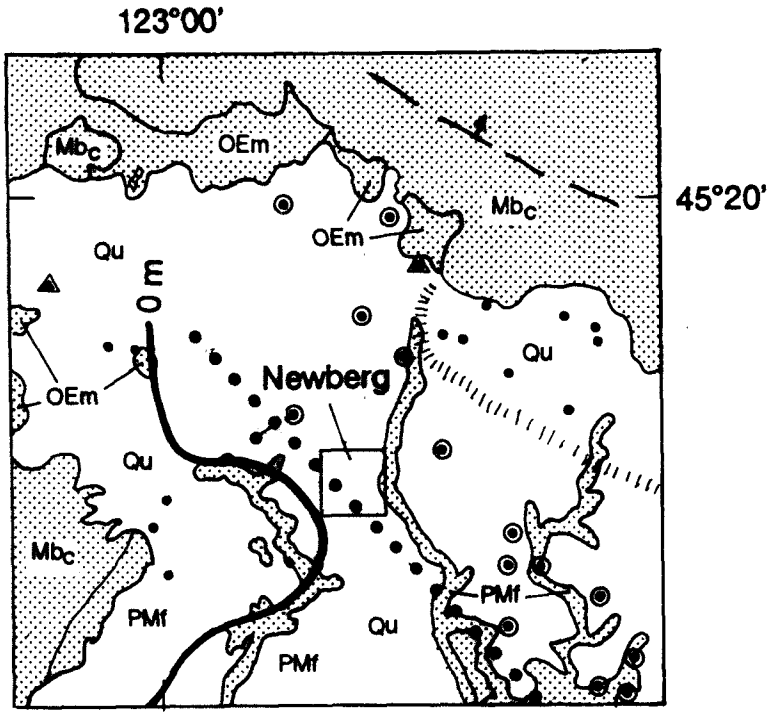


EXPLANATION

Concealed fault; ball and bar on downthrown side.

Homocline, arrow shows direction of dip.

Altitude to the top of Columbia River basalt.

Columbia River basalt - Oligocene and Eocene sedimentary rock subcrop.

Water well - reaches Columbia River basalt, located to quarter-quarter section.

Water well - Constrains altitude of contoured horizon, located to quarter-quarter section.

Water well - Constrains altitude of contoured horizon, accurately located based on Ground-Water Report.

Figure 30. Map showing the location of the Gales Creek fault or a fault en echelon to it.

clay confirming the absence of Columbia River basalt, while water wells south of the fault drill through >40 m of basalt.

Hampton [1972] originally mapped the Mt. Angel fault in the northern Willamette Valley from the edge of the Waldo Hills to just northwest of the city of Mt. Angel based on water-well data and outcropping Columbia River basalt near Mt. Angel (Figure 2). By incorporating commercial seismic-reflection data, the fault can now be extended northwestward to Woodburn (Figure 31). The southeast extent of the fault is poorly constrained due to poor exposure in the Waldo Hills. However, the fault probably continues into the Western Cascades, where it appears to have formed a barrier to three of four Silver Falls flows of the Miocene Columbia River basalt [Beeson et al., 1989a]. In addition, a Ginkgo intracanyon flow is dextrally offset approximately 1 km across the fault due to faulting or a sharp jog in the canyon [M. Beeson, personal communication, 1989].

The Mt. Angel fault vertically offsets Columbia River basalt and younger sedimentary strata down to the southwest. The amount of vertical offset on the top of Columbia River basalt increases to the southeast as shown by cross sections A-A', B-B', and C-C' (located on Figure 32). The vertical offset is approximately 100 m on seismic section A-A' (Figure 33), 200 m on seismic section B-B' (Figure 34), and 250+ m on cross section C-C' (Figure 35). The amount of offset for cross sections A-A' and B-B' is based on calculations using average velocity and stacking velocities, which are in general agreement.

The 250+ m of separation on cross section C-C' is based on the difference in altitude between the top of Columbia River basalt in a water well and the altitude of Mt. Angel (Figure 35). Mt. Angel has an elevation of 85 m above the valley floor and is composed of both Grande Ronde basalt and the younger Frenchman Springs Member of the Columbia River Basalt Group [M. Beeson, personal communication, 1990]. The presence of the Frenchman Springs member at the top of Mt. Angel indicates that little of the Columbia River basalt section has been eroded away, so the displacement is probably

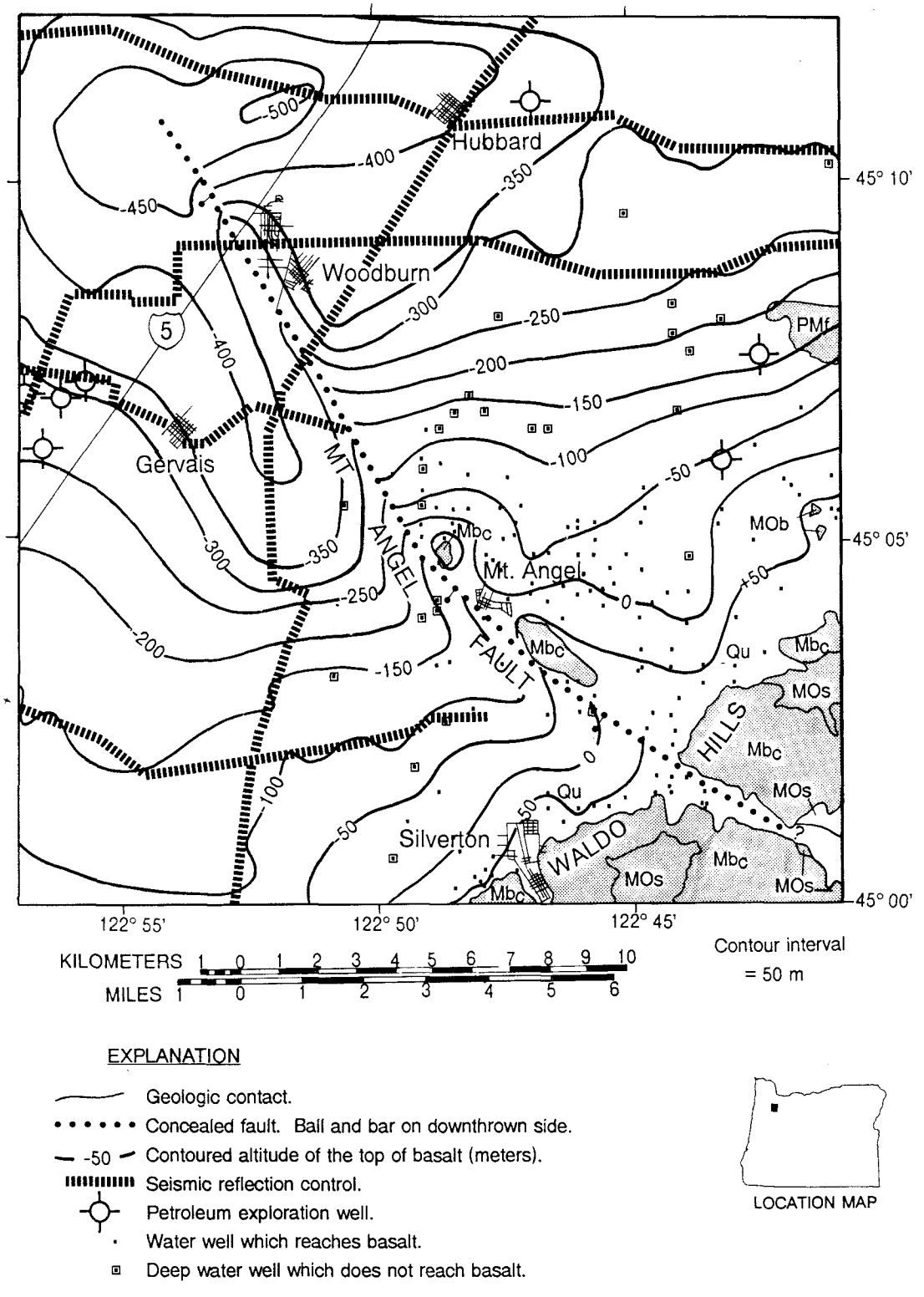


Figure 31. Contour map on the top of basalt, which is primarily Columbia River basalt except near outcropping MOb. Geologic units are labelled as follows: Qu = Quaternary undifferentiated sediment; PMf = Pliocene and Miocene fluvial and lacustrine sediment; $Mb_C$ = Miocene Columbia River basalt; MOs = Miocene and Oligocene sedimentary rock; MOb = Miocene and Oligocene basalt.

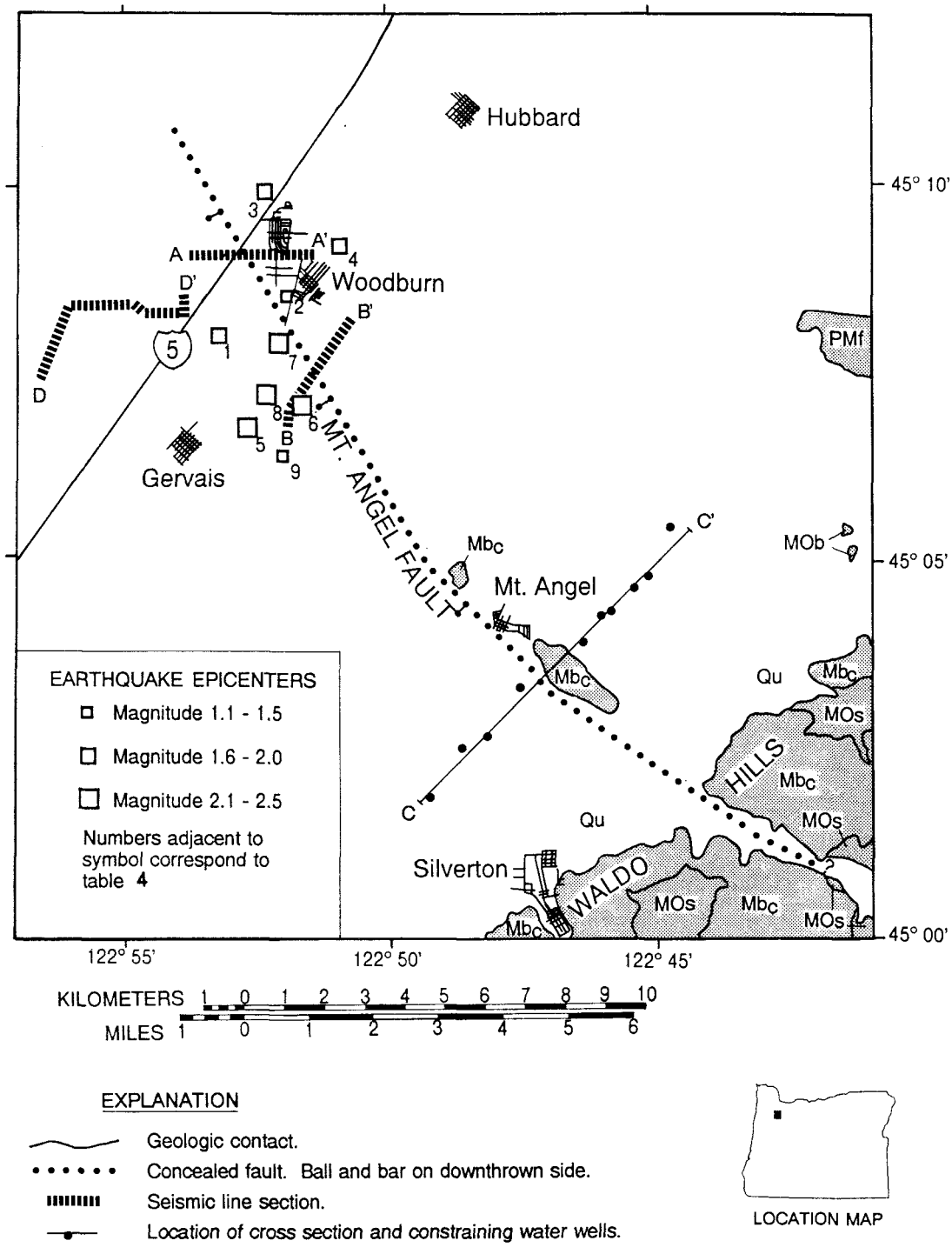


Figure 32. Epicenters of earthquakes near the Mt. Angel fault and location of seismic and water-well cross sections. Number corresponding to each earthquake refers to Table 4. Geologic units are labelled as follows: Qu = Quaternary undifferentiated sediments; PMf = Pliocene and Miocene fluvial and lacustrine sediments; $Mb_C$ = Miocene Columbia River basalt; MOs = Miocene and Oligocene sedimentary rock; MOb = Miocene and Oligocene basalt.

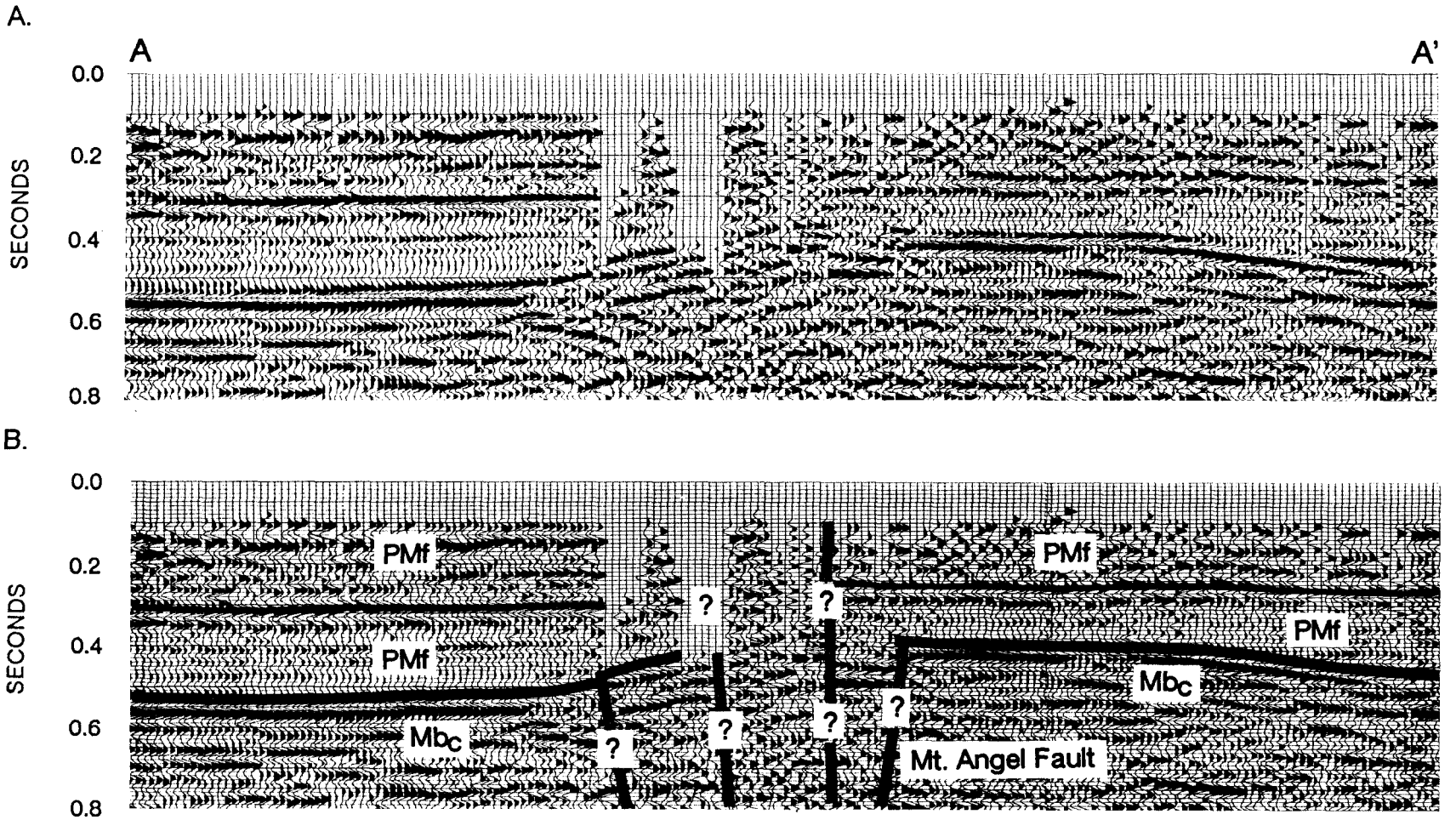


Figure 33. Seismic section A-A' across Mt. Angel fault. Location of seismic section shown in Figure 32.

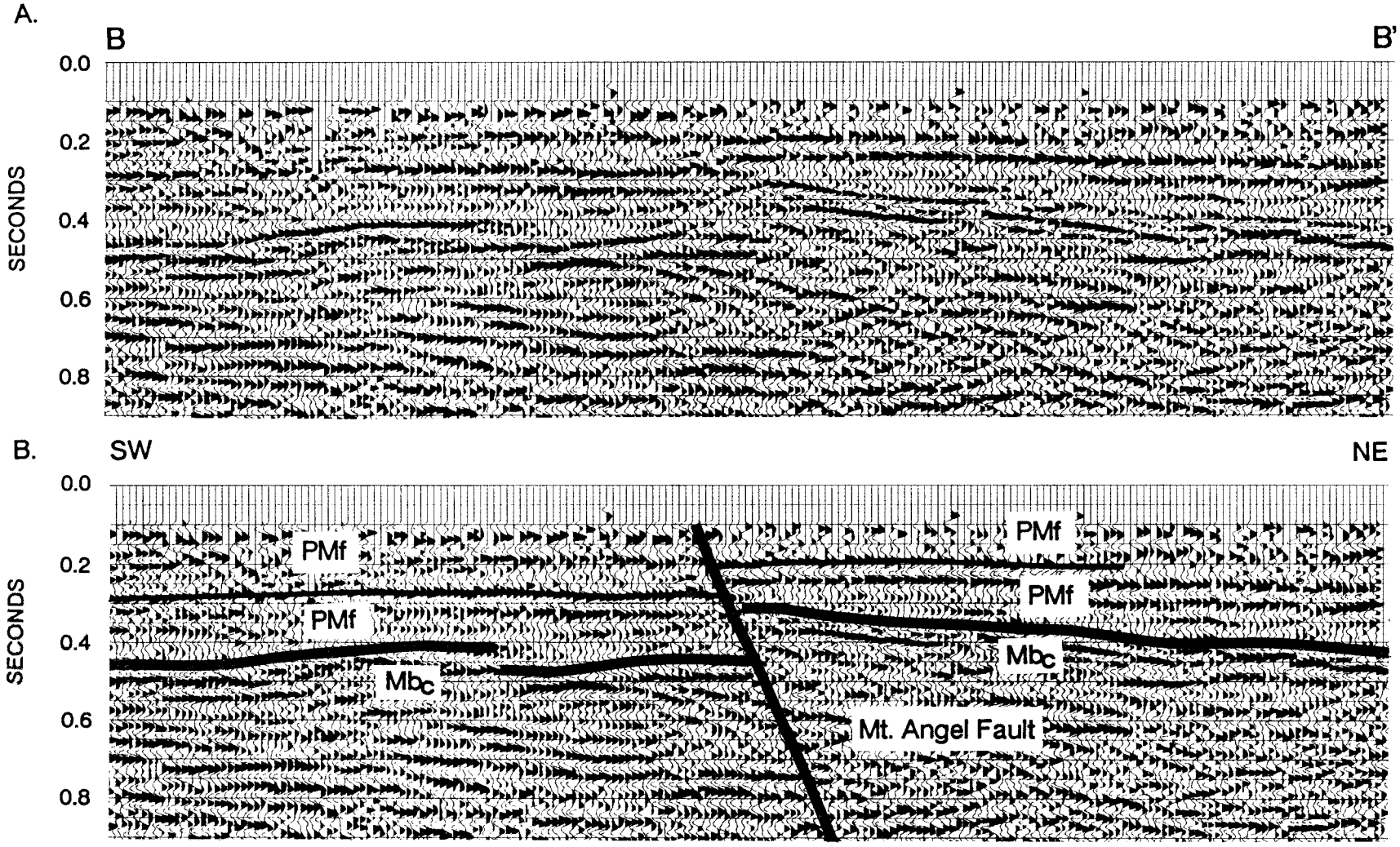


Figure 34. Seismic section B-B' across Mt. Angel fault. Location of seismic section shown in Figure 32.

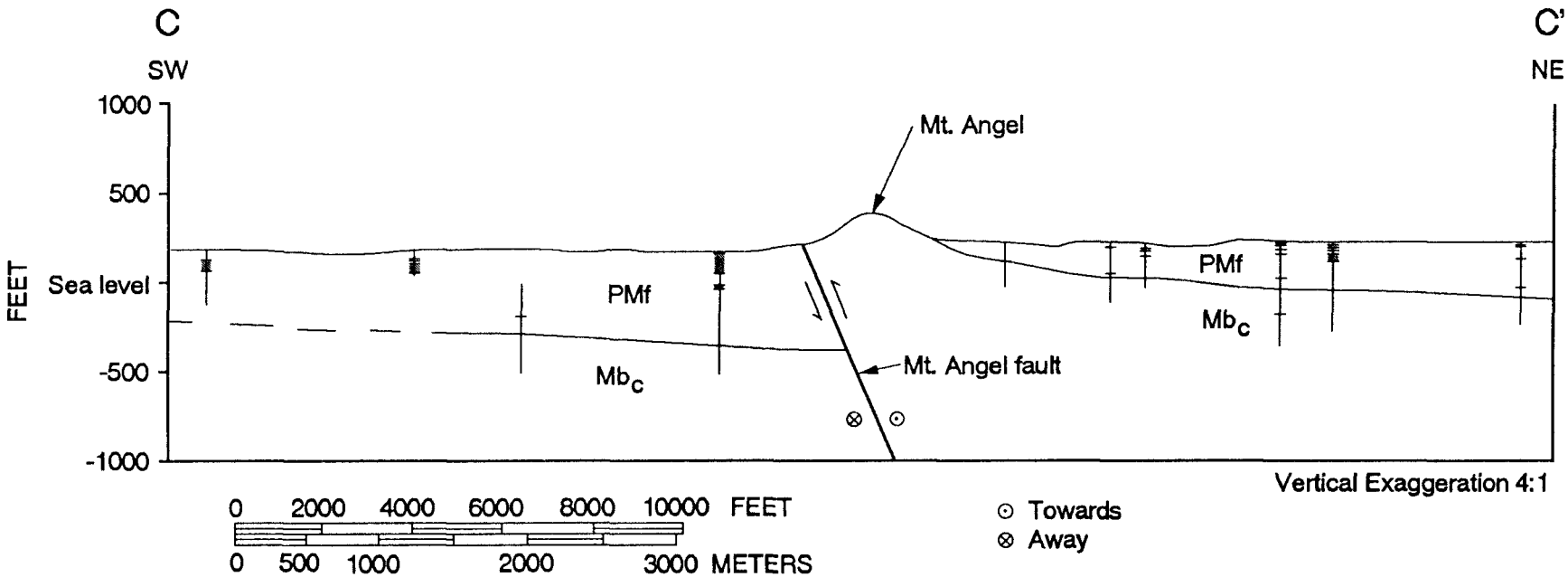


Figure 35. Structural cross section of Mt. Angel fault based on water wells. A few wells were located using personal communication with farmers or a driller from Staco Well Services. Only those parts of wells with available well logs are shown. PMf = Pliocene and Miocene fluvial and lacustrine sediments and $Mb_c$ = Miocene Columbia River basalt. The base of $Mb_c$ is unconstrained. Conglomerate intervals are indicated by two horizontal lines with shading between them. Very thin conglomerate lenses are shown by just a horizontal line. The dip on the fault is based on estimates from seismic line section B-B'. The cross section is located in Figure 32.

not much more than 250 m. The 250+ m offset determined at Mt. Angel may not represent the net vertical separation across the entire Mt. Angel fault zone. Based on the steep NE side of Mt. Angel, the topographic high of Mt. Angel and the adjacent Columbia River basalt exposure to the northwest may be caused by a positive flower or pop-up structure faulted on both sides as shown in Figure 36 [from Woodcock and Fischer, 1986].

The dip of the Mt. Angel fault is poorly constrained. Based on offset reflectors from seismic line B-B' (Figure 34), the apparent dip on the near-surface portion of the fault is about 63°; the true dip is about 66°. The fault is difficult to locate in seismic section A-A' due in part to data gaps, and it may consist of more than one splay. Therefore, it is shown to be vertical (Figure 33).

The age of deformation associated with the Mt. Angel fault based on geologic evidence extends into the Pliocene to Miocene. The fault offsets and warps not only Columbia River basalt, but younger sediments. A reflector in Pliocene and Miocene fluvial and lacustrine sediments along seismic section B-B' appears to be vertically separated across the Mt. Angel fault 41 to 96 m, depending on which reflectors are matched across the fault. The author prefers the reflector offset shown in Figure 34, an offset of 96 m. In addition, the Pliocene and Miocene sediments are warped into a syncline on the southwest side of the fault as shown in Figure 25. Structural relief on the reflector in Pliocene and Miocene sediments is approximately 45 m.

Shallow deformation associated with the Mt. Angel fault appears to have occurred both before and during deposition of Pliocene and Miocene sediments. The definition from seismic lines is inadequate to determine if the the fault deforms younger sediments. An angular unconformity at the base of Pliocene and Miocene sediments indicates pre-sediment deformation. Onlapping Pliocene and Miocene sediment reflectors are themselves warped indicating continued deformation during or after their deposition (Figures 33 and 34). In addition, the reflector corresponding to the top of Columbia River basalt is vertically

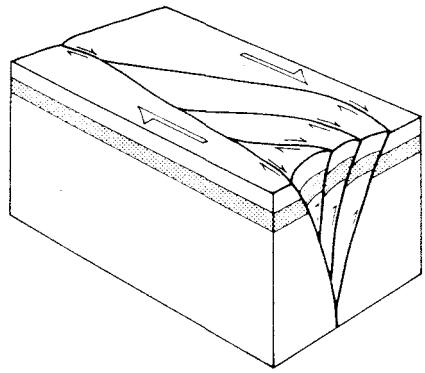

Figure 36. Schematic three-dimensional model of a Mt. Angel pop-up structure from Woodcock and Fischer [1986]. The number of splays shown does not necessarily correspond to the Mt. Angel fault.

separated across the Mt. Angel fault more than reflectors in the overlying Pliocene and Miocene fluvial and lacustrine sediments due to progressive displacement along the fault.

A series of 6 small earthquakes with coda magnitudes ($m_C$) = 2.0, 2.5, 2.4, 2.2, 2.4, 1.4, occurred on August 14, 22, and 23, 1990 with epicenters in the vicinity of the northwest end of the Mt. Angel fault near Woodburn (Figure 32, Table 4). Epicentral errors for these events are about ±2 km. Routine locations indicate a depth of about 30 km, in the lower crust, with a depth error of ±5 km. In 1980 and 1983, three events with $m_C \leq 1.7$ also occurred in this locality (Figure 32, Table 4).

The August series of events was recorded by the IRIS/OSU broadband seismic station in Corvallis (COR; epicentral distance 68 km) and the Washington Regional Seismograph Network. For all events, the waveforms recorded at any given station are remarkably similar, indicating essentially identical locations and mechanisms. Three alternative focal plane solutions, determined by J. Nábelek [written communication, 1990] and constrained by waveform modeling and first-motion data, are shown in Figure 37. The solutions were determined using a coarse grid search, i.e. varying strike from 320°-360° by 20° intervals, varying dip from 70°-110° by 20° intervals, and varying slip or rake from 140°-220° by 20° intervals [J. Nábelek, personal communication, 1990]. The preferred focal plane solution, resulting in the closest match between the forward modeled seismogram and the actual seismogram, is shown by the dashed lines. It is a right-lateral strike-slip fault with a small normal component on a plane striking N-S and dipping steeply to the west. The preferred solution is more northerly than the fault strike based on seismic-reflection data, however, small-magnitude earthquakes may occur on short en echelon fault segments oriented at up to 30° to the main fault trace.

The locations and focal mechanisms of the earthquakes are consistent with them being on a deep extension of the Mt. Angel fault. However, the association between the earthquakes and surface fault is weak because of the large depth of the earthquakes. The main point is the consistency of the tectonic stress implied by both.

Table 4. Woodburn seismicity

| Earthquake | Latitude | Longitude | Date | Magnitude |
|---|---|---|---|---|
| 1 | 45.133 | -122.886 | 7/3/80 | 1.7 |
| 2 | 45.142 | -122.874 | 8/20/83 | 1.2 |
| 3 | 45.165 | -122.871 | 9/9/83 | 1.6 |
| 4 | 45.153 | -122.847 | 8/14/90 | 2.0 |
| 5 | 45.113 | -122.877 | 8/14/90 | 2.5 |
| 6 | 45.118 | -122.860 | 8/22/90 | 2.4 |
| 7 | 45.132 | -122.867 | 8/22/90 | 2.2 |
| 8 | 45.120 | -122.871 | 8/23/90 | 2.4 |
| 9 | 45.107 | -122.866 | 8/23/90 | 1.4 |

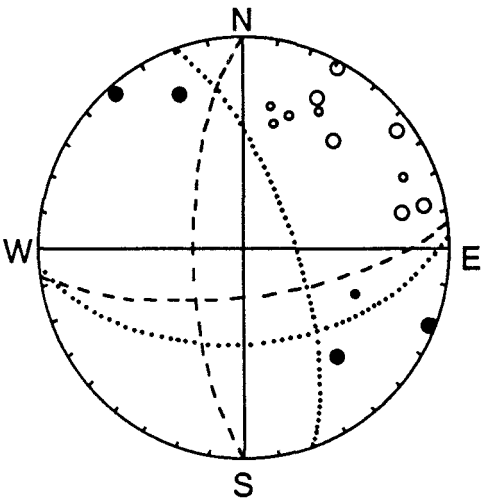


Figure 37. Composite focal mechanism for six August, 1990 earthquakes near Woodburn [from Nábelek, written communication]. Open circles indicate dilitation at a given station, filled circles indicate compression. Larger circles indicate a stronger first motion. Three separate focal mechanisms are indicated by solid, dashed, and dotted lines. The dashed focal mechanism is preferred.

## FOLDS

### Northern Willamette Basin

Plates I and II include a contour map on top of basalt which should correspond to Columbia River basalt throughout most of the basin except near La Butte and Marquam and possibly near Aurora and Curtis (Plate I and II). Within the northern Willamette basin, the top of the Columbia River basalt provides a useful surface for mapping post middle-Miocene deformation [Wells, 1989; Sherrod and Pickthorn, 1989; Beeson and Tolan, 1989]. The Columbia River basalt provides a useful surface to contour, because (1) it was extruded over a relatively short period of time, (2) it extends over much of the northern Willamette Valley, (3) its upper surface should have been flat at the time of emplacement, and (4) the upper surface should form an obvious density, velocity, and lithologic contrast with overlying sediments [Beeson and Tolan, 1989].

The contour map on the top of basalt forms a basin flanked steeply to the north, gently to the south, and centered just north of Woodburn (Plates I and II). The main syncline axis trends N80°E, although the trend is poorly defined. The syncline axis roughly corresponds to a another eastward plunging syncline axis along the southern Yamhill River discussed by Baldwin et al., [1955] and Brownfield [1982a] (they fail to show the syncline axis due to lack of geologic control). The top of Columbia River basalt in the northern Willamette Valley is downwarped to an altitude of less than -500 m, and total structural relief on the top of Columbia River basalt exceeds 1 km (Plate I).

Pliocene and Miocene sediments in the northern Willamette Valley are also broadly downwarped, although to a lesser degree, based on proprietary seismic-reflection data. Similarly, the contact between the Sandy River and Troutdale formations has regional dips of up to 2° in the Portland basin [Trimble, 1963; Swanson, 1986].

Timing of warping is poorly constrained. In the Yakima fold belt of central Washington, the main growth of folds of Columbia River basalt was 17-13 Ma, although folding continued into the Quaternary [Reidel, 1984; Sherrod and Smith, 1989].

However, in the northern Willamette Valley, significant folding did not appear to start until after emplacement of the Frenchman Springs member of the Wanapum basalt, based on the lack of Frenchman Springs member along the axis of the syncline. Folding appears to have continued at least into the late Miocene.

### Scotts Mills Anticline

The northeast-trending Scotts Mills anticline is one of several northeast-trending parallel folds in the Western Cascades [Miller and Orr, 1988]. Miller and Orr [1986] estimate average dips of the warped Scotts Mills and Molalla Formations are less than 10°, and closure of the fold is on the order of several hundred meters. Columbia River basalt appears to be thinner along the axis of the fold (Plates I and II), indicating that either the fold began growing before the middle Miocene or erosion removed the Columbia River basalt before deposition of the overlying Pliocene and Miocene strata. In general, fold growth in the northern Cascades occurred largely between 17 to 11 (?) Ma [Sherrod and Smith, 1989].

## INTRUSIONS AND RELATED FAULTING

Intrusion of Boring Lava played an important role in Pliocene-Quaternary deformation of the northern Willamette Valley. Intrusions outcrop at Highland Butte and La Butte, and probably occur in the subsurface near Aurora and Curtis. The intrusions at La Butte, Aurora, and Curtis are located at the southwestern end of the Bonneville-Yamhill lineament, which corresponds to several Boring Lava vents mapped by Allen [1975] in the Portland area.

Normal faults possibly associated with intrusion of Boring Lava are located at Parrett and Petes Mountain, Aurora, Curtis, and Swan Island (along the Molalla River). Generally, faulting associated with igneous intrusions is related to stretching and doming from influx of magma or to collapse associated with evacuation of the magma [Suppe, 1985].

### Faults at Parrett and Petes Mountain

The faults at Parrett and Petes Mountain, mapped by Beeson and Tolan [unpublished mapping, 1990], are based on aerial photographs and the juxtaposition of Columbia River basalt flows identified using geochemistry [Beeson et al., 1975]. Most of the faults are normal faults which form collapse features. They typically displace flows 10s of meters, although the net displacement may be as much as 100s of meters as suggested by water well data along the southern end of Petes Mountain and confirmed by M. Beeson for other faults [personal communication, 1990]. The fault pattern has a wide variety of strikes and is relatively closely spaced, typical of faulting related to igneous intrusion [Suppe, 1985]. Beeson et al. [1975] have suggested that similar faults located north of Oregon City (Lake Oswego and Gladstone 7 1/2' quadrangles) may have occurred from subsidence accompanying emptying of magma chambers and extrusion of Boring Lava.

### Aurora Intrusion

The "Aurora intrusion" appears to occur in the subsurface of the northern Willamette Valley just west of Aurora (Figure 38 or Plate I) based largely on chaotic reflectors shown in seismic section E-E' (Figure 39). The "Aurora intrusion" is 720 m wide near the surface (at a two-way time of 0.1 seconds) and appears to thin with depth. Water wells west of Aurora reach "basalt" (unknown identity) at a depth of 20 m. Minor steeply-dipping faults occur on the northern flank of the high associated with the chaotic reflectors. The faults offset the top of Columbia River basalt and overlying Pliocene and Miocene sediments. They are probably associated with stretching and updoming from intrusion of magma.

The location and timing of the "Aurora intrusion" indicate the intruding rock is Boring Lava. The intrusion is located near outcropping Boring Lava at La Butte and Highland Butte (Plate I). Timing of the intrusion is constrained by reflectors overlying the Columbia River basalt, which correspond to the lower Pliocene and Miocene sediments.

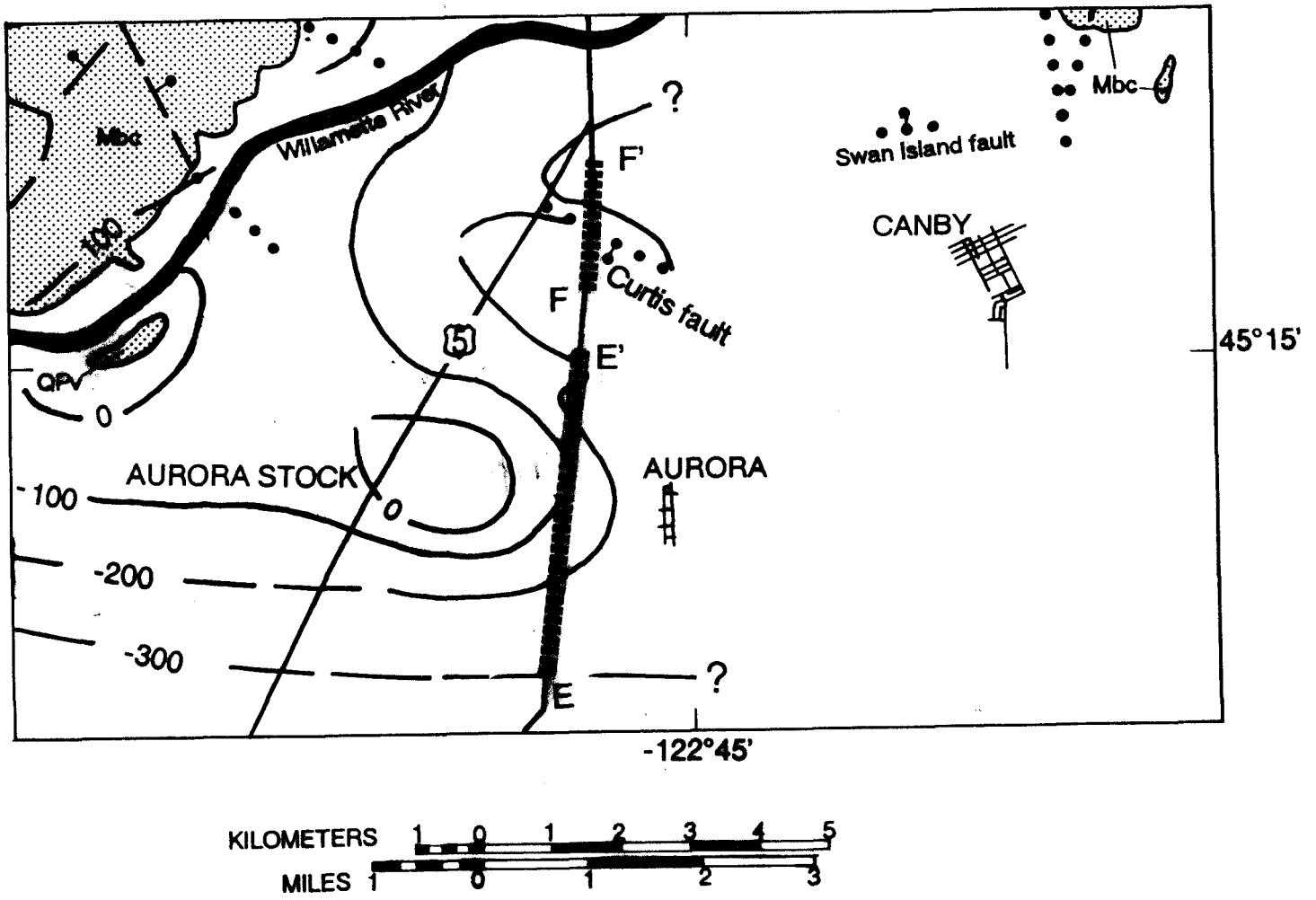


Figure 38. Location map showing seismic sections E-E' and F-F' in the northeastern part of the northern Willamette Valley. Contours correspond to subsea altitude in meters of the top of Columbia River basalt.

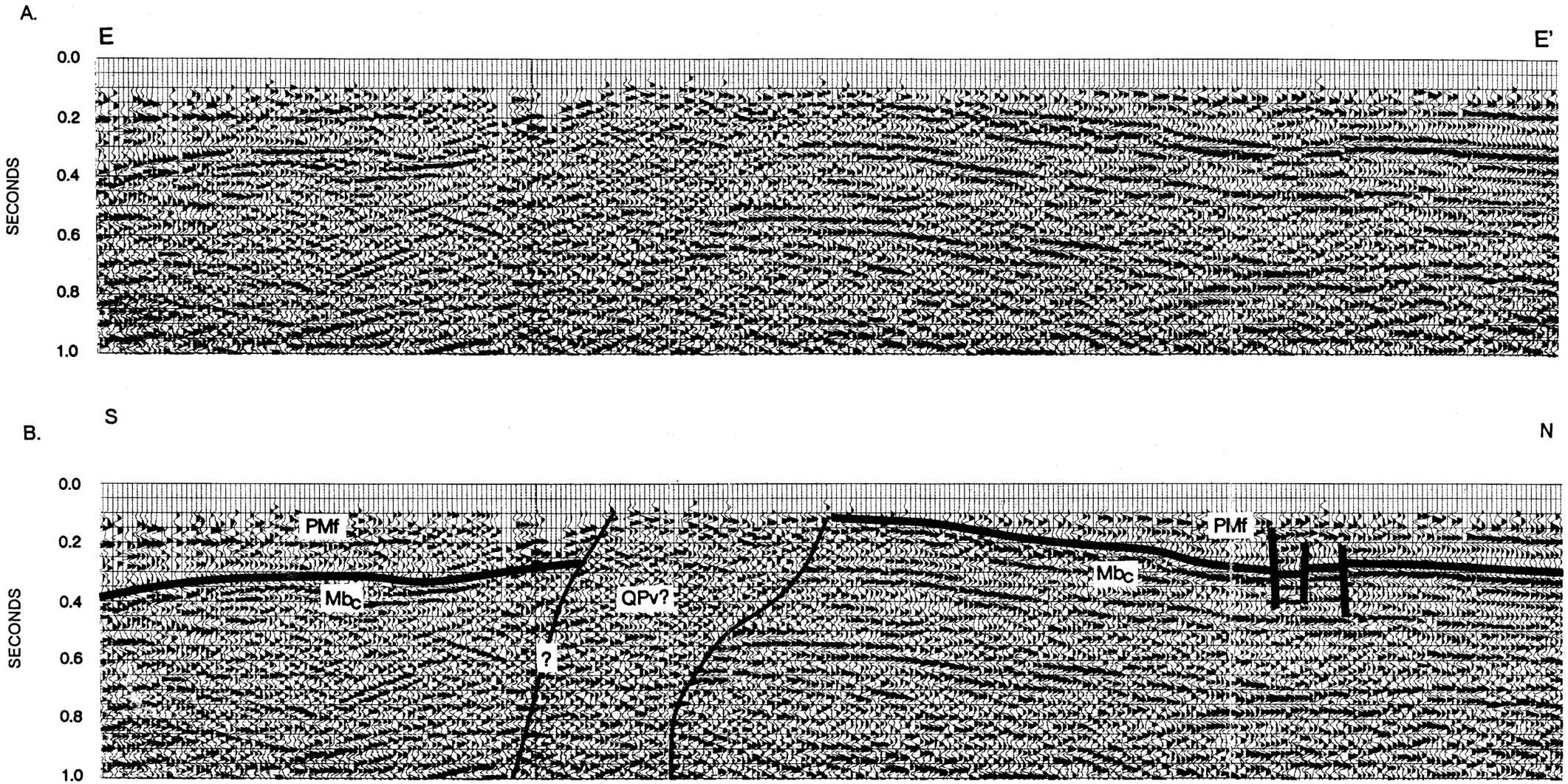


Figure 39. Seismic section E-E' showing "Aurora intrusion". Refer to Figure 38 for seismic section location. $Mb_C$ = Miocene Columbia River basalt, PMf = Pliocene and Miocene fluvial sediments, and QPv = Quaternary and Pliocene volcanics (Boring Lava).

These reflectors are warped as much as the underlying Columbia River basalt indicating the intrusion was emplaced after Columbia River basalt flowed into the northern Willamette Valley.

In the Portland area, Boring Lava appears to have been extruded primarily along pre-existing NW- and NE-trending fractures [Beaulieu, 1971; Allen, 1975; Baldwin, 1981]. Similarly, the Boring Lava at La Butte and the "Aurora intrusion" may have been emplaced along a common fracture.

**Curtis Fault**

The Curtis fault occurs in the subsurface of the northern Willamette Valley just east of Curtis (Figure 38 or Plate I), where it appears to offset Columbia River basalt as shown on seismic section F-F' (Figure 40). The Curtis fault is interpreted to be caused by intrusion of magma, possibly Boring Lava (QPv). The intrusion of magma may have caused a trapdoor uplift of sedimentary rock (?) and overlying Columbia River basalt. The top of Columbia River basalt is hinged to the south and steeply faulted to the north. The distance from hinge to fault is approximately 605 m. The top of Columbia River basalt is vertically separated about 140 m across the fault based on calculations using average velocity (from Figure 9) and about 160 m based on calculations using stacking velocities.

Timing of deformation related to the "Curtis intrusion" and the associated fault is poorly constrained by reflectors overlying the Columbia River basalt. Post-Columbia River basalt reflectors onlap the top of Columbia River basalt, suggesting they were deposited after the intrusion had largely been emplaced. Based on seismic section F-F', it is unclear if post-Columbia River basalt reflectors are also gently upwarped (figure 40). If post-Columbia River basalt reflectors are warped, then deformation continued until after deposition of Pliocene and Miocene sediments and the magma is most likely related to Boring Lava. However, the post-Columbia River basalt reflectors may be flat in which case the fault and intrusion are older.

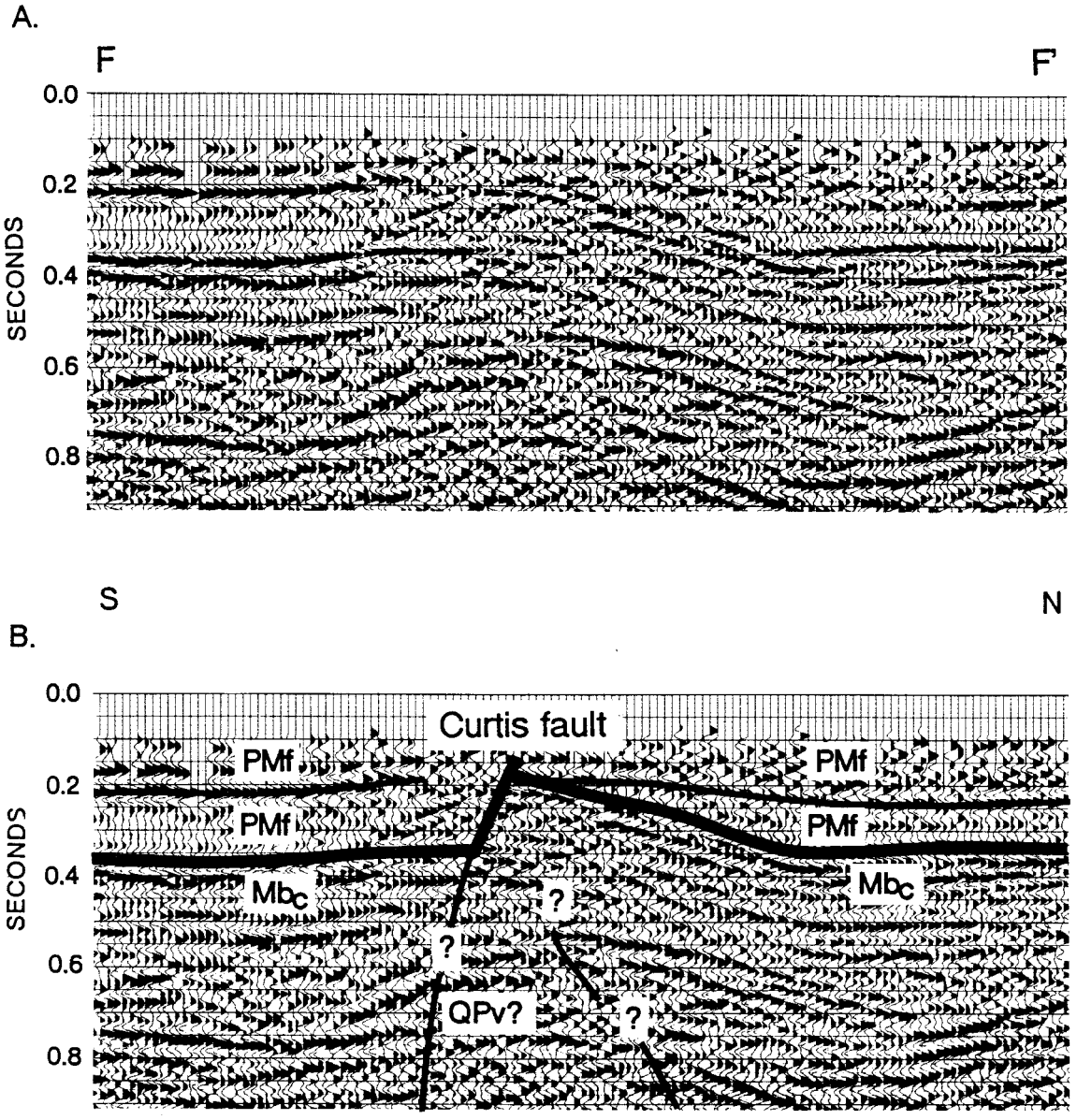


Figure 40. Seismic section F-F' showing Curtis fault. Refer to Figure 38 for seismic section location. $Mb_C$ = Miocene Columbia River basalt, PMf = Pliocene and Miocene fluvial sediments, and QPv = Quaternary and Pliocene volcanics (Boring Lava).

### Swan Island Fault

The Swan Island fault was identified by Glenn [1965] along the east bank of the Molalla River near Canby (behind Swan Lake Farms) (Plate I). The fault dips steeply to the north, and vertically separates a mud bed beneath the Willamette Formation 1 m down to the north (Figure 41). The fault does not cut the overlying Willamette Formation [Glenn, 1965].

The unit underlying the Willamette Formation appears to be the Rowland Formation, although the characteristic paleosol at the top of the Diamond Hill member is absent [Glenn, 1965], and it is possible that the mud is Pliocene or Miocene. Pliocene and Miocene fluvial and lacustrine sediments are exposed nearby at Highland Butte. Assuming the mud bed occurs in the Rowland Formation, the age of the most recent faulting event is a maximum of 28,500 yr old based on radiocarbon dates in the Diamond Hill member in the southern Willamette Valley (refer to Stratigraphy section). The fault may be related to Boring intrusion and may indicate that related doming or subsidence ended by the time the overlying Willamette Formation was deposited.


Figure 41. Photograph of the Swan Island fault taken by Glenn [1965] along the Molalla River facing northeast. Arrows show down to the north separation on the Swan Island fault. The dashed line along the ledge corresponds to interbedded mudstone. Unit I correlates to the Rowland Formation at River Bend. Unit II corresponds to the Willamette Formation.

# GRAVITY

Gravity stations in and adjacent to the northern Willamette Valley are shown in Figure 42 and Plates V and VI. Sources for the gravity data are the Defense Mapping Agency, the U.S. Geological Survey, Oregon State University, and Northwestern Geophysical Associates. These sources are denoted as filled circles on Plates V and VI. Additional sources include Goldfinger [1990] in the Corvallis area, denoted by squares on Plate V, and Beeson et al. [1975], Jones [1977], and Perttu [1981] in the Portland area, denoted by x's on Plate VI. The station density varies between tens of meters to tens of kilometers (Figure 42), so the magnitude and shape of some gravity anomalies may be controlled by relatively few stations.

## CALCULATION OF THE COMPLETE BOUGUER GRAVITY ANOMALY

The complete Bouguer gravity anomaly value for each station was calculated by the respective source using the general formula:

$$g_{CBA} = g_{obs} - g_{theor.} + \Delta g_{FA} - \Delta g_{B} + \Delta g_{T}$$

where $g_{obs}$ = observed station reading, $g_{theor.}$ = the theoretical gravitational attraction, $\Delta g_{FA}$ = the free-air correction, $\Delta g_{B}$ = the simple Bouguer correction, and $\Delta g_{T}$ = the terrain correction. The theoretical gravitational attraction depends on the latitude of the station and was determined using the International Gravity Formula of 1967 [IAG, 1971] with the 1971 Potsdam adjustment [Morelli, 1971]. The simple Bouguer correction (0.01276 * density * height in feet) was calculated for each station using a reduction density of 2.67 gm/cc, the average density for surface rocks of the earth [Nettleton, 1976]. It is assumed that the actual density does not vary significantly from 2.67 gm/cc. The terrain correction for each gravity station was determined slightly differently depending on the source.

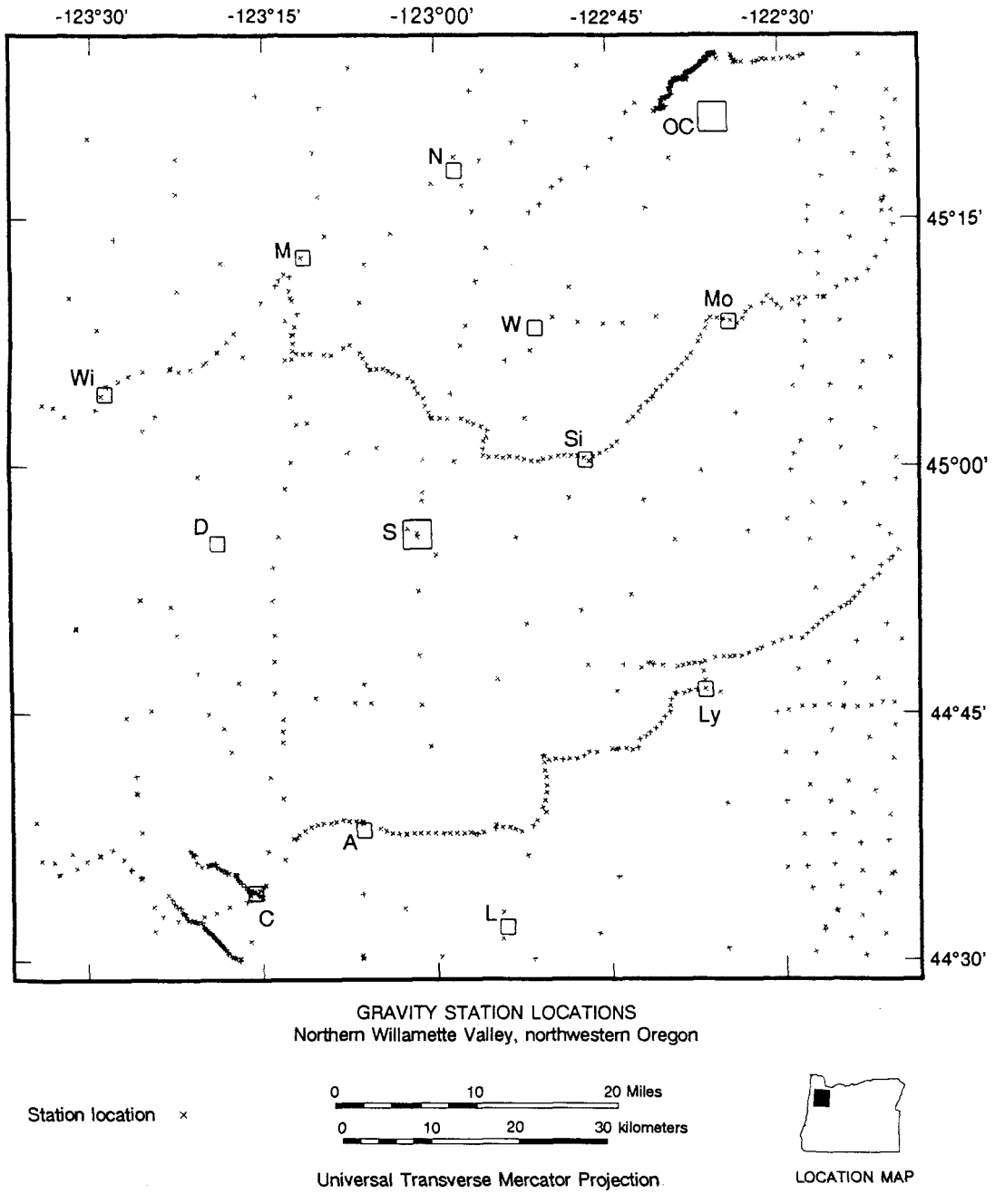


Figure 42. Gravity station locations. Sources for the gravity stations are discussed in the text. Cities are labelled from north to south as follows: OC = Oregon City; N = Newberg; M= McMinnville; Mo = Molalla; W = Woodburn; Wi = Willamina; Si = Silverton; S = Salem; D = Dallas; Ly = Lyons; A = Albany; C = Corvallis; L = Lebanon.

## COMPLETE BOUGUER GRAVITY ANOMALY MAP

Figure 43 shows the complete Bouguer gravity anomaly map of the northern Willamette Valley. The anomalies in Figure 43 range from >40 mgal in the Coast Range to <-90 mgal in the Cascades. The east-sloping gradient strikes NNE parallel to the continental margin, which is consistent with the regional gravity gradient that extends from northwestern California to southeastern Washington [Thiruvathukal, 1968; Pitts, 1979]. However, while the gradient between the Coast Range and the Cascades is relatively smooth south of Salem, a step or relatively flat area of the gradient occurs north-northeast of Salem. The relatively flat area is characterized by a series of shorter wavelength complete Bouguer gravity highs and lows which will be discussed in the residual gravity anomaly map section.

## SEPARATION OF REGIONAL AND RESIDUAL GRAVITY ANOMALIES

The separation of regional and residual gravity anomalies allows for the independent evaluation of gross large-scale anomalies and local anomalies respectively. Because the observed gravitational attraction is inversely proportional to the distance of a source body squared, increasing the depth of a given structure produces a gravity anomaly with a lower amplitude and greater wavelength [Couch et al., 1982a]. Long wavelengths are due to either deep crustal density contrasts or to broad, shallow density contrasts. Short wavelengths are due to shallow crustal density contrasts. In order to enhance shorter wavelengths, the complete Bouguer gravity anomaly was filtered using spectral separation. The technique used in this study is discussed at length by Pitts [1979], Braman [1981], and Veen [1981], and will only be briefly summarized below.

The complete Bouguer gravity values from the stations were gridded using the method of Briggs [1974], which honors data nearest the grid points, and connects the remaining grid points by minimizing local curvature; grid spacing is 0.5 km. Gravity stations shown in Figure 42 were combined with other stations between 43°45'N to 46°0'N

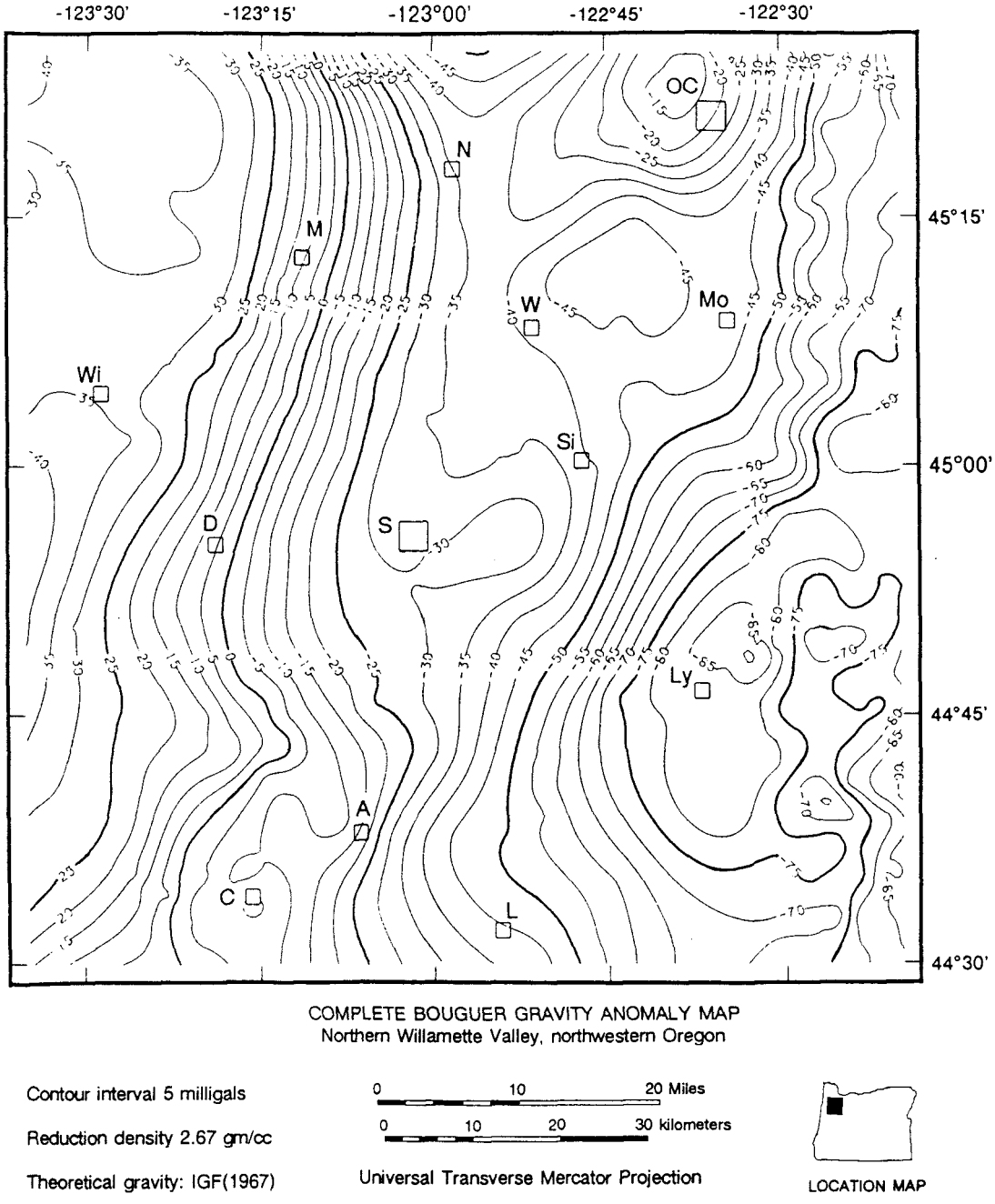


**Figure 43. Complete Bouguer gravity anomaly map of the northern Willamette Valley. Gravity stations are shown in Figure 42. Cities are labelled from north to south as follows: OC = Oregon City; N = Newberg; M= McMinnville; Mo = Molalla; W = Woodburn; Wi = Willamina; Si = Silverton; S = Salem; D = Dallas; Ly = Lyons; A = Albany; C = Corvallis; L = Lebanon.**

and -124°0'W to -122°0'W using the same sources listed above in addition to stations in Washington from the University of Puget Sound.

The gridded complete Bouguer gravity anomaly was detrended (removing a first-order plane from the data) and transferred into the frequency domain using the fast-Fourier transformation routine of Brenner [1968]. Shorter wavelengths corresponding to local effects were removed in the frequency domain using a low-pass filter. The data were filtered using the following cutoff wavelengths: 20 km, 30 km, 40 km, 50 km, and 60 km (corresponding to frequencies of 0.05 Hz, 0.033 Hz, 0.025 Hz, 0.02 Hz, 0.0166 Hz respectively). At wavelengths less than 50 km (frequencies greater than 0.02 Hz), anomalies corresponding to upper crustal geologic features become apparent on the regional gravity anomaly map. In order to avoid subtracting out these anomalies, the cutoff wavelength used for separation of regional and residual anomalies is 50 km (.02 Hz). Both the ideal filter, indicated by the dotted line, and the actual filter, indicated by the solid line, are shown in Figure 44. The actual filter is tapered and has a maximum of 6% error on both the upper and lower bands.

The filtered regional gravity anomaly was converted back to the spatial domain using a Fourier transform and retrended to produce the anomaly map shown in Figure 45. The regional gravity anomaly (Figure 45) was subtracted from the complete Bouguer gravity anomaly (Figure 43) to yield the residual gravity anomaly map (Plates V and VI; Figure 46). The residual gravity anomaly map thus contains wavelengths ≤50 km and should largely reflect density contrasts in the upper 10 km of the crust [R. Couch, personal communication, 1990].

## REGIONAL GRAVITY ANOMALY MAP

The regional gravity anomaly map (Figure 45) contains wavelengths greater than 50 km. The predominant gradient strikes north-northeast and decreases eastward from the Coast Range to the Cascades. At latitude 45°N, the regional gradient from the Coast Range

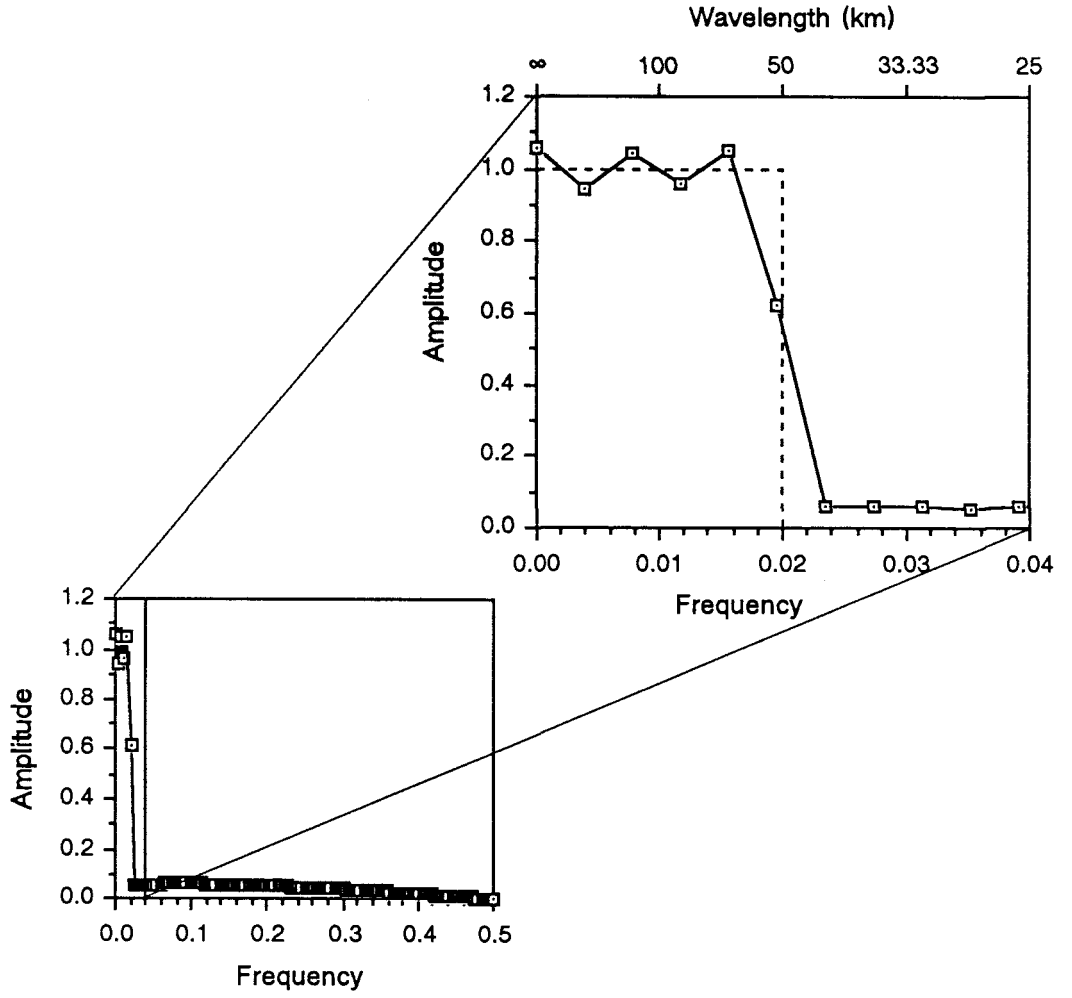


Figure 44. Amplitude spectrum of the low-pass filter used to generate regional gravity map containing 50 km and greater wavelengths.

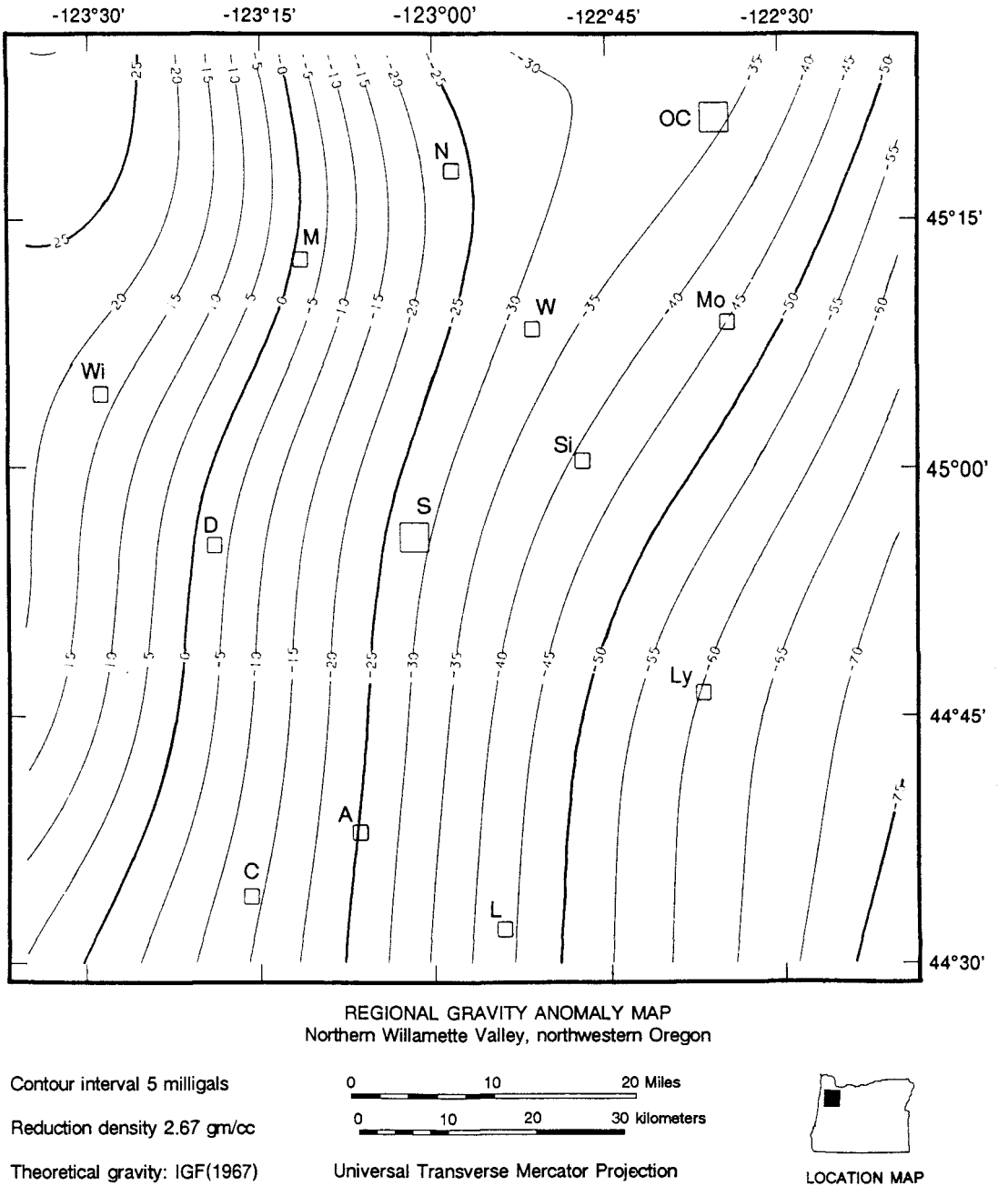


Figure 45. Regional gravity anomaly map of the northern Willamette Valley. Wavelengths less than 50 km have been filtered out. Gravity station locations are shown in figure 42. Cities are labelled from north to south as follows: OC = Oregon City; N = Newberg; M= McMinnville; Mo = Molalla; W = Woodburn; Wi = Willamina; Si = Silverton; S = Salem; D = Dallas; Ly = Lyons; A = Albany; C = Corvallis; L = Lebanon.

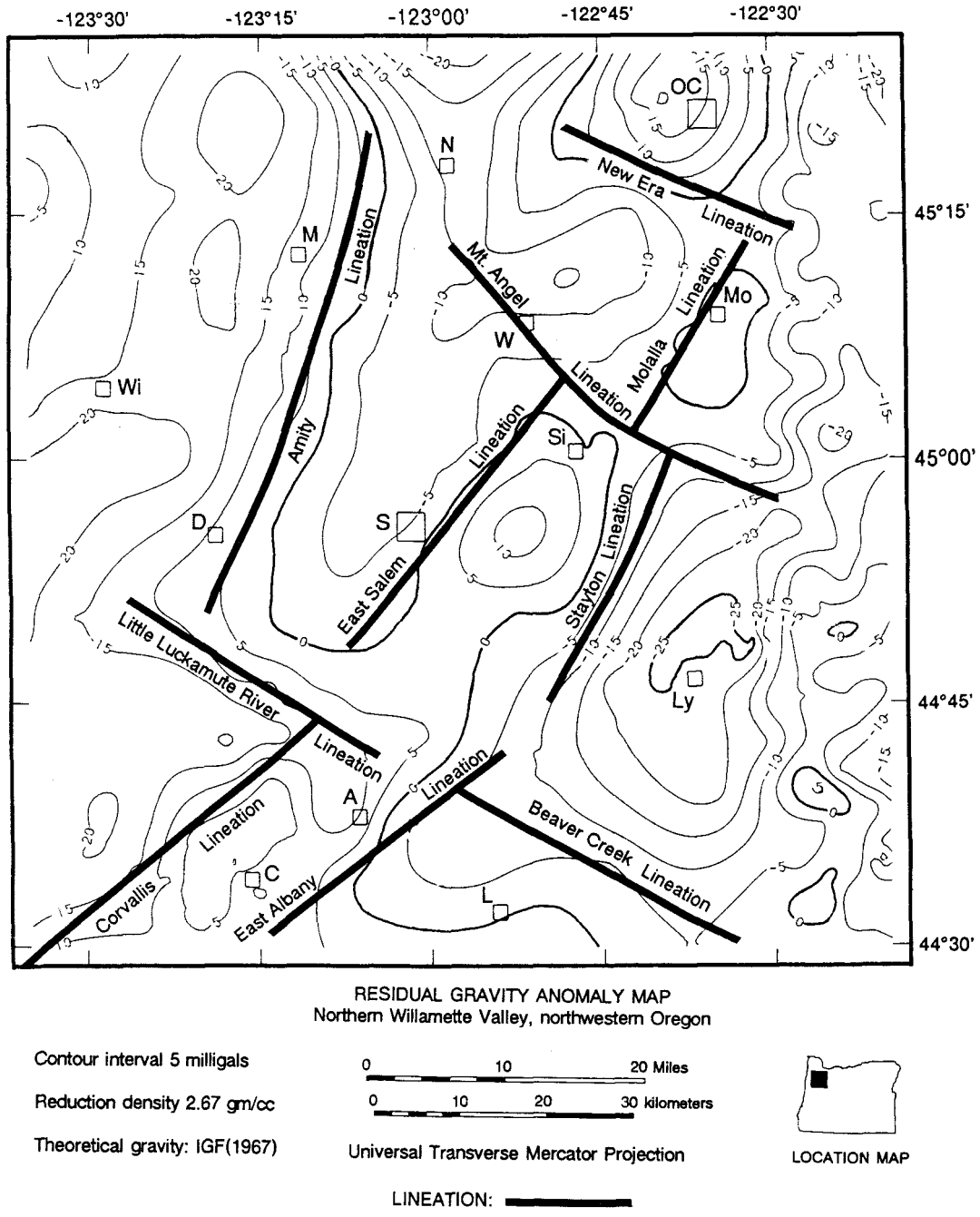


Figure 46. Gravity anomaly lineations on the residual gravity anomaly map of the northern Willamette Valley. Wavelengths longer than 50 km have been removed. Gravity station locations are shown in figure 42. Cities are labelled from north to south as follows: OC = Oregon City; N = Newberg; M= McMinnville; Mo = Molalla; W = Woodburn; Wi = Willamina; Si = Silverton; S = Salem; D = Dallas; Ly = Lyons; A = Albany; C = Corvallis; L = Lebanon.

to the Cascades (-123°30' to -122°30'W) is roughly 1.0-1.125 mgal/km. The anomalies vary from >25 mgal in the Coast Range (the Coast Range gravity high is one of the largest positive anomalies in western North America according to Simpson et al. [1986] and Blakely and Jachens [1989]), to <-75 mgal in the Cascades.

The regional gravity gradient is thought largely to be due to a rapid eastward thickening of continental crust [e.g. Dehlinger et al., 1968; Thiruvathukal et al., 1970; Couch and Riddihough, 1989], which occurs along the entire western North American margin. Cross sections by Couch and Riddihough [1989] across the borderlands of California, central California, central Oregon, and off the Queen Charlotte Islands all show abrupt crustal thickening from 15-20 km beneath the continental slope to 30-40 km about 200 km landward of the slope. Several estimates of the change in crustal thickness associated with this gradient have been made across the northern Willamette Valley. Based on a crustal thickness map of Oregon from Thiruvathukal et al. [1970], the continental crust thickens roughly 10 km (23 km to 33 km) from the Coast Range to the Western Cascades (-123°30' to -122°30') at a latitude of 45°. Similarly, independent two-dimensional gravity models by both Dehlinger et al. [1968] and Braman [1981] across the same area indicate that the Moho deepens eastward from approximately 23 km to 31 km (excludes contribution from topography).

The gradient associated with the eastern edge of the Coast Range trends north-northeast across the northern Willamette Valley, however, the gradient associated with the western edge of the Cascades rotates clockwise near Woodburn. This clockwise rotation is probably due to northward thinning of the crust beneath the Cascades. Couch et al. [1982a] estimate that the crust thins from as much as 45 km thick between the Three Sisters and Crater Lake to 30 km near the Columbia River north of Mt. Hood.

Near-surface geologic units with a sufficient density contrast and large aerial extent can also produce long-wavelength gravity anomalies. The near-surface geologic units most likely to produce long-wavelength anomalies are Eocene volcanic rocks and Columbia

River basalt. Eocene volcanic rocks crop out in the Coast Range and near Oregon City. Bromery and Snavely [1964] and Dehlinger et al. [1968] originally suggested that anomalously high Bouguer gravity anomalies over the Coast Range were largely caused by dense Eocene volcanics. Based on two-dimensional gravity and magnetic modeling across southern Washington, Finn [1989] recently confirmed that the source of the Coast Range Bouguer high is largely due to the density contrast between dense Eocene volcanics and adjacent sedimentary and volcanic rocks. The Columbia River basalt may also contribute to long wavelengths. It has a large density contrast with overlying unconsolidated sediments and is areally extensive north of Salem.

## RESIDUAL GRAVITY ANOMALY MAP

Previous small scale residual gravity anomaly maps including coverage of northwest Oregon have been completed by Bromery and Snavely [1964], Thiruvathukal [1968], Thiruvathukal et al. [1970], and Connard et al. [1984]. Large scale residual gravity anomaly maps have been completed for the Portland area by Perttu [1981] and for the Cascades by Pitts [1979], Braman [1981], Veen [1981], and Couch et al. [1982a, b]. No previous large scale residual gravity anomaly maps have been published for the northern Willamette Valley.

The residual gravity anomaly map of the northern Willamette Valley is shown at the 1:100,000 scale in Plates V and VI. The relief on the residual gravity map is >50 mgal, varying from <-28 mgal just south of Lyons to >22 mgal south of Willamina and west of McMinnville. The largest anomaly highs correspond to outcropping Eocene Coast Range volcanics (Siletz River Volcanics, Tillamook Volcanics, and basalt of Waverly Heights) and intrusive rocks (including thick sills). The deepest anomaly lows correspond to the Tualatin basin, the northern Willamette basin, and young volcaniclastic rocks in the Western Cascades.

**Residual Gravity Anomaly Highs.**

Outcropping Siletz River Volcanics correspond to residual gravity highs of >20 mgal north of Corvallis and >22 mgal south of Willamina (Plates V and VI). The density of Siletz River Volcanics is 2.7-2.8 gm/cc [Perttu, 1981; Couch et al., 1982a], while adjacent Eocene sedimentary rocks have a density of roughly 2.5 gm/cc [Perttu, 1981]. The size and shape of the gravity high south of Willamina is poorly defined by gravity stations.

The N-S trending gravity high west of McMinnville is >20 mgal and corresponds to Eocene volcanic rocks and Tertiary intrusions (chiefly thick sills). The Eocene volcanic rocks were mapped by Wells et al. [1983] as either Siletz River Volcanics or the submarine facies of the Tillamook Volcanics. The gravity anomaly may correspond to a high in Siletz River Volcanics or more likely the additional presence of Tillamook Volcanics. The gravity anomaly does not extend over outcropping Siletz River Volcanics to the west. The Coast Range intrusive rocks have a density of 3.0-3.1 gm/cc [Perttu, 1981], the highest density in the northern Willamette Valley area. More buried sills and/or source bodies may be present at depth.

A large gravity high of >20 mgal is centered between outcrops of basalt of Waverly Heights (Plate I and V). Basalt of Waverly Heights, which has a density of 2.8 gm/cc [Perttu, 1981], crops out adjacent to the Willamette River both southwest of Oregon City (Plate I) and 6 km north of the map bounds. The associated gravity high is roughly circular, consistent with a seamount or oceanic island geometry and origin. One arm of the gravity high extends southwestward towards La Butte and may be caused by a ridge of basalt of Waverly Heights and/or a source body for Boring lava which crops out there. Similarly, another arm of the gravity high extends southeastward towards Highland Butte, a known vent of Boring lava with a probable underlying source body. The density of Boring lava is roughly 2.5 gm/cc [Perttu, 1981].

Moderate gravity anomaly highs occur south of Molalla and southeast of Silverton (Plate V). The gravity high of >2 mgal located south of Molalla is centered over a vent of mafic rocks of the Miocene and Oligocene volcanic unit (Little Butte Volcanics) mapped by Peck et al. [1964]. The vent is located roughly 5 km south of Molalla. The density contrast between dense mafic vent facies or volcanic core facies associated with the vent and surrounding sedimentary and intermediate volcanic rocks is probably causing the gravity high. The Wicks well penetrates 2130+ m of volcanics and minor sedimentary rock which are presumed to be Miocene to Oligocene. A schematic representation of a mafic vent facies is shown in the upper right hand corner of Figure 19 [from Sherrod and Smith, 1989]. Densities for the Miocene and Oligocene volcanics range between 2.43-2.55 gm/cc [Couch et al., 1982a].

The residual gravity anomaly high of >12 mgal located southeast of Salem is poorly constrained by gravity stations (Plates V and VI), however, proprietary gravity data are consistent with the general shape and magnitude of the anomaly. The gravity high is similar in shape and orientation to the high just south of Molalla, however, it is 4 times larger. It may correspond to a vent complex of Miocene and Oligocene volcanics analogous to Powell Buttes located in the central Cascades. Powell Buttes is an Oligocene vent complex of the John Day formation, which is defined by a large positive gravity anomaly [Pitts, 1979] with a similar size and shape. A thick late Eocene volcanic unit is present in the Gath well indicating a possible nearby vent complex. Alternatively, the gravity high east of Salem may be due to faulting. Mapping by Hoffman [1981] in the Salem Hills shows a fault bounded horst block of Columbia River basalt projecting northeast into the Waldo Hills (Plate II); however, Hoffman [1981] inferred vertical displacements of Columbia River basalt on faults in the Salem Hills of only 15 to 30 meters.

### Residual Gravity Anomaly Lows

The main gravity lows on Plates V and VI occur in the Tualatin Valley, the northern Willamette Valley, and the Western Cascades north of Lyons. Popowski [in prep.] will discuss the gravity low associated with the Tualatin basin. The gravity low over the northern Willamette basin corresponds to a syncline of Columbia River basalt filled with unconsolidated lacustrine and fluvial sediments. The density of the post-Columbia River basalt sediments in the northern Willamette Valley has been modeled as 2.25 gm/cc by Couch et al. [1982a]. The residual gravity anomaly contours on Plates V and VI generally agree with the contour map of the top of CRB (Plates I and II). However, several features evident on the contour map of the top of CRB are absent or shifted on the residual gravity anomaly map probably largely due to poor gravity station coverage. Differences include shifting of the center of the gravity low slightly east of the center of the CRB basin, the lack of a gravity low on the southwest side of the Mt. Angel fault, and the lack of a gravity high associated with the intrusion of magma near Aurora.

The gravity low of <-28 mgal north of Lyons is the second largest negative anomaly (after the Tualatin basin) in the Willamette and Tualatin Valley areas. The anomaly trends northeast and does not directly correspond to any mapped geologic map units. It may be caused by a subsurface valley or graben filled with less dense sediment and pyroclastic fill.

## LINEATIONS

Lineations, which correspond to inflections of the contoured residual gravity anomalies, are shown in Figure 46. The most prominent residual gravity lineations in Figure 46 trend northeast, while less prominent lineations trend northwest. The orientation of lineations adjacent to the northern Willamette Valley is consistent with the orientations of regional lineations. The Cascade arc from Washington to California is characterized by

several major northeast-trending gravity lineations which extend hundreds of kilometers and are caused by sources in the upper crust [Blakely and Jachens, 1989].

**Northeast-Trending Lineations**

The northeast-trending lineations in Figure 46 are discussed from north to south. The Amity lineation trends NNE along the Eola-Amity Hills and has decreasing values to the ESE. The lineation corresponds to an eastward-dipping homocline overlying Siletz River Volcanics, which has been faulted down to the east. Two normal faults have been mapped based on E-W trending seismic reflection lines, which offset reflectors corresponding to the top of Siletz River Volcanics. The normal faults appear to thicken Yamhill Formation by approximately 500 m based on the seismic line shown in Figure 13, producing a density contrast of 0.2-0.3 gm/cc (based on densities from Perttu [1981] and Couch et al. [1982a]) between the Siletz River Volcanic and the Yamhill Formation. Using a simple slab approximation with a 500 m thick slab and a density contrast of 0.3 gm/cc, the resulting anomaly is approximately 6 mgal. The contribution of the faults to the gravity anomaly is therefore relatively small.

The east Salem lineation is poorly constrained by gravity stations. It roughly overlies the Waldo Hills, although it also extends over the southern portion of the northern Willamette basin. The lineation may correspond to a steep northwestern flank of a Miocene and Oligocene vent complex. Alternatively, the lineation may correspond to a fault with the northwest side down. The steep gradient is apparently caused by a density contrast within the Miocene and Oligocene volcanic unit, and/or between CRB with a density of 2.7-2.8 gm/cc [Perttu, 1981; Couch et al., 1982a] and adjacent Pliocene and Miocene fluvial and lacustrine sediments with a density of 2.25 gm/cc. The lineation is on trend with one minor fault mapped in the CRB by Hoffman [1981] in the Salem Hills with the correct sense of motion, however, the fault has an inferred vertical displacement of only 15 to 30 meters.

The Corvallis lineation roughly corresponds to the Corvallis fault. The lineation actually lies to the northwest of the surface trace of the fault, suggesting the main density contrast is also to the northwest. The density contrast appears to occur between Siletz River Volcanics in the hanging wall block and Eocene Spencer and Tyee strata in the footwall block [Goldfinger, 1990]. Based on two gravity models by Goldfinger [1990], the Corvallis fault is a thrust fault, which dips 20° to the northwest.

The Stayton and east Albany lineations could arguably form one lineation. The Albany lineation corresponds to the East Albany fault of Graven [1991]. The East Albany fault is based on seismic reflection lines, although its orientation was determined largely using the trend of residual gravity contours. By inference, the Stayton lineation may also correspond to a fault with an even larger displacement and/or density contrast.

### Northwest-Trending Lineations

The northwest-trending lineations are discussed from north to south (Figure 46). The New Era lineation, which is defined by few gravity stations, occurs along the southern flank of the gravity high near Oregon City. The steep gravity gradient indicates a fault or steep slope along the southern flank of the basalt of Waverly Heights. The Mt. Angel lineation roughly corresponds to the Mt. Angel fault. It appears to offset both the northern Willamette basin low and the adjacent southeastern high in a right-lateral sense. The Little Luckiamute River lineation probably corresponds to a fault due to the straight nature and steepness of the associated gradient. In addition, an uplifted hill of Spencer sandstone and sills occur nearby at Buena Vista (A. R. Niem, personal communication, 1990; Plate II). The Beaver Creek lineation corresponds to the Beaver Creek fault of Graven [1991], which is based on seismic reflection lines. Both the Little Luckiamute River and Beaver Creek lineations are discussed by Graven [1991].

# DISCUSSION

## PRE-COLUMBIA RIVER BASALT DEFORMATION

The Siletz River Volcanics were accreted to North America in early Eocene time resulting in the formation of a forearc basin located along the Coast Range and Willamette Valley. The accretion of Siletz River Volcanics also resulted in the westward stepping of the volcanic arc from the Challis axis in eastern Washington and Idaho to an axis in the Western Cascades [Wells et al., 1984]. The suture between Siletz River Volcanics and continental crust (which corresponds to the Challis subduction zone) lies east of the Eola-Amity Hills (Plate IV) based on tracing reflectors of Siletz River Volcanics basinward on the seismic reflection line shown in Figure 13. Based on aeromagnetic data, Johnsen et al. [1990] suggest that the suture is located beneath the eastern portion of the Willamette Valley. Following accretion, the Siletz River Volcanics in the northern Willamette Valley were onlapped by bathyal Yamhill mudstones (based on seismic data) and possibly the Tyee Formation in places.

Eocene structural deformation in the northern Willamette Valley includes normal faulting in the subsurface beneath the Eola-Amity Hills. The normal faults offset Siletz River Volcanics and Eocene Yamhill Formation and are associated with eastward thickening of the Yamhill Formation. They are consistent with opening or extension related to the formation of the forearc basin.

During the middle Eocene, several major volcanic centers formed in the forearc region and were important in subdividing the large Oregon Coast Range forearc basin into several shallow marine basins [Snavely and Wagner, 1963; Niem and Niem, 1984]. Both basalt of Waverly Heights and Tillamook Volcanics formed seamounts or highlands to the north and west of the northern Willamette Valley, respectively. Both form prominent gravity highs on the residual Bouguer anomaly maps (Plates V and VI; Figure 46). The

high associated with the basalt of Waverly Heights appears to be largely responsible for separation of the Willamette and Portland basins.

Cascade volcanism began as early as 48-45 Ma based largely on the gradation between the Yamhill Formation and volcaniclastics and volcanic rocks in the subsurface of the southeastern Willamette Valley [Graven, 1991]. The lower Narizian Yamhill Formation in the northeastern Willamette Valley has lessor amounts of intercalated volcanic rocks, including "basalt" (which may correspond to a sill) and "tuff", indicating a greater distance to the source. The earliest evidence of significant volcanism from a nearby vent occurs in the Gath well in the Waldo Hills, which penetrates volcanics of middle and late Eocene age (Figure 16). Volcanics in the Gath well are not present in nearby wells, therefore, they are probably from a nearby source possibly related to the large gravity high centered in the northern Waldo Hills. Similarly, a younger vent complex of Miocene and Oligocene volcanic rock mapped by Peck et al. [1964] near Molalla forms a gravity high. During the Neogene, the axis of volcanism appears to have generally migrated eastward from the Western Cascades to the High Cascades [Priest et al., 1983; Taylor, 1989].

Uplift of the Coast Range and formation of an eastward-dipping homocline of Eocene to early Oligocene marine strata occurred prior to emplacement of the Columbia River Basalt Group. The eastward-dipping homocline is evident both in the outcrop pattern along the western edge of the Willamette Valley and on seismic reflection data. However, the Nestucca Formation complicates the homoclinal outcrop pattern in the northern Willamette Valley, and was probably deposited in a local structural basin due to its increased thickness compared to the correlative Spencer Formation as well as increased paleodepths. Strata which form the eastward-dipping homocline flatten beneath the northern Willamette basin and are warped up beneath Gervais based on exploration wells (Plate IV). The upwarping appears to have formed in late Eocene to Oligocene time based on the apparently large angular unconformity between the Pittsburg Bluff and Keasey equivalents in the Werner 14-21, Werner 34-21, and DeShazer 13-22 wells (Figure 18).

The uplift of the Coast Range corresponds to a major angular unconformity shown in Figure 10 between Oligocene and Eocene sediments and overlying middle Miocene Columbia River basalt. The Oligocene and Eocene sediments appear to thin greatly beneath the center of the northern Willamette valley as show in Figure 16. Exploration wells in the northern Willamette Valley indicate that Oligocene and Eocene strata extend at least as far east as the DeShazer well and probably as far east as the Stauffer Farms well, although no foraminiferal data were available. Columbia River basalt overlies the Scotts Mills Formation (MOs) and Miocene and Oligocene volcanic rock (MOu) in the Anderson and Rose wells as well as in the Waldo Hills. The northern Willamette Valley may have been a strike valley at the time of Columbia River basalt emplacement, and much of the thinning may have occurred due to erosion before emplacement of overlying Columbia River basalt.

In the eastern portion of the basin, uplift and the northward retreat of a marine embayment toward the mouth of the Columbia River resulted in a generally shoaling-upward sequence of the Scotts Mills and Molalla formations. By early to middle Miocene time, the Coast Range had been elevated above sea-level, however, Columbia River basalt was still able to reach a coastal embayment through the Coast Range via intracanyon flows. Continued uplift, decreasing volumes of flows, and Cascade volcanism prevented the Pomona flow of Columbia River basalt from reaching the coast except along the Columbia River (Figure 23).

## POST-COLUMBIA RIVER BASALT DEFORMATION

Structural warping of the Columbia River basalt since middle Miocene time has resulted in structural relief of the northern Willamette basin of greater than 1 km. The trend of the main syncline axis in the northern Willamette Valley is ENE, and seismic reflection data indicate the syncline is at least partly closed to the east. Based on a contour map by Sherrod and Pickthorn [1989], the structural downwarp continues NE towards the Portland basin and beneath Boring Lava (Figure 47). The orientation of the main syncline

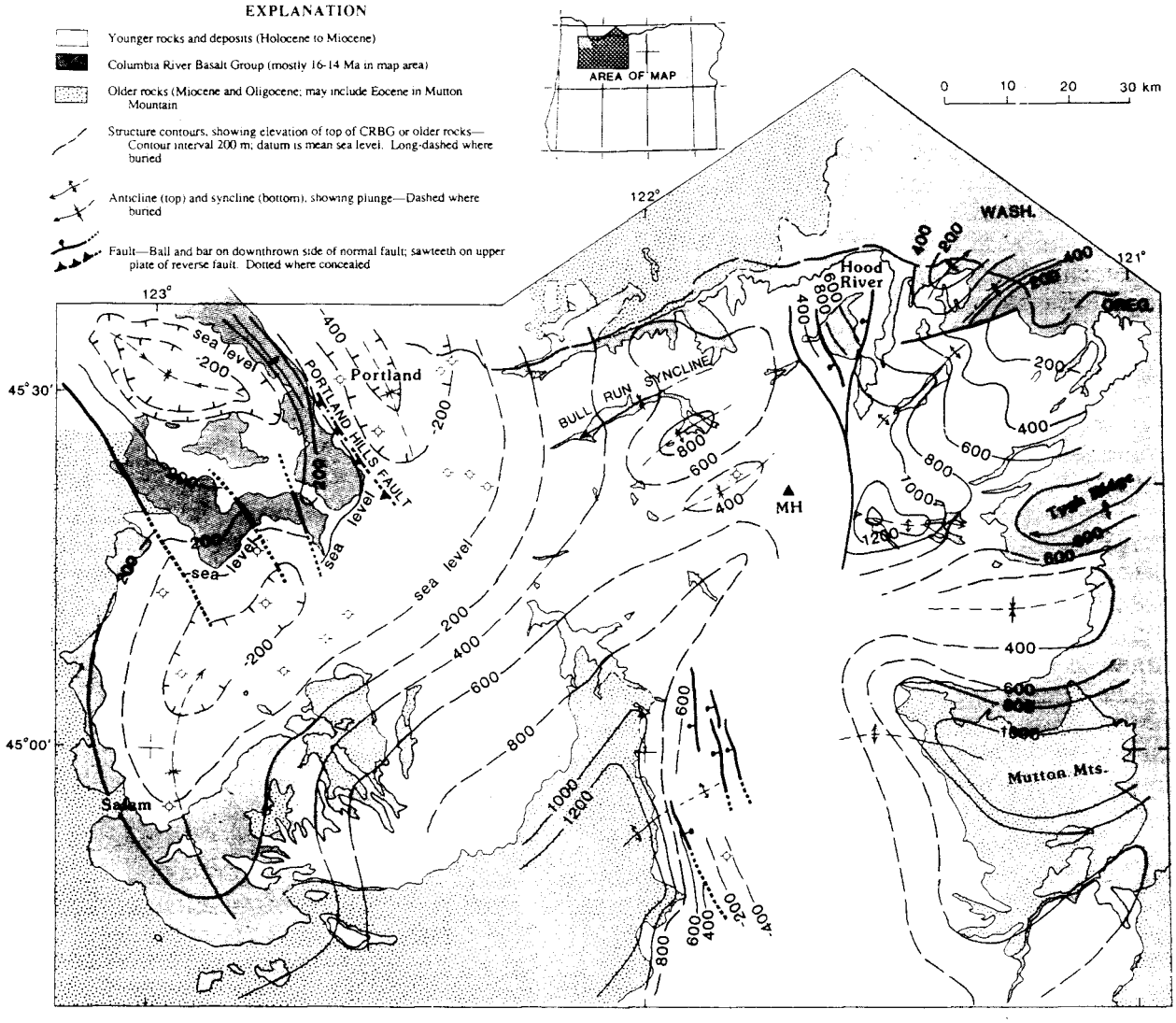


Figure 47. Regional structure-contour map showing altitude of Columbia River Basalt Group or older rocks. From Sherrod and Pickthorn [1989].

axis is consistent with the orientation of maximum horizontal compression based on dikes in the Cascades between 43° and 44°. The orientation of maximum horizontal compression based on dikes rotated from ENE in the Miocene to NNE presently [Sherrod and Pickthorn, 1989]. Deformation of the Columbia River basalt appears to correspond to a major period of underthrusting at the subduction zone interface in the late-middle Miocene due to increased plate convergence [Snavely et al., 1980].

Although seismic reflection lines indicate the top of Columbia River basalt throughout the basin is largely continuous and unbroken by major faults, several large faults are present. The large faults include possible NE-trending basin-bounding faults (whose relative importance and age is poorly known), the Gales Creek-Mt. Angel structural zone, and some intrusion-related faulting.

### Gales Creek-Mt. Angel Structural Zone

The Gales Creek and Mt. Angel faults comprise a major NW-trending linear structural zone more than 150 km long (Figure 48) [Beeson et al., 1985; 1989a]. The structural zone appears to consist of en echelon faults rather than one continuous fault. Mumford [1988] inferred right-lateral motion for the Gales Creek fault from offset NE-trending faults. Safley [1989] noted a two-meter-thick gouge zone and slickenside surface along the Gales Creek fault indicating right-lateral oblique-slip motion; the rake of the slickensides is 25°SE. Similarly, motion along the Mt. Angel fault appears to be largely right-lateral based on the linearity of the zone, the possible 1 km dextral offset of the Miocene Ginkgo intracanyon flow, and the composite focal mechanism from August, 1990 seismicity near Woodburn. Right-lateral motion along both the Mt. Angel and Gales Creek faults is consistent with the current N-S direction of maximum horizontal compression determined by borehole breakout data in western Oregon.

However, dip-slip motion is also evident along the Gales Creek and Mt. Angel faults. Mumford [1988] noted approximately 200 m of vertical separation along the Gales

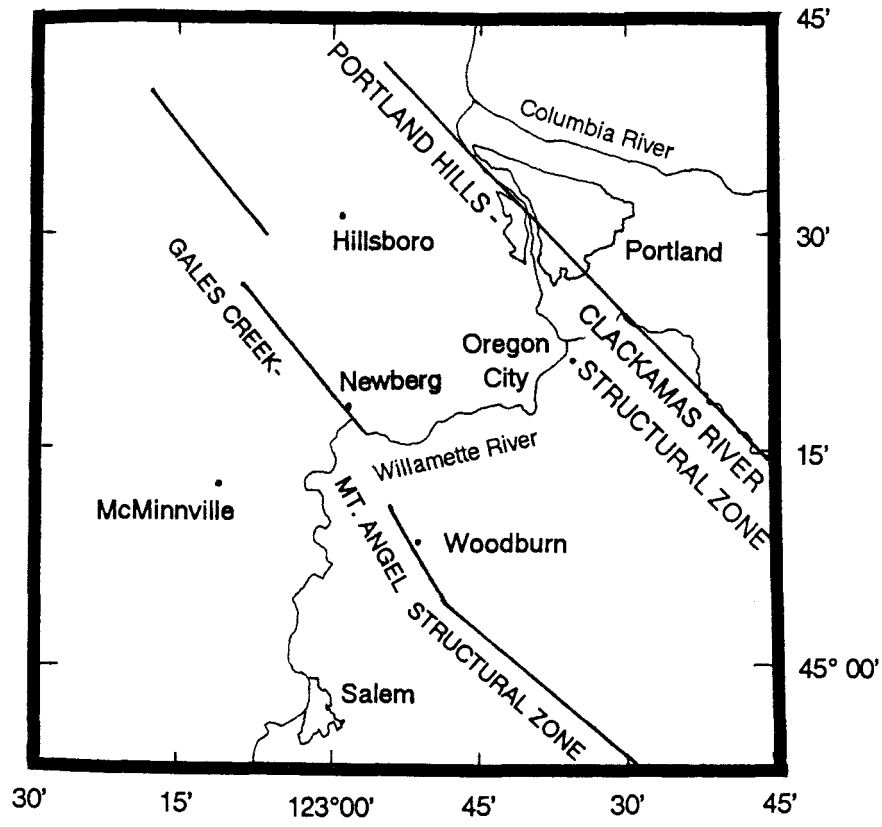


Figure 48. Map showing the Gales Creek-Mt. Angel structural zone and Portland Hills-Clackamas River structural zone.

Creek fault in southeast Clatsop County. Similarly, seismic lines as well as the topographic high of Mt. Angel indicate 100-250+ m of vertical separation (northeast side up) increasing to the southeast along the Mt. Angel fault. The vertical separation is not due to dextral strike-slip motion, since the Columbia River basalt is generally dipping northeastward in the Mt. Angel area (Figure 31). There, dextral strike-slip motion along the Mt. Angel fault would serve to counteract uplift on the northeast side of the fault.

The trend and sense of motion of the Gales Creek-Mt. Angel structural zone are similar to those of the Portland Hills-Clackamas River structural zone in the Portland area (Figure 48). The Portland Hills-Clackamas River structural zone is a major structural feature consisting of faults and folds generated in response to dextral movement [Beeson et al., 1989]. Recent seismicity, including a $M_W = 5.1$ earthquake on November 6, 1962, with its epicenter in the Portland area, appears to be related to motion along the Portland Hills-Clackamas structural zone [Yelin and Patton, in press]. Together, the Gales Creek-Mt. Angel and Portland Hills-Clackamas River structural zones may take up dextral shear imposed on the upper plate by oblique subduction of the Juan de Fuca plate beneath the North American plate.

Dextral shear has been noted by Wells and Heller [1988] and Wells [1990] as an important mechanism for generating rotation observed in paleomagnetic results. Wells and Heller [1988] conclude that dextral shear is responsible for about 40% of post-15 Ma rotation. The average rotation for coastal sites of 15 Ma flows of Grande Ronde basalt is 22° clockwise when compared to sites on the Columbia River Plateau; rotation decreases from the coast eastward [Wells and Heller, 1988]. Tectonic models explaining the paleomagnetic results have varyed from rotation of a single Coast Range block to distributed shear on many smaller faults [Sheriff, 1984; Wells and Heller, 1988]. Wells and Heller [1988] argue that the tectonic processes responsible for rotation are operating on an intermediate scale ($10^2$ - $10^4$ m). Such a scale is consistent with the model of rotation shown in Figure 49 [after Christie-Blick and Biddle, 1985] between the Portland Hills-

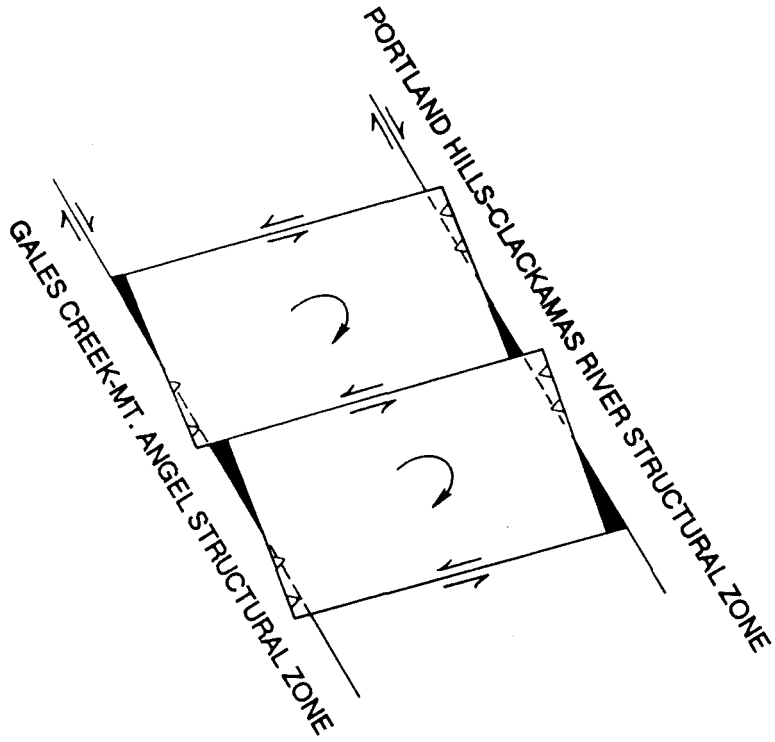


Figure 49. Model for block rotation between the Gales Creek-Mt. Angel structural zone and Portland Hills-Clackamas River structural zone. From a model applied to rotation of blocks near intersection of San Andreas and San Jacinto faults, California by Christie-Blick and Biddle [1985].

Clackamas River and Gales Creek-Mt. Angel structural zones. Wells and Coe [1985] demonstrate rotation in southwestern Washington along similar major dextral NNW-trending faults and WNW-trending sinistral R' Reidel shears.

Rotation of intermediate-sized blocks leads to space problems and differential local compression and extension along shear zones as shown in Figure 49. The differential compression associated with rotation could in turn explain the different amounts of vertical separation along the Mt. Angel fault. Alternatively the combination of right-lateral motion and vertical offset could be caused by wrench faulting.

The Gales Creek-Mt. Angel structural zone appears to have been active from Columbia River basalt time to possibly the present. Motion on the fault in the middle Miocene resulted in the formation of a barrier by the time the Silver Falls flows were extruded. Warping and offset of Pliocene and Miocene sediments indicates deformation continued during the Neogene. The Gales Creek-Mt. Angel structural zone may presently be active, if the August 1990 seismicity in fact occurred on a deep extension of the Mt. Angel fault.

**Boring Lava and Related Faulting**

Boring Lava is present in the northeastern portion of the northern Willamette Valley, both as shield volcanoes (Highland Butte) and intrusions. Updoming from influx of magma and/or collapse associated with evacuation of magma appears to have been important in generating Quaternary faulting. Many faults in the northeastern part of the northern Willamette Valley are probably related to Boring intrusion based on their random orientation, short lengths, normal sense of displacement, age, and proximity to nearby vents or intrusions of Boring Lava. The seismic hazard associated with Boring intrusion is probably minimal. However, Boring Lava is an important modifier of basin structure and may be important in controlling intensity of ground shaking.

# CONCLUSIONS

(1.) Seismic reflection data indicate that Eocene to Oligocene sedimentary strata along the western side of the northern Willamette Valley generally form a gently eastward dipping homocline. The homocline is interrupted by two steeply-dipping subsurface normal faults which offset the Siletz River Volcanics and Yamhill Formation down to the east and thicken the Yamhill Formation approximately 500 m. Petroleum exploration wells indicate local upwarping and thinning of Oligocene and Eocene strata beneath the central northern Willamette basin (near Woodburn).

(2.) The northern Willamette Valley corresponds to a residual gravity anomaly low. Several Eocene and Oligocene volcanic centers composed of Siletz River Volcanics, Tillamook Volcanics, basalt of Waverly Heights, and Cascade volcanics correspond to residual gravity anomaly highs and lineations.

(3.) The northern Willamette basin is formed by downwarped Columbia River basalt and to a much lessor extent downwarped overlying Pliocene and Miocene fluvial and lacustrine sediments. The main syncline axis trends ENE and the minimum altitude to the top of Columbia River basalt is <-500 m. The basin is bounded to the south by the NE-trending Waldo Hills range-front fault, and to the north by the NE-trending Yamhill River-Sherwood structural zone.

(4.) The Mt. Angel fault extends NNW from the town of Mt. Angel to Woodburn based on water-well and seismic reflection data. Locally, the fault vertically offsets the top of Columbia River basalt 250+ m and appears to offset a reflector corresponding to Pliocene and Miocene fluvial and lacustrine sediments 96 m. Structural relief on the Pliocene and Miocene fluvial and lacustrine sediments, which form a syncline along the south side of the fault, is 45 m.

A series of small earthquakes of $m_C$ = 2.0, 2.5, 2.4, 2.2, 2.4, and 1.4 occurred on August 14, 22, and 23, 1990 with epicenters located at the northwest end of the Mt. Angel

fault. Routine locations indicate a depth of about 30 km. The preferred composite focal mechanism solution is a right-lateral strike-slip fault with a small normal component on a plane striking north and dipping steeply to the west. The locations and focal mechanisms of the earthquakes are consistent with them being on a deep extension of the Mt. Angel fault, however, the association between the surface fault and seismicity is weak because of the large depth of the earthquakes.

The Mt. Angel fault is part of the Gales Creek-Mt. Angel structural zone, which may take up dextral shear imposed on the upper plate by subduction of the Juan de Fuca plate beneath the North American plate.

(5.) The "Aurora intrusion", probably composed of Boring Lava, occurs in the subsurface near Aurora based on interpretation of seismic reflection data and water wells which reach "basalt" as shallow as 20 m. The intrusion warps up Columbia River basalt and overlying sediments. Minor faulting appears to be associated with doming or evacuation of magma. Other Boring Lava related faulting appears to include the Curtis fault, a fault near Canby (Swan Island fault) which offsets a mud layer in the Pleistocene Rowland formation 1 m, and several other faults which offset Columbia River basalt at Parrett and Petes mountains.

## REFERENCES

Adams, J., 1984, Active deformation of the Pacific Northwest continental margin: Tectonics, v. 3, p. 449-472.

Al-Azzaby, F. A., 1980, Stratigraphy and sedimentation of the Spencer Formation in Yamhill and Washington Counties, Oregon: unpub. M.S. thesis, Portland State University, Portland, Oregon, 104 p.

Allen, J. E., 1975, Volcanoes of the Portland area, Oregon: The Ore Bin, v. 37, p. 145-157.

Allison, I. S., 1932, Glacial erratics in the Willamette Valley: Geological Society of America Bull., v. 46, p. 615-632.

-----, 1935, Glacial erratics in Willamette Valley: Geological Society of America Bull., v. 46, p. 615-632.

-----, 1936, Pleistocene alluvial stages in northwestern Oregon: Science, v. 83, p. 441-443.

-----, 1953, Geology of the Albany quadrangle, Oregon: Oregon Department of Geology and Mineral Industries Bull. 37, 18 p.

-----, 1978, Late Pleistocene sediments and floods in the Willamette Valley: The Ore Bin, v. 40, no. 11, p. 177-191 and no. 12, p. 193-202.

Allison, I. S., and Felts, W. M., 1956, Reconnaissance geologic map of the Lebanon quadrangle, Oregon: Oregon Department of Geology and Mineral Industries, QM-4, scale 1:62,500.

Anderson, E. M., 1951, The Dynamics of Faulting and Dyke Formation with Application to Britain, 2nd edition: Oliver and Boyd, London, 206 p.

Armentrout, J. M., Hull, D. A., Beaulieu, J. D., and Rau, W. W., 1983, Correlation of Cenozoic stratigraphic units of western Oregon and Washington: Oregon Department of Geology and Mineral Industries Oil and Gas Investigations 7, 90 p.

Armentrout, J. M., and Suek, D. H., 1985, Hydrocarbon exploration in western Oregon and Washington: A.A.P.G. Bull., v. 69, no. 4, p. 627-643.

Babcock, E. A., 1978, Measurement of subsurface fractures from dipmeter logs: A.A.P.G. Bull., v. 62, p. 1111-1126.

Baker, L. J., 1988, The stratigraphy and depositional setting of the Spencer Formation, west-central Willamette Valley, Oregon; a surface subsurface analysis: unpub. M.S. thesis, Oregon State University, Corvallis, 159 p.

Baldwin, E. M., 1981, Geology of Oregon: Kandall/Hunt Publishing Co., 170 p.

Baldwin, E. M., Brown, R. D., Jr., Gair, J. E., and Pease, M. H., Jr., 1955, Geology of the Sheridan and McMinnville quadrangles, Oregon: U.S. Geological Survey Oil and Gas Inv., Map OM 155.

Balster, C. A., and Parsons, R. B., 1969, Late Pleistocene stratigraphy, southern Willamette Valley, Oregon: Northwest Science, v. 43, p. 116-129.

Beaulieu, J. D., 1971, Geologic formations of western Oregon (west of longitude 121 30'): Oregon Department of Geology and Mineral Industries Bull. 70, 72 p.

Beeson, M. H., Fecht, K. R., Reidel, S. P., and Tolan, T. L., 1985, Regional correlations within the Frenchman Springs Member of the Columbia River Basalt Group: New insights into the Middle Miocene tectonics of northwestern Oregon: Oregon Geology, v. 47, no. 8, p. 87-96.

Beeson, M. H., Johnson, A. G., and Moran, M. R., 1975, Portland environmental geology -- Fault identification: Final technical report, U.S. Geological Survey contract no. 14-08-0001-14832, Geology Department, Portland State University, Portland, Oregon, 107 p.

Beeson, M. H., and Moran, M. R., 1979, Columbia River Basalt Group stratigraphy in western Oregon: Oregon Geology, v. 41, no. 1, p. 11-14.

Beeson, M. H. and Tolan, T. L., 1989, The Columbia River Basalt Group in the Cascade Range: a middle Miocene reference datum for structural analysis: in Muffler, L.J. P., Weaver, C. S., and Blackwell, D. D., eds., Proceedings of Workshop XLIV, Geological, geophysical, and tectonic setting of the Cascade Range, U.S. Geological Survey Open-file Report 89-178, p. 257-290.

Beeson, M. H., Tolan, T. L., and Anderson, J. L., 1989a, The Columbia River Basalt Group in western Oregon; geologic structures and other factors that controlled flow emplacement patterns: in Reidel, S. P., and Hooper, P. R., eds., Volcanism and tectonism in the Columbia River flood-basalt province, Geological Society of America Special Paper 239, p. 223-246.

Beeson, M. H., Tolan, T. L., and Madin, I. P., 1989b, Geologic map of the Lake Oswego quadrangle, Clackamas, Multnomah, and Washington counties, Oregon: Oregon Department of Geology and Mineral Industries Geologic Map Series GMS-59.

Bela, J. L., 1981, Geology of the Rickreall, Salem West, Monmouth, and Sidney 7 1/2' quadrangles, Marion, Polk, and Linn Counties, Oregon: Oregon Department of Geology and Mineral Industries, GMS-18.

Bell, J. S., and Gough, D. I., 1979, Northeast-southwest compressive stress in Alberta: Evidence from oil wells: Earth and Planet. Sci. Lett., v. 45, p. 475-482.

Berkman, T. A., 1990, Surface-subsurface geology of the middle to upper Eocene sedimentary and volcanic rock units, western Columbia county, northwest Oregon: unpub. M.S. thesis, Oregon State University, Corvallis, 413 p.

Blakely, R. J., and Jachens, R. C., 1989, Volcanism, isostatic residual gravity, and regional tectonic setting of the Cascade volcanic province: in L. P. Muffler, D. D. Blackwell, and C. S., Weaver, eds., Geologic, geophysical and tectonic setting of the Cascade Range, U.S. Geological Survey Open-File Report 89-178, p. 16-30.

Bolt, B. A., Lomnitz, C., and McEvilly, T. V., 1968, Seismological evidence on the tectonics of central and northern California and the Mendocino escarpment: Bull. Seismol. Soc. Am., v. 58, p. 1725-1767.

Braman, D. E., 1981, Interpretation of gravity anomalies observed in the Cascade Mountain province of northern Oregon: unpub. M.S. thesis, Oregon State University, Corvallis, 144 p.

Brenner, N., 1968, FOR2d subroutine package for multi-dimensional FFT: MIT Lincoln Laboratory, Boston, Massachusetts.

Briggs, I. C., 1974, Machine contouring using minimum curvature: Geophysics, v. 39, no. 1, p. 39-48.

Brown, R. D., 1951, The geology of the McMinnville quadrangle, Oregon: unpub. M. S. thesis, University of Oregon, Eugene, 54 p.

Brownfield, M. E., 1982a, Geologic map of the Sheridan quadrangle, Polk and Yamhill Counties, Oregon: Oregon Department of Geology and Mineral Industries, GMS-23, scale 1:24,000.

-----, 1982b, Geologic map of the Grand Ronde quadrangle, Polk and Yamhill Counties, Oregon: Oregon Department of Geology and Mineral Industries, GMS-24, scale 1:24,000.

-----, 1982c, Preliminary geologic map of the Ballston Quadrangle, Oregon: Oregon Department of Geology and Mineral Industries Open-File Report 0-82-2, scale 1:24,000.

Brownfield, M. E., and Schlicker, H. G., 1981a, Preliminary geologic map of the Amity and Mission Bottom quadrangles, Oregon: Oregon Department of Geology and Mineral Industries Open-File Report 0-81-05, scale 1:24,000.

Brownfield, M. E., and Schlicker, H. G., 1981b, Preliminary geologic map of the McMinnville and Dayton quadrangles, Oregon: Oregon Department of Geology and Mineral Industries Open-File Report 0-81-06, scale 1:24,000.

Bromery, R. W., and Snavely, P. D., Jr., 1964, Geologic interpretation of reconnaissance gravity and aeromagnetic surveys in northwestern Oregon: U.S. Geological Survey Bull. 1181-N, 13 p.

Bruer, W. G., Alger, M. P., Deacon, R. J., Meyer, H. J., Portwood, B. B., and Seeling, A. F., project coordinators, 1984, Correlation section 24, northwest Oregon: Pacific section, A.A.P.G.

Cheeney, R. F., 1983, Statistical methods in geology for field and lab decisions: George Allen & Unwin, London, 169 p.

Christie-Blick, N., and Biddle, K. T., 1985, Deformation and basin formation along strike-slip faults: in Biddle, K. T., and Cristie-Blick, N., eds., Strike-slip deformation, basin deformation, and sedimentation, Society of Economic Paleontologists and Mineralogist Special Publication 37, p. 1-35.

Connard, G., Couch, R., Pitts, G. S., Roy, J., Keeling, K., Pitts, P., Watkins, R., and Peper, J., 1984, Residual Bouguer gravity anomalies: in Kulm et al., eds., Western North American continental margin and adjacent ocean floor of Oregon and Washington: Ocean margin drilling program: Regional Atlas Series.

Couch, R. W., Gemperle, M., and Peterson, R., 1985, Total field aeromagnetic anomaly map Cascade Range, northern Oregon: Oregon Department of Geology and Mineral Industries Geological Map Series GMS-40.

Couch, R., Johnson, S., and Gallagher, J., 1968, The Portland earthquake of May 13, 1968 and earthquake energy release in the Portland area: The Ore Bin, v. 30, p. 185-190.

Couch, R. W., Pitts, G. S., Gemperle, M., Braman, D. E., and Veen, C. A., 1982a, Gravity anomalies in the Cascade Range in Oregon: structural and thermal implications: Oregon Department of Geology and Mineral Industries Open-File Report 0-82-9, 66 p.

Couch, R. W., Pitts, G. S., Gemperle, M., Veen, C. A., and Braman, D. E., 1982b, Residual gravity maps of the northern, central, and southern Cascade Range, Oregon: 122°30' to 121°00'E by 42°00' to 45°45'N: Oregon Department of Geology and Mineral Industries Geologic Map Series GMS-26.

Couch, R. W., and Riddihough, R. P., 1989, The crustal structure of the western continental margin of North America: in Pakiser, L., and Mooney,W., eds., Geophysical Framework of the Continental United States, GSA Memoir 172., p. 103-128.

Couch, R., Thrasher, G., and Keeling, K., 1976, The Deschutes Valley earthquake of April 12, 1976: The Ore Bin, v. 38, p. 151-161.

Crosson, R. S., 1972, Small earthquakes, structure, and tectonics of the Puget Sound region: Bull. Seismol. Soc. Amer., v. 62, p. 1133-1171.

Crosson, R. S., and Frank, D., 1975, The Mt. Rainier earthquake of July 18, 1973, and its tectonic significance: Bull. Seismol. Soc. Am., v. 65, p. 393-401.

Crosson, R. S., and Lin, J., 1975, A note on the Mt. Rainier earthquake of April 20, 1974: Bull. Seismol. Soc. Am., v. 65, p. 549-556.

Dehlinger, P., Bowen, R. G., Chiburis, E. F., and Westphal, W. H., 1963, Investigations of the earthquake of November 5, 1962, north of Portland: The Ore Bin, v. 25, p. 53-68.

Dehlinger, P., Couch, R. W., and Gemperle, M., 1968, Continental and oceanic structure from the Oregon coast westward across the Juan de Fuca Ridge: Can. J. Earth Sci., v. 5, p. 1079-1090.

Duncan, R. A., 1982, A captured island chain in the Coast Range, Oregon and Washington: J. Geophys. Res., v. 87, p. 10827-10837.

EMSLAB Group, 1988, The EMSLAB electromagnetic sounding experiment: EOS Transactions, American Geophysical Union, v. 69, no. 7, p. 89, 98, 99.

Engelder, T., and Sbar, M. L., 1984, Near-surface in situ stress: Introduction: J. Geophys. Res., v. 89, p. 9321-9322.

Evarts, R. C., Ashley, R. P., and Smith, J. G., 1987, Geology of Mount St. Helens area: Record of discontinuous volcanic and plutonic activity in the Cascade arc of southern Washington: J. Geophys. Res., v. 92, p. 10155-10169.

Fiebelkorn, R. B., Walker, G. W., MacLeod, N. S., McKee, E. H., and Smith, J. G., 1983, Index to K-Ar determinations for the State of Oregon: Isochron/west, no. 37, p. 3-46.

Finn, C., 1989, Structure of the convergent Washington margin: U.S. Geological Survey Open-File Report 89-178, p. 291-317.

Frank, F. J., and Collins, C. A., 1978, Groundwater in the Newberg area, northern Willamette Valley, Oregon: Oregon Water Resources Department, Ground Water Report no. 27, 77 p.

Fuchs, K., and Clauß, B., 1988, Borehole breakout method for stress determination theory and practice: Geophysikalisches Institut, Universität Fridericiana Karlsruhe, unpub., 17 p.

Gephart, J. W., and Forsyth, D. W., 1984, An improved method for determining the regional stress tensor using earthquake focal mechanism data: Application to the San Fernando earthquake sequence: J. Geophys. Res., v. 89, p. 9305-9320.

Glenn, J. L., 1965, Late Quaternary sedimentation and geological history of the north Willamette Valley, Oregon: unpub. Ph.D. dissertation, Oregon State University, Corvallis, 231 p.

Goldfinger, C., 1990, Evolution of the Corvallis fault, and implication for the Oregon Coast Range: unpub. M.S. thesis, Oregon State University, Corvallis, 138 p.

Gough, D. I., and Bell, J. S., 1982, Stress orientations from borehole wall fractures with examples from Colorado, east Texas, and northern Canada: Can. J. Earth Sci., v. 19, p. 1358-1370.

Grant, W. C., and Weaver, C. S., 1986, Earthquakes near Swift Reservoir, Washington, 1958-1963: seismicity along the southern St. Helens Seismic Zone: Bull. Seismol. Soc. Am., v. 76, p. 1573-1587.

Graven, E. P., 1991, Structure and tectonics of the southern Willamette Valley: unpub. M.S. thesis, Oregon State University, Corvallis, in press.

Hampton, E. R., 1963, Records of wells, water levels and chemical quality of ground water in the Molalla-Salem slope area, northern Willamette Valley, Oregon: Oregon Water Resources Department, Ground Water Report no. 2, 174 p.

-----, 1972, Geology and groundwater of the Molalla-Salem slope area, Northern Willamette Valley, Oregon: U.S. Geological Survey Water-Supply Paper 1997, 83 p.

Harper, H. E., 1946, Preliminary report on the geology of the Molalla quadrangle, Oregon: unpub. M.S. thesis, Oregon State University, Corvallis, 29 p.

Hart, D. H., and Newcomb, R. C., 1965, Geology and ground water of the Tualatin Valley Oregon: U.S. Geological Survey Water-Supply Paper 1697, 172 p.

Hearn, B. C., Jr., Pecora, W. T., and Swadley, W.C., 1963, Geology of the Rattlesnake Quadrangle, Bearpaw Mountains, Blaine County, Montana: U.S. Geological Survey Bull. 1181-B, 66 p.

Heaton, T. H., and Hartzell, S. H., 1986, Source characteristics of hypothetical subduction earthquakes in the northwestern United States: Bull. Seismol. Soc. Am., v. 76, p. 675-708.

Heaton, T. H., and Hartzell, S. H. 1987, Earthquake hazards on the Cascadia subduction zone: Science, v. 236, p. 162-168,.

Heinrichs, D. F., and Pietrafesa, L. J., 1968, The Portland earthquake of January 27, 1968: The Ore Bin, v. 30, p. 37-40.

Hickman, S. H., Healy, J. H., and Zoback, M. D., 1985, In situ stress, natural fracture distribution, and borehole elongation in the Auburn geothermal well Auburn, New York: J. Geophys. Res., v. 90, p. 5497-5512.

Hodge, E. T., 1933, Age of Columbia River and lower canyon (abstr.): Geol. Soc. Amer. Bull., v. 44, p. 156-157.

Hoffman, C. W., 1981, A stratigraphic and geochemical investigation of ferruginous bauxite deposits in the Salem Hills, Marion County, Oregon: unpub. M.S. thesis, Portland State University, Portland, Oregon, 105 p.

International Association of Geodesy, 1971, Geodetic reference system 1967, Bull. of Geodesy Spec. Pub. No. 3.

Jackson, M. K., 1983, Stratigraphic relationships of the Tillamook Volcanics and the Cowlitz Formation in the upper Nehalem River-Wolf Creek area, northwestern Oregon: unpub. M.S. thesis, Portland State University, Portland, Oregon, 81 p.

Johnsen, P. R., Zietz, I., and Bond, K. R., 1990, U.S. west coast revisited: An aeromagnetic perspective: Geology, v. 18, p. 332-335.

Jones, T. D., 1977, Analysis of a gravity traverse south of Portland: unpub. M.S. thesis, Portland State University, Portland, Oregon, 54 p.

Keach II, R. W., 1986, Cenozoic active margin and shallow Cascades structure: COCORP results from western Oregon: unpub. M.S. thesis, Cornell University, Ithica, New York, 51 p.

Kelsey, H. M., 1990, Late Quaternary deformation of marine terraces on the Cascadia subduction zone near Cape Blanco, Oregon: EOS Trans. AGU, v. 71, p. 367.

Kleinpell, R. M., 1938, Miocene stratigraphy of California: Tulsa, Okla., A.A.P.G., 416 p.

Kulm, L. D., and Fowler, G., 1974, Oregon continental margin structure and stratigraphy: A test of the imbricate thrust model: in C. A. Burk and C. L. Drake, eds., The geology of the continental margins, Springer-Verlag, New York, p. 261-283.

Leonard, A. R., and Collins, C. A., 1983, Ground water in the northern part of the Clackamas County, Oregon: Oregon Water Resources Department, Ground-Water Report 29, 85 p.

Luedke, R. G., and Smith, R. L., 1982, Map showing the distribution, composition, and age of late Cenozoic volcanic centers in Oregon and Washington: U.S. Geological Survey Map, I-1091-D, scale 1:1,000,000.

Lux, D. R., 1982, K-Ar and $^{40}Ar$-$^{39}Ar$ ages of Mid-Tertiary volcanic rocks from the Western Cascade Range, Oregon: Isochron/West, no. 33, p. 27-32.

Ma, L., 1988, Regional tectonic stress in western Washington from focal mechanisms of crustal and subcrustal earthquakes: M.S. Thesis, Univ. of Washington, Seattle, 84 p.

MacLeod, N. S., 1969, Geology and igneous petrology of the Saddleback area, central Oregon Coast Range: Santa Barbara, California, University of California Ph.D., 205 p.

Macleod, N. S., and Sherrod, D. R., 1988, Geologic evidence for a magma chamber beneath Newberry Volcano, Oregon: J. Geophys. Res., v. 93, p. 10067-10079.

Madin, I. P., 1990, Earthquake-Hazard geology maps of the Portland metropolitan area, Oregon: Text and map explanation: Oregon Department of Geology and Mineral Industries Open-File Report 0-90-2, 21 p.

Magee, M. E., and Zoback, M. L., 1989, Present state of stress in the Pacific Northwest (abstr.): EOS Trans. AGU, v. 70, p. 1332-1333.

Mallory, V. S, 1959, Lower Tertiary biostratigraphy of the California Coast Ranges: Tulsa Oklahoma, A.A.P.G., 416 p.

Mardia, K. V., 1972, Statistics of directional data: Academic Press, Orlando, Florida, 357 p.

McDowell, P. F., in press, Quaternary stratigraphy and geomorphic surfaces of the Willamette Valley, Oregon: in Morrison, R. B., ed., Quaternary non-glacial geology of North America, Geological Society of America, Decade of North American Geology Series.

McDowell, P. F., and Roberts, M. C., 1987, Field guidebook to the Quaternary stratigraphy, geomorphology and soils of the Willamette Valley, Oregon: Field trip no. 3, Association of American Geographers 1987 annual meeting, Portland, Oregon, 75 p.

McInelly, G. W., and Kelsey, H. M., 1990, Late Quaternary tectonic deformation in the Cape Arago-Bandon region of coastal Oregon as deduced from wave-cut platforms: J. Geophys. Res., in press.

McKeel, D. R., 1980, Micropaleontological study of five wells, western Willamette Valley, Oregon: Oregon Department of Geology and Mineral Industries Open-File Report 0-80-01, 21 p.

-----, 1984, Biostratigraphy of exploratory wells, northern Willamette basin, Oregon: Oregon Department of Geology and Mineral Industries Oil and Gas Investigations 12, 19 p.

-----, 1985, Biostratigraphy of exploratory wells, southern Willamette basin, Oregon: Oregon Department of Geology and Mineral Industries Oil and Gas Investigations 13, 17 p.

McWilliams, R. G., 1968, Paleogene stratigraphy and biostratigraphy of central-western Oregon: unpub. Ph.D. dissertation, University of Washington, Seattle, 140 p.

-----, 1973, Stratigraphic and biostratigraphic position of the Yamhill Formation in central western Oregon: Geological Society of America Abstracts with Program, v. 5, p 79.

-----, 1980, Eocene correlations in western Oregon-Washington: Oregon Geology, v. 42, no. 9, p. 151-158.

Miller, P. R., and Orr, W. N., 1984a, Geologic map of the Wilhoit quadrangle, Oregon: Oregon Department of Geology and Mineral Industries, GMS-32, scale 1:24,000.

Miller, P. R., and Orr, W. N., 1984b, Geologic map of the Scotts Mills quadrangle, Oregon: Oregon Department of Geology and Mineral Industries, GMS-33, scale 1:24,000.

Miller, P. R., and Orr, W. N., 1986, The Scotts Mills Formation: Mid-Tertiary geologic history and paleogeography of the central Western Cascade Range, Oregon: Oregon Geology, v. 48, p. 139-151.

Miller, P. R., and Orr, W. N., 1988, Mid-Tertiary transgressive rocky coast sedimentation: Central Western Cascade Range, Oregon: Jour. Sed. Pet., v. 58, no. 6, p. 959-968.

Morelli, C., 1971, International gravity standardization net 1971: International Association of Geodesy Sp. Pub. No. 4.

Mullineaux, D. R., Wilcox, R. E., Ebaugh, W. F., Fryxell, R., and Rubin, M., 1978, Age of the last major scabland flood in the Columbia Plateau in eastern Washington: Quaternary Research, v. 10, p. 171-180.

Mumford, D. F., 1988, Geology of the Elsie-lower Nehalem River area, south-central Clatsop and northern Tillamook Counties, northwestern Oregon: unpub. M.S. thesis, Oregon State University, Corvallis, 392 p.

Nakamura, K., 1977, Volcanoes as possible indicators of tectonic stress orientations: Principles and proposal: Jour. Volc. and Geothermal Res., v. 2, p. 1-16.

Nakamura, K., and Uyeda, S., 1980, Stress gradient in arc-back arc regions and plate subduction: J. Geophys. Res., v. 85, p. 6419-6428.

Nelson, D. E., 1985, Geology of the Fishhawk Falls-Jewell Area, Clatsop County, Northwest Oregon: unpub. M.S. Thesis, Oregon State University, Corvallis, 360 p.

Nettleton, L. L., 1976, Gravity and magnetics in oil prospecting: McGraw-Hill Book Company, New York, 464 p.

Niem, A. R., and Niem, W. A., 1984, Cenozoic geology and geologic history of western Oregon, in Kulm, L. D. et al., eds., Atlas of the Ocean Margin Drilling Program,

Western Oregon-Washington, Continental Margin and Adjacent Ocean Floor, Region V: Ocean Margin Drilling Program Regional Atlas Series, Atlas 1, Marine Science International, Woods Hole, Massachusetts, Sheets 17 and 18.

Niem, A. R., and Niem, W. A., 1985, Oil and Gas Investigations of the Astoria Basin, Clatsop and northernmost Tillamook Counties, northwestern Oregon: Oregon Department of Geology and Mineral Industries Oil and Gas Invest. 14, scale 1:100,000.

Olbinski, J. S., 1983, Geology of the Buster Creek-Nehalem Valley area, Clatsop County, northwest Oregon: unpub. M.S. Thesis, Oregon State University, Corvallis, 204 p.

Orr, W. N., and Miller, P. R., 1984, Geologic map of the Stayton NE quadrangle, Oregon: Oregon Department of Geology and Mineral Industries, GMS-34, scale 1:24,000.

Orr, W. N., and Miller, P. R., 1986a, Geologic map of the Drake Crossing quadrangle, Marion County, Oregon: Oregon Department of Geology and Mineral Industries, GMS-50, scale 1:24,000.

Orr, W. N., and Miller, P. R., 1986b, Geologic map of the Elk Prairie quadrangle, Marion and Clackamas Counties, Oregon: Oregon Department of Geology and Mineral Industries, GMS-51, scale 1:24,000.

Paillet, F. L., and Kim, K., 1987, Character and distribution of borehole breakouts and their relationship to in situ stresses in deep Columbia River basalts: J. Geophys. Res., v. 92, p. 6223-6234.

Parker, M. J., 1990, The geology of the Oligocene and Miocene rocks of the Tillamook embayment, Tillamook County, northwestern Oregon: unpub. M.S. Thesis, Oregon State University, Corvallis, 492 p.

Parrish, R. R., Haugerud, R. A., and Price, R. A., 1990, The Eocene tectonic transition, Oregon to Alaska: Geol. Soc. Am. News and Information, v. 12, p. 124-125.

Peck, D. L., Griggs, A. B., Schlicker, H. G., Wells, F. G., and Dole, H. M., 1964, Geology of the central and northern parts of the Western Cascades, Oregon: U.S. Geological Survey Professional Paper 449, 56 p.

Perttu, J. C., 1981, An analysis of gravity surveys in the Portland Basin, Oregon: unpub. M.S. thesis, Portland State University, Portland, Oregon, 106 p.

Peterson, C. P., 1983, Geology of the Green Mountain-Young's River area, Clatsop County, northwest Oregon: unpub. M.S. thesis, Oregon State University, Corvallis, 215 p.

Peterson, C. D., and Darienzo, M. E., 1989, Episodic, abrupt tectonic subsidence recorded in late Holocene deposits of the South Slough syncline: An on-land expression of shelf fold belt deformation from the southern Cascadia margin (abstr.): Cordilleran section GSA, v. 21, p. 129.

Peterson, C. P., Kulm, L. D., and Gray, J. J., 1986, Geologic map of the ocean floor off Oregon and the adjacent continental margin: Oregon Department of Geology and Mineral Industries Geol. Map Series 42, scale 1:500,000.

Piper, A. M., 1942, Ground-water resources of the Willamette Valley, Oregon: U.S. Geological Survey Water-Supply Paper 890, 194 p.

Pitts, G. S., 1979, Interpretation of gravity measurements made in the Cascade Mountains and adjoining Basin and Range province in central Oregon: unpub. M.S. thesis, Oregon State University, Corvallis, 186 p.

Plumb, R. A., and Cox, J. W., 1987, Stress directions in eastern North America determined to 4.5 km from borehole elongation measurements: J. Geophys. Res., v. 92, p. 4805-4816.

Plumb, R. A., and Hickman, S. H., 1985, Stress-induced borehole elongation: A comparison between the four-arm dipmeter and the borehole televiewer in the Auburn geothermal well: J. Geophys. Res., v. 90, p. 5513-5521.

Popowski, T., in prep., Structure and tectonics of the Tualatin basin, northwestern Oregon: unpub. M.S. thesis, Oregon State University, Corvallis.

Price, D., 1961, Records of wells, water levels and chemical quality of ground water in the French Prairie-Mission Bottom area, northern Willamette Valley, Oregon: Oregon Water Resources Department, Ground Water Report no. 1, 314 p.

-----, 1967a, Geology and water resources in the French Prairie area, northern Willamette Valley, Oregon: U.S. Geological Survey Water Supply Paper 1833, 98 p.

-----, 1967b, Ground water in the Eola-Amity Hills area northern Willamette Valley, Oregon: U.S. Geological Survey Water Supply Paper 1847, 66 p., scale 1:48,000.

Price, D., and Johnson, N. A., 1965, Selected ground water data in the Eola-Amity Hills area, northern Willamette Valley, Oregon: Oregon Water Resources Department, Ground-Water Report no. 7, 55 p.

Priest, G. R., 1989, Volcanic and tectonic evolution of the Cascade volcanic arc, 44° 00" to 44° 52' 30" N: in Muffler, L.J. P., Weaver, C. S., and Blackwell, D. D., eds., Proceedings of Workshop XLIV, Geological, geophysical, and tectonic setting of the Cascade Range, U.S. Geological Survey Open-file Report 89-178, p. 430-489.

Priest, G. R., Wolter, N. M., Black, G. L., and Evans, S. H., 1983, Chapter 2. Overview of the geology of the central Oregon Cascade Range: in Geology and geothermal resources of the central Oregon Cascade Range, Oregon Department of Geology and Mineral Industries, Special Paper 15, p. 3-28.

Raleigh, C. B., Healy, J. H., Bredehoeft, J. D., 1972, Faulting and crustal stress at Rangely, Colorado: in H. C. Heard et al., eds., Flow and Fracture of Rocks, AGU Geophys. Monogr. Ser., v. 16, p. 275-284.

Rarey, P. J., 1986, Geology of the Hamlet-North Fork of the Nehalem River area, southern Clatsop and northernmost Tillamook counties, northwest Oregon: unpub. M.S. thesis, Oregon State University, Corvallis, 457 p.

Reidel, S. P., 1984, Saddle Mountains: The evolution of an anticline in the Yakima fold belt: Amer. J. Science, v. 284, p. 942-978.

Riddihough, R. P., 1977, A model for recent plate interactions off Canada's west coast: Can. J. Earth Sci., v. 14, p. 384-396.

-----, 1984, Recent movements of the Juan de Fuca plate system: J. Geophys. Res., v. 89, p. 6980-6994.

Roberts, M. C., 1984, The late Cenozoic history of an alluvial fill: the southern Willamette Valley, Oregon: in Mahaney, W. C., ed., Correlation of Quaternary chronologies, Norwich, England, Geo Books, p. 491-504.

Roberts, M. C., and Whitehead, D. R., 1984, The palynology of a nonmarine Neogene deposit in the Willamette Valley, Oregon: Review of Paleobotony and Palynology, v. 41, p. 1-12.

Safley, L. E., 1989, Geology of the Rock Creek-Green Mountain area, southeast Clatsop and northernmost Tillamook Counties, northwest Oregon: unpub. M.S. thesis, Oregon State University, Corvallis, 245 p.

Salvador, A., 1981, Final revision of Cosuna chronostratigraphic and numerical time scale, in O. E. Childs, ed., Fifth annual progress report of correlation of stratigraphic units of North America "COSUNA": U.S. Geological Survey Fiscal Year 1981 Report.

Sbar, M. L., 1982, Delineation and interpretation of seismotectonic domains in western North America: J. Geophys. Res., v. 87, p. 3919-3928.

Schenck, H. G., and Kleinpell, R. M., 1936, Refugian stage of Pacific Coast Tertiary: A.A.P.G. Bull., v. 20, p. 215-225.

Schlicker, H. G., and Finlayson, C. T., 1979, Geology and geologic hazards of northwestern Clackamas County, Oregon: Oregon Department of Geology and Mineral Industries Bull. 99, 79 p.

Sheriff, S. D., 1984, Paleomagnetic evidence for spatially distributed post-Miocene rotation of western Washington and Oregon: Tectonics, v. 3, p. 397-408.

Sherrod, D. R., and Pickthorn, L. G., 1989, Some notes on the Neogene structural evolution of the Cascade Range in Oregon: in Muffler, L. P., Weaver, C. S., and Blackwell, D. D., eds., Geology, geophysics, and tectonic setting of the Cascade Range, U.S. Geological Survey Open-File Report 89-178, p. 351-368.

Sherrod, D. R., and Smith, J. G., 1989, Preliminary map of upper Eocene to Holocene volcanic and related rocks of the Cascade Range, Oregon: U.S. Geological Survey Open-File Report 89-14, 20 p.

Simpson, R. W., Jachens, R. C., Blakely, R. J., and Saltus, R. W., 1986, A new isostatic map of the conterminous United States with a discussion on the significance of isostatic residual anomalies, J. Geophys. Res., v. 91, p. 8348-8372.

Smith, R. B., 1977, Intraplate tectonics of the western North American plate: Tectonophysics, v. 37, p. 323-336.

Snavely, P. D., Jr., and Baldwin, E. M., 1948, Siletz River volcanic series, northwestern Oregon: A.A.P.G. Bull., v. 32, p. 806-812.

Snavely, P. D., Jr., and MacLeod, N. S., 1977, Evolution of Eocene continental margins of western Oregon and Washington: Geological Society of America Abstracts with Programs, v. 9, p. 1183

Snavely, P. D., Jr., MacLeod, N. S., and Rau, W. W., 1969, Geology of the Newport area, Oregon: The Ore Bin, v. 31, p. 25-71.

Snavely, P. D., Jr., MacLeod, N. S., and Wagner, H. C., 1968, Tholeiitic and alkalic basalts of the Eocene Siletz River Volcanics, Oregon Coast Range: Am. Jour. of Science, v. 266, p. 454-481.

Snavely, P. D., Jr., and Vokes, H. E., 1949, Geology of the coastal area between Cape Kiwanda and Cape Foulweather, Oregon: U.S. Geological Survey Oil and Gas Investigation Map 97.

Snavely, P. D., and Wagner, H. C., 1964, Geologic sketch of northwestern Oregon: U.S. Geological Survey Bull. 1181-M, 17 p.

Snavely, P. D., Jr., Wagner, H. C., and Lander, D. L., 1980, Interpretation of the Cenozoic geologic history, central Oregon continental margin: Cross-section summary: Geological Society of America Bull., v. 91, Part 1, p. 143-146.

Spence, W., 1989, Stress origins and earthquake potentials in Cascadia: J. Geophys. Res., v. 94., p. 3076-3088.

Springer, J. E., 1987, Stress orientations from well bore breakouts in the Coalinga region: Tectonics, v. 6, p. 667-676.

Suppe, J., 1985, Principles of structural geology: Prentice-Hall, Inc., Englewood Cliffs, New Jersey, 537 p.

Sutter, J. F., 1978, K-Ar ages of Cenozoic rocks from the Oregon Cascades west of 121°30': Isochron/West, no. 21, p. 15-21.

Swanson, R. D., 1986, A stratigraphic-geochemical study of the Troutdale Formation and Sandy River Mudstone in the Portland basin and lower Columbia River Gorge: unpub. M.S. thesis, Portland State University, Portland, Oregon, 103 p.

Swanson, D. A., Wright, T. L., Hooper, P. R., and Bentley, R. D., 1979, Revisions in stratigraphic nomenclature of the Columbia River Basalt Group: U.S. Geological Survey Bull. 1457-G, 59 p.

Taylor, E. M., in press, Volcanic history and tectonic development of the central High Cascade Range, Oregon: in Muffler, L.J. P., Weaver, C. S., and Blackwell, D. D., eds., Proceedings of Workshop XLIV, Geological, geophysical, and tectonic setting of the Cascade Range, U.S. Geological Survey Open-file Report 89-178, p. 369-394.

Thayer, T. P., 1939, Geology of the Salem Hills and the North Santiam River basin, Oregon: Oregon Department of Geology and Mineral Industries Bull. 15, 40 p.

Thiruvathukal, J. H., 1968, Regional gravity of Oregon: unpub. Ph.D. thesis, Oregon State University, Corvallis, 92 p.

Thiruvathukal, J. H., Berg, J. W., Jr., Heinrichs, D. F., 1970, Regional gravity of Oregon: Geological Society of America Bull., v. 81, p. 725-738.

Tolan, T. L., and Beeson, M. H., 1984, Intracanyon flows of the Columbia River Basalt Group in the lower Columbia River Gorge and their relationship to the Troutdale Formation: Geological Society of America Bull., v. 95, p. 463-477.

Tolan, T. L., Reidel, S. P., Beeson, M. H., Fecht, K. R., Anderson, J. L., and Swanson, D. A., 1989, Revisions to the estimates of the areal extent and volume of the Columbia River Basalt Group: in Reidel, S. P., and Hooper, P. R., eds., Volcanism and tectonism in the Columbia River flood-basalt province, Geological Society of America Special Paper 239. p. 1-20.

Treasher, R. C., 1942, Geologic history of the Portland area: State of Oregon Department of Geology and Mineral Industries, GMI Short Paper no. 7, 17 p.

Trimble, D. E., 1963, Geology of Portland, Oregon and adjacent areas: A study of Tertiary and Quaternary deposits, lateritic weathering profiles, and of Quaternary history of part of the Pacific Northwest, U.S. Geological Survey Bull. 1119, 119 p.

Turner, F. E., 1938, Stratigraphy and mollusca of the Eocene of western Oregon: Geological Society of America Special Paper no. 10, 98 p.

Veen, C. A., 1981, Gravity anomalies and their structural implications for the southern Oregon Cascade Mountains and adjoining Basin and Range province: unpub. M.S. thesis, Oregon State University, Corvallis, 86 p.

Verplanck, E. P., 1985, Temporal variations in volume and geochemistry of volcanism in the Western Cascades, Oregon: unpub. M.S. Thesis, Oregon State University, Corvallis, 115 p.

Weaver, C. S., and Baker, G. E., 1988, Geometry of the Juan de Fuca plate beneath Washington and northern Oregon from seismicity: Bull. Seismol. Soc. Am., v. 78, p. 264-275.

Weaver, C. S., Grant, W. C., Malone, S. D., and Endo, E. T., 1981, Post May 18 seismicity: Volcanic and tectonic implications: U.S. Geological Survey Prof. Paper 1250, p. 109-121.

Weaver, C. S., Grant, W. C., and Shemata, J. E., 1987, Local crustal extension at Mount St. Helens, Washington: J. Geophys. Res., v. 92, p. 10170-10178.

Weaver, C. S., Green, S. M., and Iyer, H. M., 1982, Seismicity of Mount Hood and structure as determined from teleseismic P wave delay studies: J. Geophys. Res., v. 87, p. 2782-2792.

Weaver, C. S., and Smith, S. W., 1983, Regional tectonic and earthquake hazard implications of a crustal fault zone in southwestern Washington: J. Geophys. Res., v. 88, p. 10371-10383.

Wells, F. G., 1956, Geology of the Medford quadrangle, Oregon-California: U.S. Geological Survey Quadrangle Map GQ-89, scale 1:96,000.

Wells, R. E., 1990, Paleomagnetic rotations and the Cenozoic tectonics of the Cascade arc, Washington, Oregon, and California: J. Geophys. Res., v. 95, p. 19409-19417.

Wells, R. E., and Coe, R. S., 1985, Paleomagnetism and geology of Eocene volcanic rocks of southwest Washington, implications for mechanisms of tectonic rotation: J. Geophys. Res., v. 90, p. 1925-1947.

Wells, R. E., Engebretson, D. C., Snavely, P. D., Jr., and Coe, R. S., 1984, Cenozoic plate motions and the volcano-tectonic evolution of western Oregon and Washington: Tectonics, v. 3, p. 275-294.

Wells, R. E., and Heller, P. L., 1988, The relative contribution of accretion, shear, and extension to Cenozoic tectonic rotation in the Pacific Northwest: Geol. Soc. Amer. Bull., v. 100, p. 325-338.

Wells, R. E., Niem, A. R., Macleod, N. S., Snavely, P. D., Jr., and Niem, W. A., 1983, Preliminary geologic map of the west half of the Vancouver (Washington-Oregon) 1° x 2° quadrangle, Oregon: Oregon Department of Geology and Mineral Industries Open-File Report 0-83-06, scale 1:250,000.

Woodcock, N. H., and Fisher, M., 1986, Strike-slip duplexes: J. Stuct. Geol., v. 8, p. 725-735.

Yelin, T. S., and Patton, H. J., 1989, Seismotectonics of the Portland, Oregon region (abstr.): EOS Trans. AGU, v. 70, p. 1330.

Yelin, T. S., and Patton, H. J., 1990, Seismotectonics of the Portland, Oregon region: submitted to Bull. Seis. Soc. Am.

Zoback, M. D., Moos, D., Mastin, L., and Anderson, R. N., 1985, Well bore breakouts and in situ stress: J. Geophys. Res., v. 90, p. 5523-5530.

Zoback, M. D., Moos, D., Mastin, L., and Anderson, R. N., 1986, Reply: J. Geophys. Res., v. 91, p. 14163-14164.

Zoback, M. L., and Zoback, M. D., 1980, State of stress in the conterminous United States: J. Geophys. Res., v. 85, p. 6113-6156.

Zoback, M. L., and Zoback, M. D., 1989, Tectonic stress field of the continental United States: in Pakiser, L., and Mooney,W., eds., Geophysical Framework of the Continental United States, GSA Memoir 172.

Zoback, M. L., Nishenko, S. P., Richardson, R. M., Hasegawa, H. S., and Zoback, M. D., 1986, Mid-plate stress, deformation, and seismicity: in Vogt, P. R., and Tucholke, B. E., eds., Geology of North America volume M, The Western North Atlantic Region, Geol. Soc. of Am., p. 297-312

Zoback, M. D., Zoback, M. L., Mount, V. S., Suppe, J., Eaton, J. P., Healy, J. H., Oppenheimer, D., Reasenberg, P., Jones, L., Raleigh, C. B., Wong, I. G., Scotti, O., and Wentworth, C., 1987, New evidence on the state of stress of the San Andreas fault system, Science, v. 238, p. 1105-1111.

Zollweg, J. E., and Crosson, R. S., 1981, The Goat Rocks Wilderness, Washington earthquake of 28 May 1981 (abstr.): EOS Trans. AGU, v. 62, p. 966.